



WPI

Development of 3D Printed Humanoid Robots

IN PARTIAL FULFILLMENT OF A MAJOR QUALIFYING PROJECT
WORCESTER POLYTECHNIC INSTITUTE

Submitted by:

Aashish Sing Alag (ME)
Zeñia Alarcon (ME)
Emily Austin (RBE/ME)
Tessa Lytle (ME)
James Van Milligen (ME)

Project Advisors:

Kaveh Pahlavan (ECE/CS)
Pradeep Radhakrishnan (ME/RBE)

This report represents the work of WPI undergraduate students submitted to the faculty as evidence of completion of a degree requirement. WPI routinely publishes these reports on its website without editorial or peer review. For more information about the projects program at WPI, please see <http://www.wpi.edu/academics/ugradstudies/project-learning.html>

Abstract

This project focused on developing two open-source 3D-printed humanoid robots, Koalby and Ava, as versatile lab assistants with a focus on lifting objects, pushing a cart, and walking. Static and dynamic analyses were carried out to guide a series of redesigns to improve strength and integrate new components. The redesigns included a new grip mechanism to lift objects, sensors to aid the walking component, and component updates to integrate new lower cost motors. The grip was an under-actuated, 3-point finger grip with an electromagnet attached to the base of the forearm. A new spine was created, attached at the chest and pelvis, to assist with stability for standing and walking. The chest and feet were redesigned to include sensors to assist in walking. To make the robots more cost effective, all of the Dynamixel motors were replaced with HerkuleX DRS motors allowing for uniformity in design and programming.

Acknowledgements

This project would not have been possible without the help of the following people:

Dr. Pradeep Radhakrishnan

Dr. Kaveh Pahlavan

Dr. Mehul Bhatia

Barbara Furhman

Peter Hefti

Cam Tu Le

The original Poppy Project team at the Flowers laboratory at Inria Bordeaux Sud-Ouest

The 2022 3D Printed Humanoid Robot MQP team

The 2023 3D Printed Humanoid Robot Software MQP team

Worcester Polytechnic Institute

Our friends and families

Table of Contents

Abstract	2
Acknowledgements	3
Table of Contents	4
Authorship	7
List of Figures	12
List of Tables	16
List of Abbreviations	17
1.0 Introduction	18
1.1 Project Overview and Goals	19
1.2 Section Overview	20
2.0 2022 MQP	21
2.1 Goal	21
2.2 Outline of Components	22
2.3 Structural Component Design Changes	22
2.4 Actuators	25
2.5 Electrical	29
2.6 Achievements	32
2.7 Recommendations	32
3.0 2022 MQP Testing	33
4.0 Literature Review	35
4.1 Humanoid Robot Application Research	35
4.2 Actuated Grips	37
4.2.1 Jamming Grip	38
4.2.2 Actuated Finger Grip Research	39
Type 1	40
Type 2	41
Type 3	42
4.3 Electrical Components	43
4.4 Exoskeleton	47
4.5 Printing	48
4.5.1 FDM Printing	49
4.5.2 Resin Printing	49
5.0 Project Goal	51
5.1 Objectives	51
6.0 Methodology	53
6.1 A-Term	53

6.2 B-Term	54
6.3 C-Term	55
6.4 D-Term	56
7.0 Structural Component Redesign	57
7.1 Analysis	57
7.1.1 ANSYS	57
7.1.2 Free Body Diagrams	59
7.1.3 FBD Equations	63
7.2 Pelvis	65
7.3 Spine	65
8.0 Walking Redesigns	66
8.1 Sensor Integration	67
8.2 Electrical Integration	69
8.3 Head Lid	69
8.4 Chest	70
8.5 Feet	72
9.0 Grip Addition	73
9.1 Grip Tools	74
9.2 Grip Matrix	75
9.3 Grip Design	78
9.4 Forearm Redesign	80
10.0 Standardizing Components	81
10.1 Motor Matrix	81
10.1.1 Torque Analysis	84
10.1.2 Comparing Specifications	86
10.2 Hip	89
10.3 Thigh	90
10.4 Shin	91
10.5 Abdomen	93
10.6 Neck	96
10.7 Head	97
10.8 Shoulder and Shoulder Connector	98
10.9 Bicep	99
11.0 Manufacturing and Assembly	101
11.1 3D Printing	101
11.1.1 Resin 3D Printing	102
11.1.2 FDM 3D Printing	103
11.2 Assembly	104

11.3 Part Compatibility	107
12.0 Discussion	108
12.1 Improve Structural Integrity	108
12.2 Design for Walking	109
12.3 Grip Addition	109
12.4 Standardize Components	110
12.5 WPI Undergraduate Research Project Showcase	110
13.0 Conclusions	112
13.1 Broader Impacts	112
13.1.1 Social and Global Impact	112
13.1.2 Environmental Impact	113
13.1.3 Economical Impact	113
13.2 Future Work	114
13.2.1 Testing	114
13.2.2 Pressure Sensors	114
13.2.3 Hazardous Resistance	115
14.0 References	116
15.0 Appendices	120
Appendix A Inventory	120
Appendix B Humanoid Robot Application Pictures [6]	120
Appendix C Motor Movement Document	121
Appendix D Motor Specification Document	121
Appendix E Part Compatibility Document	121
Appendix F Torque Analysis	122
Appendix G Electrical Diagram	125
Appendix H Printing Instructions	126
Appendix I Assembly Instruction	126
Appendix J CAD assembly	126
Appendix K Cost	126
Appendix L ANSYS	128
16.0 Reflections	133

Authorship

Section	Author	Editor
<i>Abstract</i>	Zeñia Alarcon	Everyone
<i>Acknowledgements</i>	Aashish Singh Alag	Everyone
<i>List of Figures</i>	Zeñia Alarcon	Emily Austin
<i>List of Tables</i>	Zeñia Alarcon	Tessa Lytle
<i>List of Abbreviations</i>	Tessa Lytle	Everyone
<i>Introduction</i>	Aashish Singh Alag	Emily Austin
Project Overview and Goals	Aashish Singh Alag	Emily Austin
Section Overview	James Van Milligen	Emily Austin
<i>2022 MQP</i>	Zeñia Alarcon	James Van Milligen
Goal	Zeñia Alarcon	James Van Milligen
Outline of Components	Zeñia Alarcon	James Van Milligen
Structural Component Design Changes	Tessa Lytle	Zeñia Alarcon
Actuators	Tessa Lytle	Zeñia Alarcon
Electrical	Tessa Lytle	Zeñia Alarcon
Achievements	James Van Milligen	Tessa Lytle
Recommendations	James Van Milligen	Aashish Singh Alag
<i>2022 MQP Testing</i>	James Van Milligen	Aashish Singh Alag
<i>Literature Review</i>	Zeñia Alarcon	Emily Austin
Humanoid Robot Application Research	Tessa Lytle	Emily Austin
Actuated Grips	Zeñia Alarcon	Emily Austin
Jamming Grip	Zeñia Alarcon	Emily Austin

Actuated Finger Grip Research	Zeñia Alarcon	Emily Austin
Type 1	Zeñia Alarcon	Emily Austin
Type 2	Zeñia Alarcon	Emily Austin
Type 3	Zeñia Alarcon	Emily Austin
Electrical Components	Emily Austin	Zeñia Alarcon
Exoskeleton	James Van Milligen	Emily Austin
Printing	Aashish Singh Alag	Emily Austin
FDM Printing	Aashish Singh Alag	Emily Austin
Resin Printing	Aashish Singh Alag	Emily Austin
Project Goal	Zeñia Alarcon	Aashish Singh Alag
Objectives	Zeñia Alarcon	Emily Austin
Methodology	Zeñia Alarcon	Emily Austin
A-term	Zeñia Alarcon	Emily Austin
B-term	Zeñia Alarcon	Emily Austin
C-term	Zeñia Alarcon	Emily Austin
D-term	Zeñia Alarcon	Emily Austin
Structural Component Redesign	Zeñia Alarcon	Tessa Lytle
Analysis	Zeñia Alarcon	Tessa Lytle
ANSYS	Zeñia Alarcon	Tessa Lytle
Free Body Diagrams	Zeñia Alarcon	Tessa Lytle
FBD Equations	Zeñia Alarcon	Tessa Lytle
Pelvis	James Van Milligen	Emily Austin
Spine	James Van Milligen	Emily Austin
Walking Redesigns	Emily Austin	Zeñia Alarcon

Sensor Integration	Emily Austin	Zeñia Alarcon
Electrical Integration	Emily Austin	Zeñia Alarcon
Head Lid	Tessa Lytle	Emily Austin
Chest	James Van Milligen	Zeñia Alarcon
Feet	Emily Austin	Zeñia Alarcon
<i>Grip Addition</i>	Zeñia Alarcon	Emily Austin
Grip Tools	Emily Austin	Zeñia Alarcon
Grip Matrix	Zeñia Alarcon	Tessa Lytle
Grip Design	Aashish Singh Alag	James Van Milligen
Forearm Redesign	Zeñia Alarcon	James Van Milligen
<i>Standardizing Components</i>	Zeñia Alarcon	James Van Milligen
Motor Matrix	Zeñia Alarcon	James Van Milligen
Torque Analysis	Emily Austin	James Van Milligen
Comparing Specifications	Tessa Lytle	James Van Milligen
Hip	Aashish Singh Alag	Emily Austin
Thigh	Tessa Lytle	Emily Austin
Shin	Aashish Singh Alag	Emily Austin
Abdomen	Tessa Lytle	Aashish Singh Alag
Neck	Tessa Lytle	Aashish Singh Alag
Head	Emily Austin	Aashish Singh Alag
Shoulder and Shoulder Connector	Aashish Singh Alag	Emily Austin
Bicep	Aashish Singh Alag	Emily Austin
<i>Manufacturing and Assembly</i>	Aashish Singh Alag	Tessa Lytle
3D Printing	Aashish Singh Alag	Tessa Lytle

Resin 3D Printing	Aashish Singh Alag	Tessa Lytle
FDM 3D Printing	Aashish Singh Alag	Tessa Lytle
Assembly	Aashish Singh Alag	Tessa Lytle
Part Compatibility	Tessa Lytle	Aashish Singh Alag
Discussion	Tessa Lytle	Aashish Singh Alag
Improve Structural Integrity	Tessa Lytle	Aashish Singh Alag
Design for Walking	Tessa Lytle	Aashish Singh Alag
Grip Addition	Tessa Lytle	Aashish Singh Alag
Standardize Components	Tessa Lytle	Aashish Singh Alag
WPI Undergraduate Research Project Showcase	Tessa Lytle	Aashish Singh Alag
Conclusion	Tessa Lytle	Aashish Singh Alag
Broader Impacts	Aashish Singh Alag	Zeñia Alarcon
Social and Global Impact	Aashish Singh Alag	Zeñia Alarcon
Environmental Impact	Aashish Singh Alag	Zeñia Alarcon
Economic Impact	Aashish Singh Alag	Zeñia Alarcon, James Van Milligen
Future Work	Aashish Singh Alag	Zeñia Alarcon
Testing	Aashish Singh Alag	James Van Milligen
Pressure Sensors	Aashish Singh Alag	James Van Milligen
Hazardous Resistance	Aashish Singh Alag	Zeñia Alarcon
References	Zeñia Alarcon	Everyone
Appendices	Everyone	Everyone
Appendix A Inventory	Tessa Lytle	Everyone
Appendix B Humanoid Robot Application Pictures [6]	Tessa Lytle	Everyone

Appendix C Motor Movement Document	Tessa Lytle	Everyone
Appendix D Motor Specification Document	Tessa Lytle	Everyone
Appendix E Part Compatibility Document	Tessa Lytle	Everyone
Appendix F Torque Analysis	Emily Austin	Everyone
Appendix G Electrical Diagram	Emily Austin	Everyone
Appendix H Printing Instructions	Tessa Lytle, Aashish Singh Alag, & James Van Milligen	Everyone
Appendix I Assembly Instruction	Tessa Lytle & Aashish Singh Alag	Everyone
Appendix J CAD Assembly	Tessa Lytle & Aashish Singh Alag	Everyone
Appendix K Cost	Zeñia Alarcon	Everyone
Appendix L ANSYS	Zeñia Alarcon	Everyone

List of Figures

Figure 1.1a: 2022 Koalby Project.....	19
Figure 2.1a: Full Assembly of Koalby.....	21
Figure 2.3a: Original Poppy Chest Piece with Handle	22
Figure 2.3b: Koalby Redesign to Fit on Print Bed	23
Figure 2.3c: Two Part Shin Redesign reproduced as is from [3]	23
Figure 2.3d: Shin Platforms to Store Battery	24
Figure 2.3e: Foot Range of Motion Redesign, original (left) and redesign (right) reproduced as is from [3].....	25
Figure 2.4a: 25 Motors in Koalby.....	26
Figure 2.4b: Two Horn Dynamixel MX-28 Motor reproduced as is from [3].....	27
Figure 2.4c: HerkuleX DRS-0201 Motor CAD with the Motor Adapter Prints Attached reproduced as is from[3]	27
Figure 2.4d: Comparison of original Dynamixel double rotation assembly (left) and the HerkuleX version (right) reproduced as is from [3]	27
Figure 2.4e: Abdomen Assembly in Koalby.....	28
Figure 2.4f: Comparison of original Dynamixel servo horn hole pattern (left) and the HerkuleX version (right) reproduced as is from [3].....	28
Figure 2.4g: Original Pelvis Assembly (left) and Modified Pelvis Assembly (right) reproduced as is from [3].....	29
Figure 2.5a: 7.4V Batteries in Koalby's Legs.....	30
Figure 2.5b: 11.1V Battery in Koalby's Head.....	30
Figure 2.5c: Koalby Electronics Setup reproduced as if from [3].....	31
Figure 2.5d: Serial Port Usage of Koalby reproduced as is from[3].....	31
Figure 3.0a: Initial Condition of Koalby.....	33
Figure 3.0b: Broken Pelvis.....	34
Figure 3.0c: Broken Pelvis and Abdomen.....	34
Figure 4.2a: 2022 MQP Grip reproduced as is from [3].....	37
Figure 4.2.1a: Jamming Gripper reproduced as is from reproduced as is from [12].....	39
Figure 4.2.2a: Type of grasp reproduced as is from [13].....	39

Figure 4.2.2b: Grip finger distance.....	39
Figures 4.2.2c: The Claw reproduced as is from [14].....	41
Figure 4.2.2d: Our printed prototype of The Claw.....	41
Figure 4.2.2e: ALARIS finger design reproduced as is from [15].....	42
Figure 4.2.2f: Blueprint of ALARIS finger design with motor reproduced as is from [15].....	42
Figure 4.2.2g: Blueprint of ALARIS finger design reproduced as is from [15].....	42
Figure 4.2.2h: Full ALARIS grip design reproduced as is from [15].....	42
Figure 4.2.2i: Model O various pivot connections reproduced as is from [16].....	43
Figure 4.2.2j: Model O grip orientation reproduced as is from [16].....	43
Figure 4.3a: Ultrasonic sensor reproduced as is from [17].....	44
Figure 4.3b: Infrared transmitter (white) and receiver (black) reproduced as is from [18].....	44
Figure 4.3c: LiDAR sensor reproduced as is from [19].....	44
Figure 4.3d: Diagram of IR sensor functionality.....	45
Figure 4.3e: Diagram of ultrasonic sensor functionality reproduced as is from [22].....	45
Figure 4.3f: Diagram of LiDAR sensor functionality reproduced as is from [23].....	45
Figure 4.3g: Diagram of pressure sensor functionality reproduced as is from [26].....	46
Figure 4.3h: Diagram of force sensor functionality reproduced as is from [27].....	46
Figure 4.3i: Diagram of an IMU's 3-axis gyroscope and accelerometer reproduced as is from [28].....	46
Figure 4.4a Rigid Style Exoskeleton reproduced as is from [32].....	48
Figure 4.4b Personal Lift Augmentation Device reproduced as is from [31].....	48
Figure 4.5.1a: FDM Printers.....	49
Figure 4.5.2a: Resin printer.....	50
Figure 7.1.1a: Pelvis ANSYS set up.....	58
Figure 7.1.1b: Pelvis ANSYS deformation.....	59
Figure 7.1.1c: Pelvis ANSYS stress.....	59
Figure 7.1.2a: Full body reference for FBD.....	60
Figure 7.1.2b: Head FBD about Z-axis.....	60
Figure 7.1.2c: Shin FBD about Z-axis.....	60
Figure 7.1.2d: Thigh FBD about Z-axis.....	61
Figure 7.1.2e: Hip FBD about Z-axis.....	61

Figure 7.1.2f: Arm FBD about Z-axis.....	61
Figure 7.1.2g: Foot FBD about Z-axis.....	61
Figure 7.1.2h: Chest FBD about the X-axis.....	62
Figure 7.1.2i: Forearm FBD about the X-axis.....	62
Figure 7.1.2j: Abdomen FBD about the X-axis.....	62
Figure 7.1.2k: Hip FBD about the X-axis.....	62
Figure 7.1.2m: Pelvis FBD about the Y-axis.....	63
Figure 7.2a: Full pelvis part.....	65
Figure 7.2b: Zoomed in pelvis.....	65
Figure 7.3a: Spine addition.....	66
Figure 8.3a: 2022 MQP Team Head Lid Design.....	69
Figure 8.3b: Redesigned Head Lid.....	70
Figure 8.3c: Head Assembly.....	70
Figure 8.4a: Front Chest Design.....	71
Figure 8.4b: Back Chest Design.....	71
Figure 8.4c: Breast Plate.....	72
Figure 8.4d: IMU Holder.....	72
Figure 8.5a: Widened Foot.....	73
Figure 8.5b: Foot Printed in TPE.....	73
Figure 8.5c: Foot with PVC Attached.....	73
Figure 8.5d: Foot with IMU Integration.....	73
Figure 9.1a: Lab Tools.....	74
Figure 9.3a: Implemented grip design.....	79
Figure 9.3b: Electromagnet.....	79
Figure 9.3c: Wrist connection with palm of grip assembly.....	79
Figure 9.4a: Forearm redesign assembly.....	80
Figure 10.1.2a: Dynamixel MX-64AT Motor.....	86
Figure 10.1.2b: HerkuleX DRS-0601 Motor.....	87
Figure 10.1.2c: HerkuleX DRS-0101 Motor.....	88
Figure 10.1.2d: Dynamixel AX-12 Motor.....	88
Figure 10.2a: Redesigned Hip Piece.....	89

Figure 10.3a: Redesigned Thigh Part.....	90
Figure 10.3b: Custom Servo Horn for HerkuleX DRS-0601 Motor.....	90
Figure 10.3c: Thigh Sub-Assembly.....	91
Figure 10.4a: Redesigned Top Shin Part.....	92
Figure 10.4b: Redesigned Bottom Shin Part.....	93
Figure 10.5a: Abdomen Horn Holder.....	94
Figure 10.5b: Abdomen Motor Connector.....	94
Figure 10.5c: Large Abdomen Piece.....	94
Figure 10.5d: Abdomen Assembly.....	95
Figure 10.5e: Abdomen Location in Full Assembly.....	95
Figure 10.6a: Neck Piece.....	96
Figure 10.6b: Head Assembly with Neck Piece.....	96
Figure 10.7a: Head Bracket.....	97
Figure 10.7b: Head Base.....	97
Figure 10.7c: Full Head Assembly.....	97
Figure 10.8a: Redesigned Shoulder Part.....	98
Figure 10.8b: Redesigned Shoulder Connector Part.....	99
Figure 10.9a: Right Hand Bicep Piece.....	100
Figure 11.1a: CHITUBOX setup.....	103
Figure 11.2a: Leg Subassembly.....	104
Figure 11.2b: Arm Subassembly.....	104
Figure 11.2c: Torso Subassembly	105
Figure 11.2d: Head Sub Assembly	105
Figure 11.2e: Ava Assembly without Grip Attached.....	106
Figure 11.3a: Right Hip Deviation.....	107
Figure 11.3b: Rib Deviation.....	107
Figure 12.5a: Mechanical and Materials Engineering Department Presentation.....	111
Figure 12.5b: Ava and Koalby at the Mechanical and Materials Engineering Department Presentation.....	111

List of Tables

Table 2.4a: Comparing Dynamixel MX-28 and HerkuleX DRS-0201 Motors.....	25
Table 4.1a: Humanoid Robot Application Examples.....	35
Table 8.1a: Sensor Decision Matrix.....	68
Table 9.1a: Lab Tool Specifications.....	75
Table 9.2a: Grip Decision Matrix:	77
Table 10.1a: Upper Body Motor Decision Matrix.....	82
Table 10.1b: Lower Body Motor Decision Matrix.....	83
Table 10.1.1a: Elbow Torque: Arm is resting at the side and the elbow is bent 90 degrees where the palm is facing the ceiling.....	84
Table 10.1.1b: Shoulder Torque (y-axis): At the shoulder, the arm was held straight out to the right (horizontal) and the palm of the hand was rotated to face the ceiling.....	84
Table 10.1.1c: Shoulder Torque (x-axis): At the shoulder, the arm was held out straight to the right (horizontal) and the elbow was bent inwards 90 degrees where the palm was facing the ground.....	85
Table 10.1.1d: Chest Torque: At the shoulder, the arm was held out straight to the right (horizontal) and analysis was done about the central chest connection point.....	85
Table 10.1.1e: Leg Torque: Hip was bent upward 90 degrees, and the knee joint was bent downward at 45 degrees.....	85
Table 11.1a: Physical Properties of Hard-Tough Resin.....	102

List of Abbreviations

Abbreviation	Meaning
IMU	Inertial Measurement Unit
LiDAR	Light Detection and Ranging
DOF	Degrees of Freedom
CoM	Center of Mass
MQP	Major Qualifying Project
AI	Artificial Intelligence
FBD	Force Body Diagram
DLP	Digital Light Processing
FDM	Fused Deposition Modeling
TPE	Thermoplastic Elastomer
PVC	Polyvinyl Chloride
PLA	Polylactic Acid
ABS	Acrylonitrile Butadiene Styrene
MME	Mechanical and Materials Engineering

1.0 Introduction

Humanoid robots designed to resemble human shape and movements are being used in various fields including healthcare, education, entertainment, and research. Currently, there are several humanoid robots in the field such as Asimo by Honda, Atlas by Boston Dynamics and Ameca by Engineering Arts. Equipped with a variety of sensors and cameras to facilitate motion, the robots are rapidly advancing the field of robotics in areas such as artificial intelligence, computer vision, and 3D printing [1].

3D printing has been used in the field of robotics to reduce the cost and complexity of manufacturing. The ability to create intricate human-like shapes and designs allows for production of complex parts that would have been difficult or nearly impossible to create using traditional subtractive and machining techniques. Additionally, 3D printing can be used to shorten the manufacturing time required to create the robot and also enable various customization of the design to fit specific needs.

The Koalby Project, a 3D-printed Humanoid Robot, aimed to reproduce the functionality of the original Poppy Project Robot while reducing the cost of creation by using 3D printing techniques [2]. This recreation of Poppy, named Koalby (seen in Figure 1.1a) is a 4 kg, 85 cm tall humanoid robot with 27 degrees of freedom. Successful in reproducing the functionalities of the original Poppy, the team was able to achieve their goal of cost reduction of approximately ~\$3000. In addition to this, the project also aimed to untether the robot by providing fully onboard battery power and wifi capabilities for remote operation, both major steps towards enabling Koalby to walk. Overall, their project demonstrated the potential of using 3D printing technology to create small scaled, cost-effective humanoid robots with human-like capabilities while exhibiting the potential for future advancement in the field.

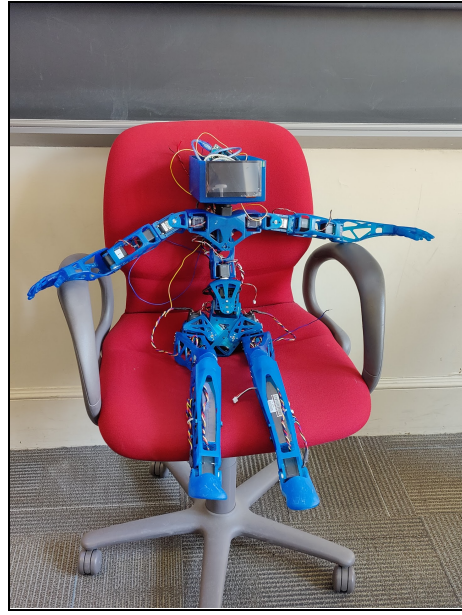


Figure 1.1a: 2022 Koalby Project

1.1 Project Overview and Goals

Our goal was to design and build an Open-Source 3D printed humanoid robot, based on Koalby, that could be recreated for supply managers or engineers looking for an efficient and effective lab assistant. Ava, our new iteration of a humanoid robot, involved a series of changes from the original Koalby design. These key adjustments made from Koalby were standardizing components like motors and parts, adding gripping functionality, adding walking capabilities, and improving the overall structural integrity.

The first objective was to increase Ava's structural integrity such that she could withstand the motions she would be performing. This required a redesign of multiple components to improve their overall strength while providing additional stability and balance. The second objective was to implement walking capabilities into Ava's design. This involved integrating sensors and cameras that would help assess the robot's surroundings and assist with walking. The third objective was to integrate gripping functionality into Ava's design. To do this, we had to consider the compatibility of various gripping mechanisms and their ability to be made modular and adjustable to suit various lab environments. This would allow us to create a robot that could pick up and manipulate objects with ease, accuracy and precision.

While they had many successes, last year's team was unable to fully simplify the Poppy design and reduce the number of parts and fasteners for the assembly. Hence, we aimed to standardize and reduce several of Ava's components to achieve both time and cost efficiency, as well as facilitate quick and efficient maintenance and repairs. By using readily available and economical motors and implementing various manufacturing techniques, we were able to create a cost-effective robot that is comparable to its larger counterparts.

In summary, our goal with Ava was to create a lab assistant that would be efficient, effective, and cost-effective. Through various redesigns and improvements, we were able to make significant progress to ensure that Ava meets the needs and demands of the lab environment.

1.2 Section Overview

Section 2 will talk about the 2022 3D Printed Humanoid Robot MQP Team and what they were able to achieve. Section 3 focuses on the observation of the prior robot and what testing was accomplished. Section 4 shows the literature review completed, with information on humanoid robot applications, actuated grips, electrical components, exoskeletons, and 3D Printing. Section 5 talks about the goals of this MQP's project, and Section 6 focuses on how we went about achieving those goals. Section 7 then highlights the redesign of several structural components. This includes the analysis completed on the prior robots parts and the design to fix the problems coming from this. Section 8 displays the sensor and electrical integration along with designs to aid with walking. Section 9 looks at the gripper designs and the forearm attachment. Section 10 talks about the remaining design changes made in order to accommodate motor changes and decrease the amount of fasteners. Section 11 talks about the manufacturing and assembly of the new humanoid robot as well as the compatibility of the new parts. Section 12 is where we discuss what we were able to achieve, and Section 13 focuses on the broader impact and future works of this MQP. Finally, Section 14 contains the references and Section 15 the appendices.

2.0 2022 MQP

In this section, we will discuss the Koalby Project, the 2022 MQP [3]. This includes the goals of the Koalby Project along with the various components that have been changed to create Koalby. We will address what they achieved and their recommendations.

2.1 Goal

Beazley et al. worked on the Koalby Project, which was originally based on the Poppy Project. Figure 2.1a shows Koalby. The changes from Poppy to Koalby included the following: HerkuleX DRS-0201 motors usage over Dynamixel MX-28 motors and a battery powered design rather than a tethered design. The key objectives for Koalby were to identify alternative components to reduce the cost and give Koalby the ability to walk on his own. A record/play system was also implemented to allow a human operator to manually position the robot, record those positions for later playback, and highlight the capabilities of individual systems of the robot. The Koalby project proved to be successful in producing a full humanoid robot based on the Poppy Project with modifications to allow for accessibility and autonomous functionality.



Figure 2.1a: Full Assembly of Koalby

2.2 Outline of Components

The Koalby Project Team, Beazley et al., was able to recreate a humanoid robot to be more cost effective and have untethered functionality to allow for walking capabilities. Koalby had 68 resin printed parts. These parts were created using a Digital Light Processing (DLP) which uses a LCD screen to cure layers of liquid resin. Koalby used 4 Dynamixel MX-64AT Motors, 2 Dynamixel AX-12A Motors, and 19 HerkuleX DRS-0201. Additionally, Koalby uses custom Dynamixel servo horns for the MX-64 motors. There were ~500 M3 Socket head screws when Koalby was fully assembled. For electronics, Koalby had a Raspberry Pi 4, Arduino Mega Clone, and Raspberry Pi Screen. Additionally, two 7.4V batteries were installed in the shins, and an 11.1V battery was installed in the head to eliminate the need to be tethered to a power source. The Koalby Project total cost of motors and electrical components was \$4,197.56, a \$2,752.50 reduction from Poppy [3].

2.3 Structural Component Design Changes

Several additional design changes were made from the Poppy design for Koalby. First, the torso was redesigned to fit on the Elegoo Saturn resin print bed; the torso handle from Poppy was removed, as shown in Figure 2.3a and 2.3b

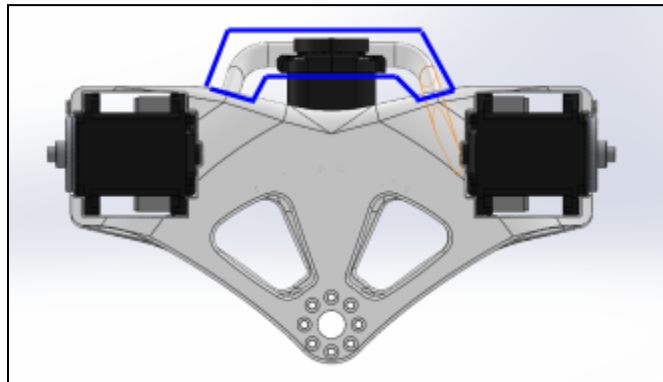


Figure 2.3a: Original Poppy Chest Piece with Handle reproduced as is from [3]

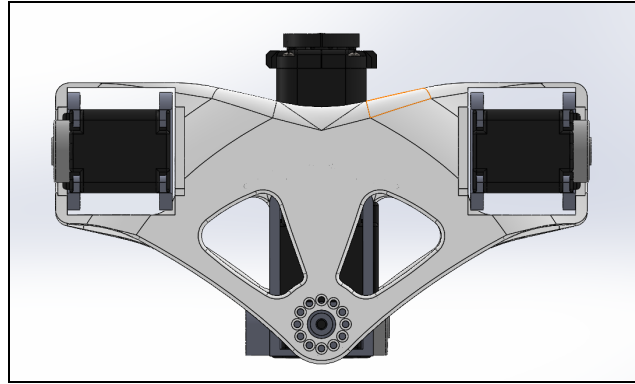


Figure 2.3b: Koalby Redesign to Fit on Print Bed reproduced as is from [3]

Koalby differs from Poppy in that the power is supplied by onboard batteries, rather than being plugged into a wall. This feature required design changes to store the batteries within Koalby. It was decided to store the batteries in the shin since it had a cavity large enough to accommodate the LiPo battery. This location of the batteries kept the center of mass around the lower chest, ideally closer to the ground. The thigh motors, Dynamixel MX-64AT with a stall torque of 6Nm, were calculated to be strong enough to lift the legs with batteries in the shins. To fit the batteries, the shin was made 30mm taller and 19mm longer (front to back), and the bottom of the thigh was lengthened by 8.48mm, and brought 5.29mm lower, so that it properly interacted with the redesigned shin. This design did not fit on the DLP printer so this was split into two pieces, as shown in Figure 2.3c.

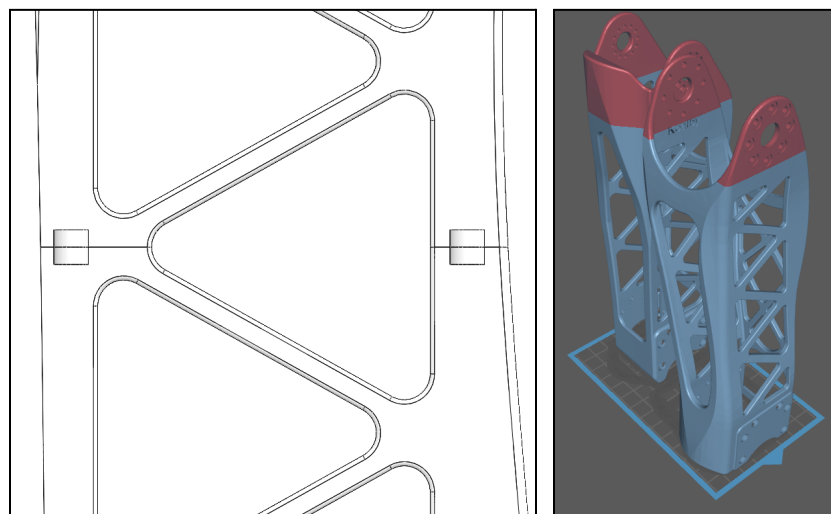


Figure 2.3c: Two Part Shin Redesign reproduced as is from [3]

A battery holding platform and upper stop were added to the shin to keep the battery from interfering with the motors, as shown in Figure 2.3d.

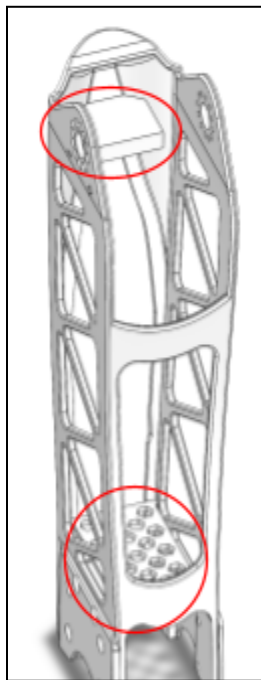


Figure 2.3d: Shin Platforms to Store Battery

The longer shin now restricts the ankle joint's upward motion. Restricting elevation from the intended 30° to 10° . This was improved by redesigning the bottom of the shin and top of the ankle to decrease interference and in the foot's range of motion, as shown in Figure 2.3e.

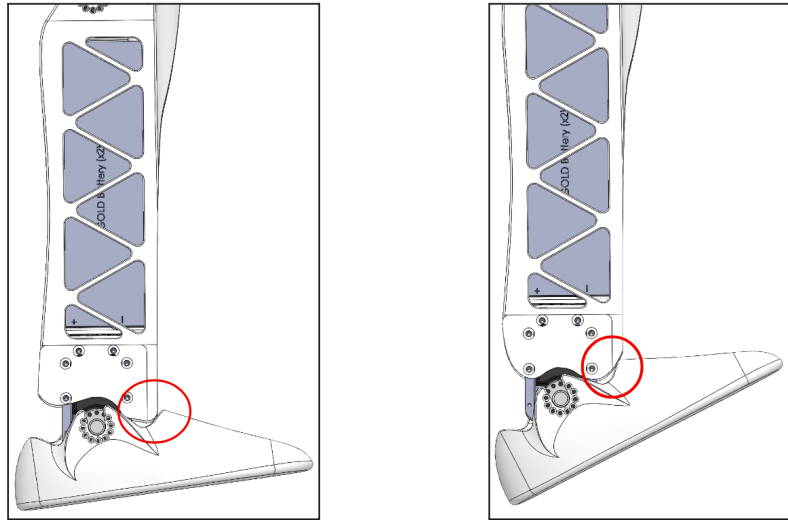


Figure 2.3e: Foot Range of Motion Redesign, original (left) and redesign (right) reproduced as is from [3]

2.4 Actuators

To reduce cost of Koalby, the Dynamixel MX-28 motors used in the Poppy project were swapped for the cheaper HerkuleX DRS-0201. As of last year's team's work, the motors used in Koalby are two Dynamixel AX-12 motors in the neck, four Dynamixel MX-64AT motors in the abdomen and hips, and 19 HerkuleX DRS-0201 motors throughout the limbs which is shown in Figure 2.4a. This differs from the original Poppy project which had Dynamixel MX-28AT motors throughout the body. All 19 of the Dynamixel MX-28 motors were replaced with the HerkuleX DRS-0201 reducing the total cost by ~\$2500. The motor comparison between Dynamixel MX-28AT and HerkuleX DRS-0201 are shown in Table 2.4a.

Table 2.4a: Comparing Dynamixel MX-28 and HerkuleX DRS-0201 Motors

Motor	Cost	Stall Torque (Nm)	No load speed (RPM)	Form Factor (mm)
Dynamixel MX-28	\$260	2.5	55	32 x 50 x 40
HerkuleX DRS-0201	\$132	2.35	68	24.0 x 45 x 31

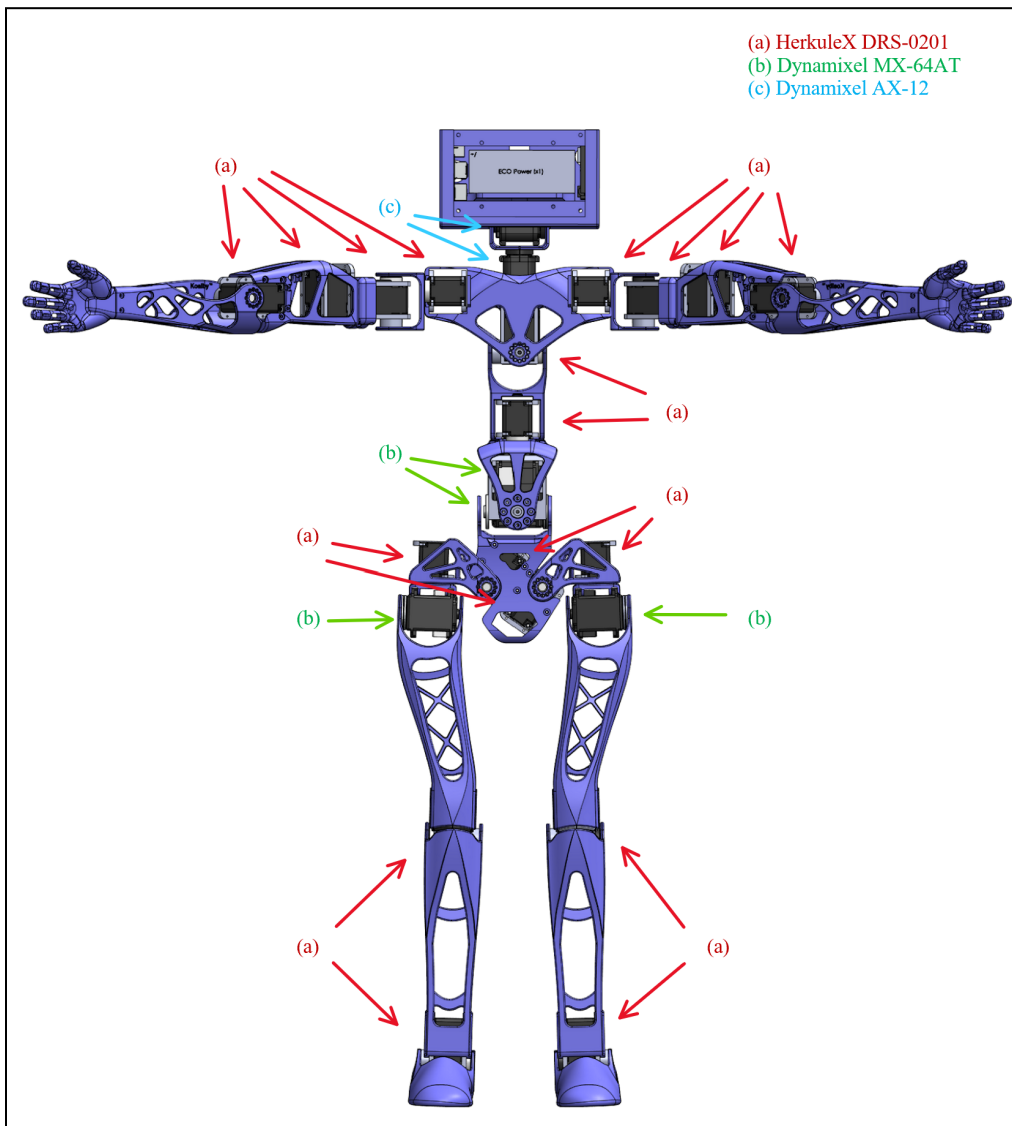


Figure 2.4a: 25 Motors in Koalby

The HerkuleX DRS-0201 motors (24.0 x 45 x 31 [mm]) are significantly thinner and slightly smaller than the MX-28 motors (32 x 50 x 40 [mm]) in most other dimensions. This meant they fit in the space previously filled by MX-28 motors, but their mounting holes do not align with the existing mounting points. A motor adapter was designed and printed to realign the mounting holes, and a spacer was designed to allow the HerkuleX motors to fit in the spaces originally designed for Dynamixel motors. Figure 2.4b shows the original two horn Dynamixel

MX-28, and Figure 2.4c shows the HerkuleX DRS-0201 motors with the motor adapter prints attached.

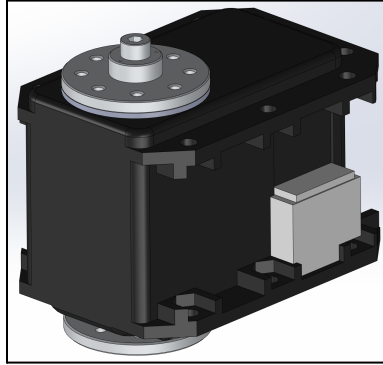


Figure 2.4b: Two Horn Dynamixel MX-28
Motor reproduced as is from [3]

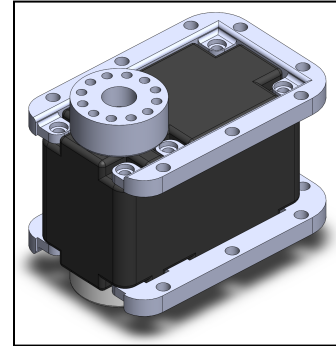


Figure 2.4c: HerkuleX DRS-0201 Motor
CAD with the Motor Adapter Prints Attached
reproduced as is from [3]

Next, a middle linking piece was created to connect the HerkuleX DRS-0201 motors to link to motors together to accomplish the original functionality allowing for rotation on two separate axes. Figure 2.4d shows the assembly of the original and new abdomen assemblies. The piece where the spacer is mounted is positioned to give a 2.5mm buffer for a screw to be mounted without scraping the motor itself. Figure 2.4e shows where this abdomen assembly fits into the torso on Koalby.

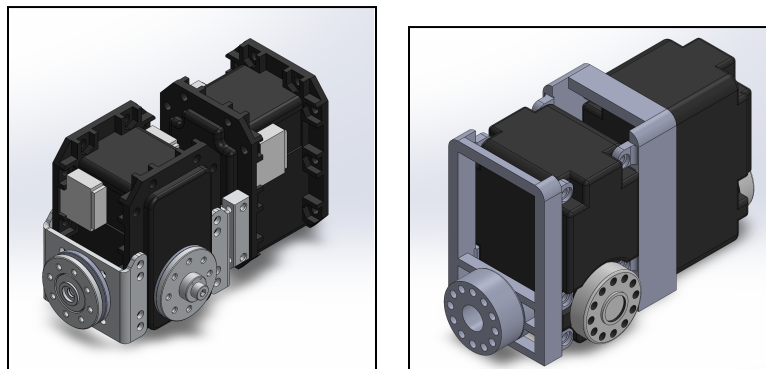


Figure 2.4d: Comparison of original Dynamixel double rotation assembly (left) and the
HerkuleX version (right) reproduced as is from [3]

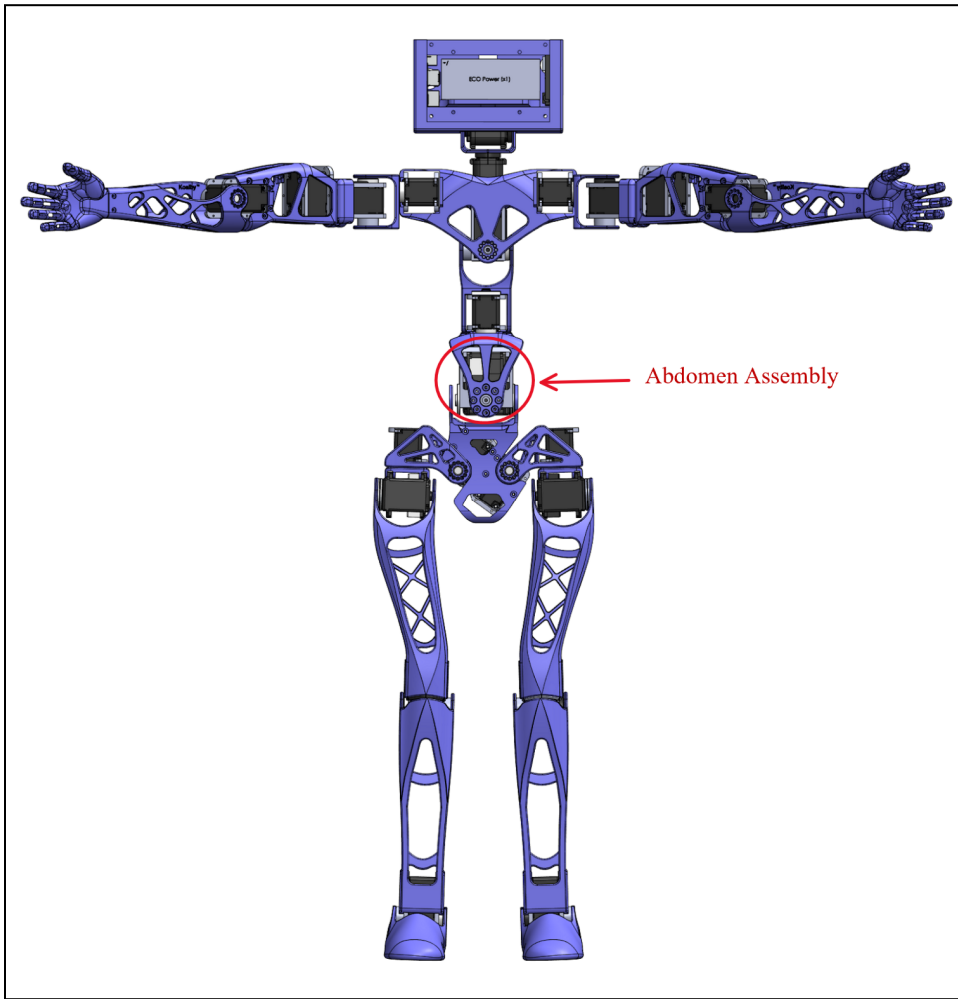


Figure 2.4e: Abdomen Assembly in Koalby

Also, the servo horn patterns were redesigned from an 8-hole design to a 12-hole design to accommodate the motor change from Dynamixel to HerkuleX, as shown in figure 2.4f.

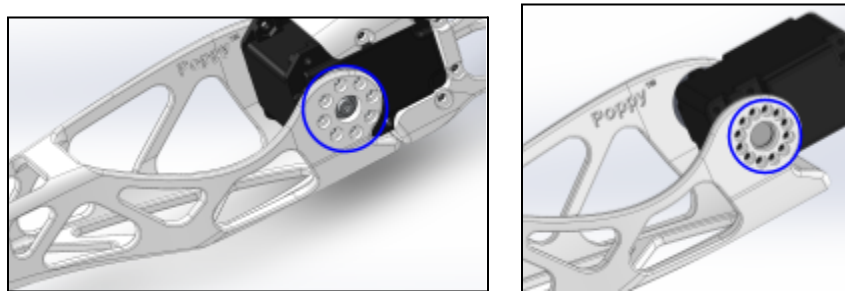


Figure 2.4f: Comparison of original Dynamixel servo horn hole pattern (left) and the HerkuleX version (right) reproduced as is from [3]

Minimal changes were made to the pelvis design; the motor mounting holes at the hip joint were moved so the motors are at the same height, as shown in Figure 2.4g.

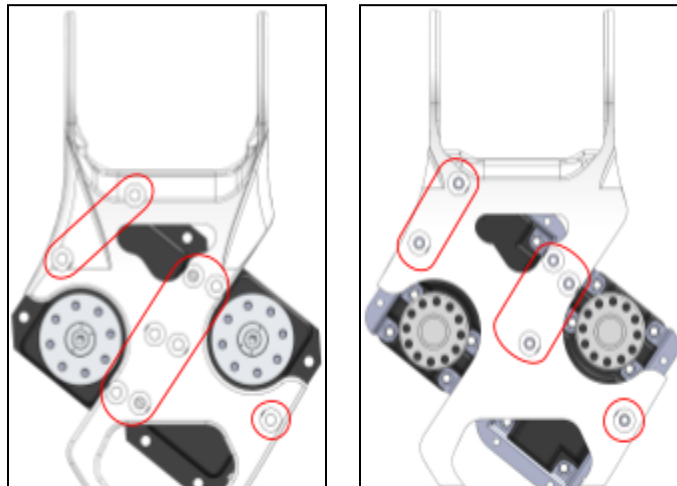


Figure 2.4g: Original Pelvis Assembly (left) and Modified Pelvis Assembly (right) reproduced as is from [3]

2.5 Electrical

Koalby differs from Poppy in that the power is supplied by onboard batteries rather than being plugged into a wall outlet [3]. The control wiring runs signals to the Arduino from the separate HerkuleX and Dynamixel bus systems. Koalby was powered with two 7.4V batteries and one 11.1V lithium polymer battery. The two 7.4V batteries have a capacity of 5200mAh and contain two cells. Figure 2.5a shows where the 7.4V batteries are stored in Koalby's shins. The third 11.1V battery has a capacity of 2200 mAh with three cells. Figure 2.5b shows where the 11.1V battery is stored in Koalby's head. The two 7.4V batteries were placed in parallel to power the Herkluex motors (which can run on anywhere from 6-9V), a Raspberry Pi 3 and an Arduino Mega. The Arduino Mega has an integrated voltage regulator, so it can be powered directly from the 7.4V batteries. The Raspberry Pi does not have a voltage regulator, so a LM7805CV linear voltage regulator (which supplies up to 1.8A) was used to power the Raspberry Pi, which needs

1.6A to operate. The third 11.1V battery was used to power the Dynamixel motors and Dynamixel Shield.

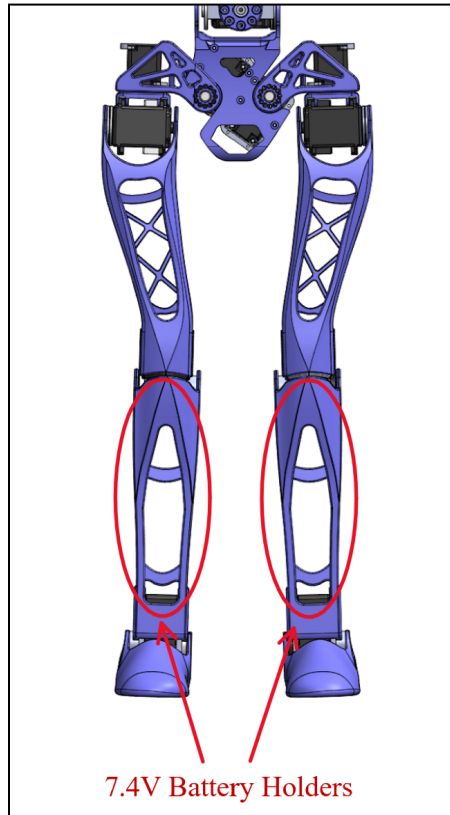


Figure 2.5a: 7.4V Batteries in Koalby's Legs

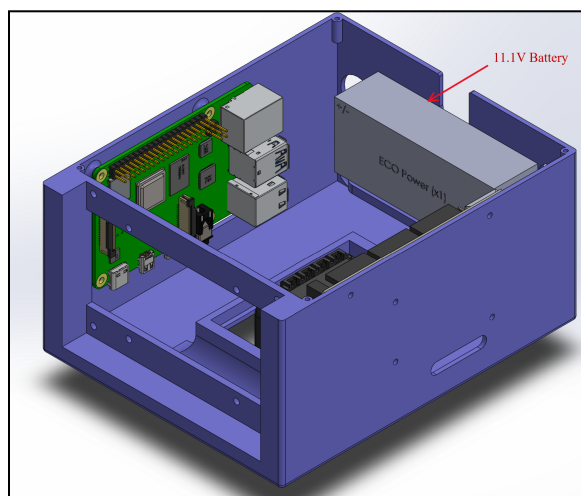


Figure 2.5b: 11.1V Battery in Koalby's Head

The Poppy robot connected the Dynamixel motors directly to the Raspberry Pi via a custom built PCB; this custom PCB connected directly to the GPIO pins of the board [3]. This board was not available in the US and the HerkuleX motors used a different four wire bus standard than the three wire Dynamixel setup [3]. Therefore, an Arduino Mega was used in Koalby to replace the smaller adapter board. The HerkuleX motors can be controlled directly by the Arduino, while the Dynamixel motors require an additional shield, a Dynamixel Motor Shield. Figure 2.5c shows the electronics setup of Koalby, as previously described.

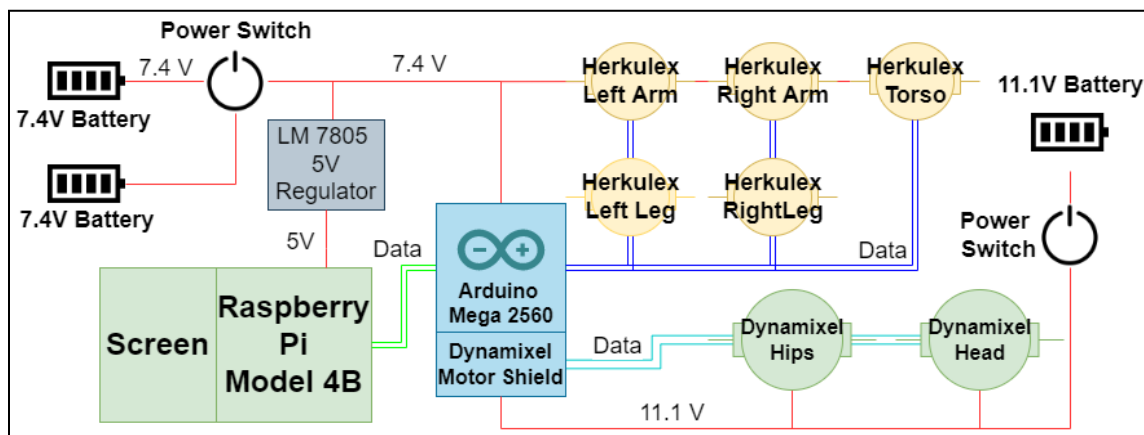


Figure 2.5c: Koalby Electronics Setup reproduced as if from [3]

Serial communication between the Arduino and Raspberry Pi was accomplished via a USB-serial adapter. This was necessary because the Arduino uses the serial pins for the USB port. The adapter connected pins from the Raspberry Pi's USB port to the Serial2 pins of the Arduino. Figure 2.5d shows Koalby's serial port usage.

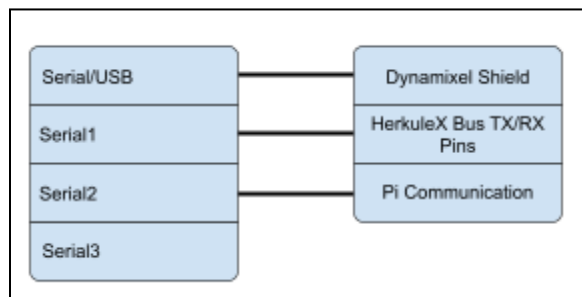


Figure 2.5d: Serial Port Usage of Koalby reproduced as is from [3]

2.6 Achievements

The 2022 3D Printed Humanoid Robot MQP team successfully accomplished the goals put forth by its team. Koalby demonstrated the ability to build an open source robot. Motor changes were made to successfully decrease the cost by ~\$2,500. These motor changes were integrated into the previous design with the aid of a motor mount to fit the old style of motors. With the addition of internal batteries, Koalby can operate untethered from an external power source allowing for a wider range of functions. Basic actions, like shaking hands and waving, were successfully recorded with the ability to be replayed. These actions were successfully demonstrated at the TouchTomorrow and WPI Project Presentation Day events.

2.7 Recommendations

The 2022 3D Printed Humanoid Robot MQP Team made recommendations for the continuation of this project. Firstly, they proposed expanding the gripper design or creating a new one. The team also suggested redesigning the robot to minimize the number of printed parts. The team also noted that the batteries in Koalby's shin were harder to access and recommended finding an easier port to reach the batteries. It was also recommended to reevaluate the motors to determine if all of them remain the best choice. In order to aid with stable motion, the team recommended adding sensors such as an IMU.

3.0 2022 MQP Testing

After receiving Koalby, the team noted several observations about its condition and components as shown in Figure 3a. The pelvis was broken at the start of the project (shown in Figures 3b), with multiple breaks at the motor connection as well as in the back, where the switch was located. While the 2023 3D Printed Humanoid Robot Software MQP Team began to actuate the robot, to test motion, the pelvis continued to break in these same spots. The abdomen, thigh, and hip also broke at the respective motor connection points. The team conducted an inventory of the printed and leftover parts (see Appendix A) and inspected all previous components to identify design problems. (see Appendix A).



Figure 3.0a: Initial Condition of Koalby



Figure 3b: Broken Pelvis

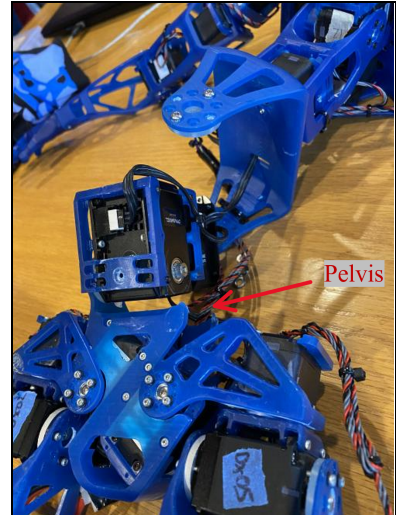


Figure 3c: Broken Pelvis and Abdomen

One significant problem was the lack of proper wire management which caused tangling and restricted the motion in the limbs. The torso also lacked real stability, as it is composed of multiple smaller pieces without extra support. There were also the motor connections that seemed problematic. A motor movement document (see Appendix C) was created to understand the axes and range of motion of each motor. This document was also used to note any problematic areas such as broken connections and poor wire management. The biggest one was the use of motor mounts since these were not always effective and did not hold the part properly. The Spine part showed bowing outward at the bottom due to this issue. The head needed rework to fit any sensors or cameras. The same for the forearm, since it was not big enough to fit a proper gripping hand.

4.0 Literature Review

Our literature review was conducted on humanoid robot applications, grip designs, sensor types, and spines. These topic summaries can be found below in Sections 4.1- 4.5 respectively.

4.1 Humanoid Robot Application Research

In order to have a clear objective for this project, current humanoid robot applications needed to be explored. Some of these applications included medicine, industry, service, space exploration, and outreach. In order to understand the potential applications within these industries, various humanoid robots were examined (see Table 4.1). Photos of each Humanoid Robot are in Appendix B.

Table 4.1: Humanoid Robot Application Examples

Industrial Field	Service / Medical	Space	Outreach/Interaction
Digit (Ford Agility Robotics)	T-HR3 (Toyota) - mobility service	Vyammitra	Sophia (Hanson Robotics) - human/robot interaction
Nextage (Kawada Robotics)	Kime (Macco Robotics) - bartender	Fedar	Surena Robot (Iranian U) - inspire students
	Robothespian - actor	Robonaut 2 (NASA)	
	Smart Field Hospital	Valkyrie (NASA)	

In the industrial field, humanoid robots have been used to assist in warehouse management and maintain production for manufacturing companies. For example, Digit, created by Agility Robotics, was incorporated into a factory setting by Ford [4]. Digit is a headless humanoid robot that can navigate stairs, obstacles, varied terrains, balance on one foot, pick up

and stack boxes weighing up to 40 pounds, and fold itself for compact storage. The future application envisioned for Digit is to assist in package deliveries; Digit would ride in a driverless car and deliver packages to customers, automating the entire delivery process. A second example of humanoid robots used in industry is Nextage by Kawada Robotics [5]. Nextage was developed to perform maintenance tasks alongside human workers in industrial settings. This robot was designed as only a torso with two 6 DOF arms for high functionality in process management and object manipulation [6].

Humanoid robots have also been designed for acts of service ranging from medical aid to bartending and entertainment. In the medical field, humanoid robots have been used at the Smart Field Hospital in Wuhan, China. This usage started in March 2020 during the COVID-19 pandemic [6]. During such times, humanoid robots could relieve overworked nurses to do basic cleaning and delivery tasks. These robots are also being used as medical assistants to disinfect surfaces, measure temperatures, deliver food and medicine, and entertain medical staff and patients. Additionally, the T-HR3 by Toyota was designed to provide service and skills, such as surgery, while operated by a person located elsewhere. This humanoid robot can mimic the movements of its human operators and walk. [6].

Kime by Macco Robotics was designed to be a food and beverage serving robot with a human-like head, torso, and arms. Kime was tested at gas stations throughout Europe and in a Spanish brewery; this robot can serve up to 300 glasses per hour and has 14-20 degrees of freedom, smart sensors, and uses machine learning to improve its skills [7]. For entertainment, Robothespian is a robot actor that comes with a library of impressions, greetings, songs, and gestures [6]. Multiple Robothespians can be incorporated to become a robotics theater with movement tracks, animation software, touchscreen control, lighting, and sound.

Furthermore, several humanoid robots have been developed for space exploration research, termed “robonauts”. Two key examples developed by NASA include Robonaut 2 and Valkyrie. Robonaut 2 successfully traveled to space and spent seven years on the International Space Station [6]. Valkyrie is a more recent robonaut designed to withstand harsh environments similar to those on the moon and Mars [6]. Developed by the Indian Space Research Organization, Vyommitra, another humanoid robot, was intended to conduct microgravity experiments to help prepare future crewed missions [8]. Lastly, Fedar by Final Experimental Demonstration Object Research was a Russian remote-controlled humanoid that flew to the

International Space Station in 2019 [6]. Fedar simulated repairs during a spacewalk and later returned to Earth.

Humanoid robots have also been developed for research and collaborative purposes. Sophia, by Hanson Robotics, is a social humanoid robot who serves as a robotic ambassador to advance research related to robotics and human-robot interactions [9]. Sophia can move, talk, show some emotions, draw, and sing. Additionally, Surena Robot by Iranian University of Tehran is an adult-sized humanoid robot capable of face and object detection, speech recognition and generation, and can walk with a speed of 0.7 km/hr [10]. Surena has 43 DOF and hands that can grip different shapes. It is currently being used to research bipedal locomotion, artificial intelligence, and for outreach to attract students to careers in engineering.

Overall, this research showed the various humanoid robot applications that are currently being explored including industry, service, and outreach. Based upon this, our team decided to focus our application towards service as a lab assistant. This is because service applications have positive broader and societal impacts and humanoid robots in lab settings are currently less explored compared to factory and medical settings.

4.2 Actuated Grips

With the desire to create a humanoid robot that would act as a supply room assistant, we needed a type of grip that would give the robot the ability to lift a variety of objects. The 2022 MQP [3] created a 2-finger grip located in Figure 4.2a. This type of grip was a good starting point; however, it lacked the ability to lift complicated objects. Since the grip only had 2-fingers, it did not have enough strength or versatility. For the purpose of a lab assistant, the grip struggled to lift objects that were flat like a wrench. We wanted to investigate ways to improve this grip.



Figure 4.2a: 2022 MQP Grip reproduced as is from [3]

Finding the perfect grip would determine how effective the robot would be in a role as a supply room assistant. We imagined in this particular role, certain objects needed to be lifted like an adjustable wrench, a vice grip, a battery, a mallet, and much more. We have a more in-depth list of these various objects in Section 8.1.

When looking for the best grip, we took into consideration the following: the size of the grip, the weight of grip, the number of actuators needed, the accessibility of attaching/detaching, and the various shapes the grip could lift. More information on these factors can be located in Section 8.2. For our humanoid robot, we focused on researching jamming grips and 3-finger actuated grips.

4.2.1 Jamming Grip

The jamming grip method utilizes pneumatics to lift objects, and it consists of an elastic ball filled with a granular material [11]. The granular material, which could be any material with a consistency of something like coffee grinds, is used to fill the ball. A granular material allows for the ball to take any shape, essentially creating flexibility. The ball is made out of a nonporous elastic bag, a material similar to a balloon, in order to be strong enough to not rip upon contact with an object while remaining elastic enough to conform to any object that the robot may wish to pick up [11]. When the gripper approaches an object, a compressed air tank connected to the ball via a tube removes all the air from the ball, forming a vacuum and allowing it to attach to the desired object. As such, it does not matter what shape the object is, because the ball adjusts itself to that object. Figure 4.2.1a shows how the jamming grip picks up a complex shape like a jack but also something as fragile as an egg.

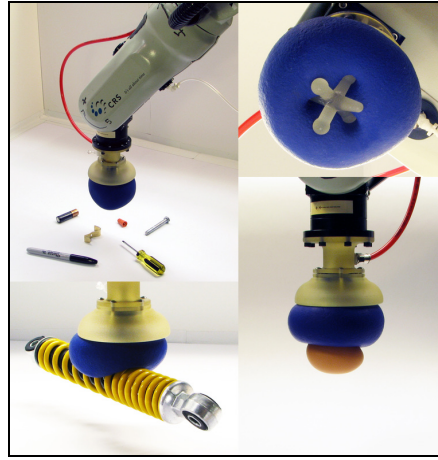


Figure 4.2.1a: Jamming Gripper reproduced as is from [12]

A jamming grip has more versatility because there are no limitations as to what it can or cannot grab. It can pick up something as small as a penny or as big as a wrench. In order to implement the jamming grip, we would have to find the proper pressure needed to pick up the objects listed in Figure 4.2.1a. Knowing the correct pressure would allow us to find the correct tank size.

Due to its seemingly infinite degrees of freedom, the jamming grip can be seen as a beneficial gripping mechanism. However, there are some areas of concern. Due to pneumatic tanks weighing $\sim 3.8\text{kg}$, this grip may be too heavy for our 3D printed robot to support. Additionally, running air tubes through the robot may complicate the overall wiring, and a ball-shaped hand filled with coffee grinds would take away from the humanoid aspect.

4.2.2 Actuated Finger Grip Research

There are several different types of 3-point grips. A 3-point grip tends to be 3 fingers that are either equidistant from one another or slightly askew as shown in Figure 4.2.2b. Depending on the grip model, some fingers can wrap around an object producing an encompassing grip, while other fingers will remain straight and pinch an object with tips to lift it [13]. Figure 4.2.2a below shows an encompassing grip in comparison to the fingertip grip.

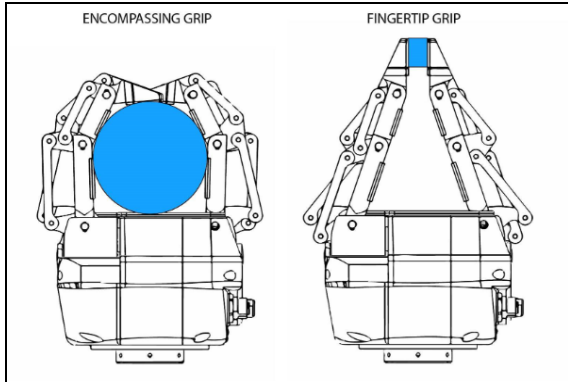


Figure 4.2.2a: Type of grasp reproduced as is from [13]

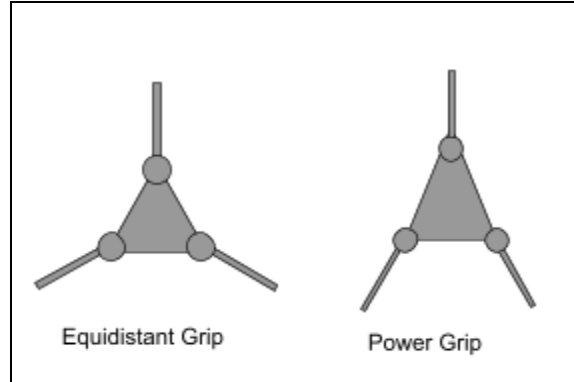
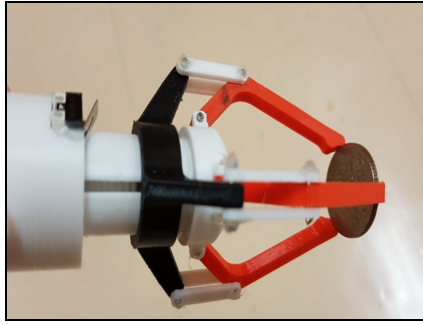


Figure 4.2.2b: Grip finger distance

Type 1

One of the first 3-finger grips we looked at was The Claw shown in Figures 4.2.2c and 4.2.2d [14]. This grip uses a N20 DC motor that moves a worm gear in the center. As the gear moves up and down, the ‘fingers’ will close to pick up an item or widen to release. The largest finger component, which is measured to be 30mm, has a bend which allows it to surround the item it is trying to pick up. This component moves along a pin to create the grip motion. The smaller pieces that make up the grip are held together by screws. The smaller pieces move with the motor, and they are connected to the larger component to assist with the movement. This grip method is considered to be the most simple option and the design is more human-like compared to the jamming grip as it has three “fingers”. However, the surface area of the grip is not as wide, which limits what the grip is able to lift. Additionally, since the “fingers” are equidistant, it may be hard to pick up certain objects. For example, this grip can grab a cylindrical shape from the top, given that the bottom is not too heavy, but not the side of the cylinder because there would be a finger preventing it.



Figures 4.2.2c: The Claw reproduced as is from [14]

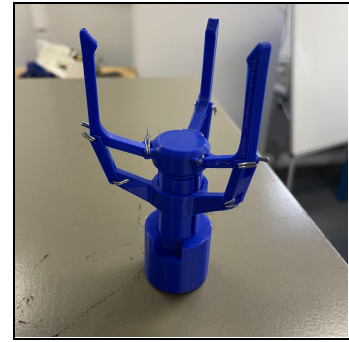


Figure 4.2.2d: Our printed prototype of The Claw

Type 2

The next grip we researched was the Underactuated Robotic Grip by ALARIS [15]. This grip is a mechanical linkage system for fingers with an underactuated worm wheel gear transmission. The servo actuator, a Dynamixel MX-28 servo motor, is connected to “two phalanges, two links, an extension spring and a worm wheel” [15]. The worm gear ensures simultaneous movement between all fingers creating uniformity since there is one pivot point for all of the fingers. Meanwhile, the gear train transmission system allows for alternate torque and speed depending on the need of the grip. The fingers are 3D-printed out of ABS (Acrylonitrile Butadiene Styrene) and each finger has 2 degrees of freedom. Figures 4.2.2e-4.2.2h show the design of this grip, more specifically Figure 4.2.2g shows an in depth assembly of the grip. The fingers move as individual rigid bodies; phalanx 1 of the fingers engages in contact with the item being lifted while phalanx 2 is engaged with a pivot point to allow for a full encompassing movement of the grip [15]. This grip is able to grab cylindrical and spherical shapes. Similar to the Type 1 grip, it has an equidistant grip. However, this grip has a greater surface area and uses a stronger motor.



Figure 4.2.2e: ALARIS finger design reproduced as is from [15]

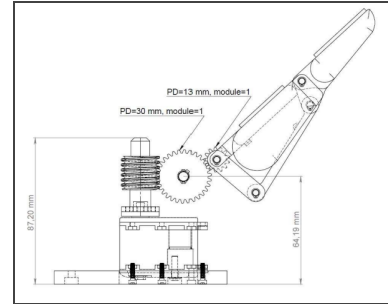


Figure 4.2.2f: Blueprint of ALARIS finger design with motor reproduced as is from [15]

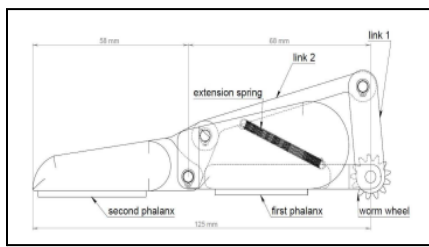


Figure 4.2.2g: Blueprint of ALARIS finger design reproduced as is from [15]

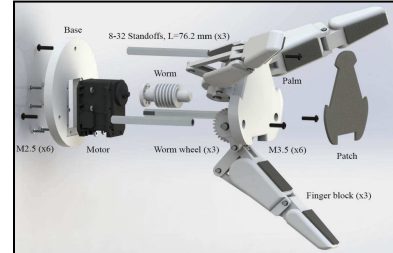


Figure 4.2.2h: Full ALARIS grip design reproduced as is from [15]

Type 3

Finally, we looked into the The Yale OpenHand Project [16]. The Yale OpenHand Project is working towards advancing “the design and use of robotic hands designed and built through rapid-prototyping techniques in order to encourage more variation and innovation in mechanical hardware” [16]. Of the many robotic hands designed through The Yale OpenHand Project, we focused on the Model O design. The Model O design has two possible design options which both use four Dynamixel XM430-W350-R motors, and torsional springs at the base of the palm to help move the 3D-printed fingers. One option for the Model O is to have a pivot-pivot connection in the joint of the finger. This method uses a pin to attach the two links of the fingers and includes an extension spring to create the underactuated design that would help in the bending of the fingers when it comes in contact to grasp the object.. Option 2 for Model O is to

have a pivot-flexure connection for the joint of the fingers. The flexure is made of urethanes which allows for a “a monolithic component and exhibits a greater degree of adaptability and robustness to collisions due to the joints’ out-of-plane compliance” [16]. This flexure is a resin piece placed between two links of the fingers shown in Figure 4.2.2i. The flexure allows for more adaptability compared to the pivot-pivot option.

The layout of the Model O fingers resembles “a thumb and two opposing fingers” creating more of an isosceles triangle look. This design is the best for a human-like quality as it has a thumb shown in Figure 4.2.2j.

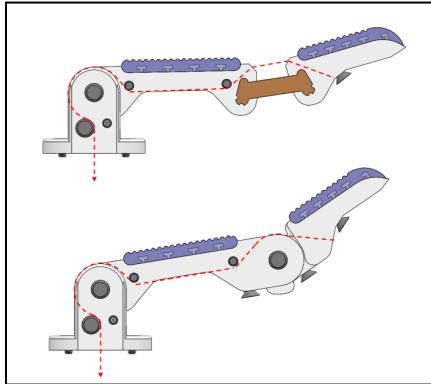


Figure 4.2.2i: Model O’s various pivot connections reproduced as is from [16]

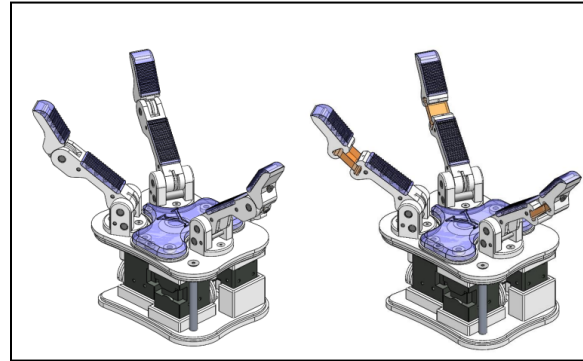


Figure 4.2.2j: Model O grip orientation reproduced as is from [16]

4.3 Electrical Components

Robots must have the ability to sense their surroundings in order to successfully walk and relocate objects. This can be done by implementing a camera as well as a series of sensors that can measure distance, force, orientation and acceleration.

For example, distance sensors such as Ultrasonic sensors (Figure 4.3a), Infrared (IR) sensors (Figure 4.3b), and LiDAR sensors (Figure 4.3c), can be used to tell the robots how close they are to objects that surround them as they traverse through their environment, while force or pressure sensors on their grippers can tell them whether or not they have successfully grabbed an object.



Figure 4.3a: Ultrasonic sensor reproduced as is from [17]



Figure 4.3b: Infrared transmitter (white) and receiver (black) reproduced as is from [18]



Figure 4.3c: LiDAR sensor reproduced as is from [19]

Of the distance sensors mentioned, IR sensors, which use infrared light to detect objects (Figure 4.3d), are less reliable, and have the shortest maximum measurement length. Meanwhile, ultrasonic sensors, which use sonic waves to detect objects (Figure 4.3e), are not only more reliable, but also have the ability to accurately detect a larger range of materials compared to the IR sensors and have a longer maximum measurement range [20]. However, the LiDAR sensor, which uses laser pulses to detect objects (Figure 4.3f), was found to be the most reliable and versatile as it can measure 3D structures without being inhibited by light interference. Additionally, they tend to have a greater measurement distance than that of the ultrasonic [21]. Although the LiDAR is larger than the other two distance sensors, it is still small enough that it can be attached to a variety of areas on the robot such as the ankles, torso, or head. By attaching it to the ankles, the robots will be able to determine whether or not they are about to kick their

foot into something. Meanwhile placing them in the torso or head will allow the robots to gauge how close they are to an object and whether or not they can move in that direction without hitting anything.

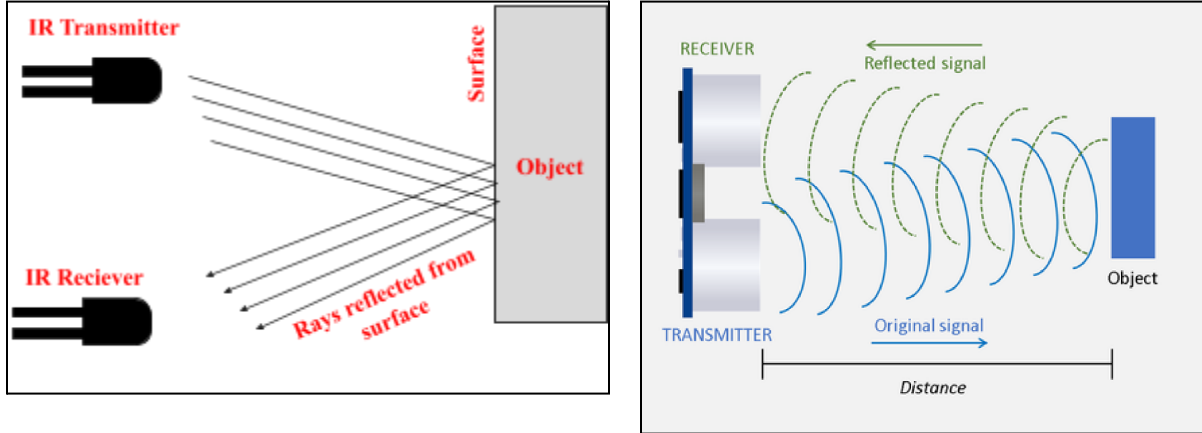


Figure 4.3d: Diagram of IR sensor functionality

Figure 4.3e: Diagram of ultrasonic sensor functionality reproduced as is from [22]

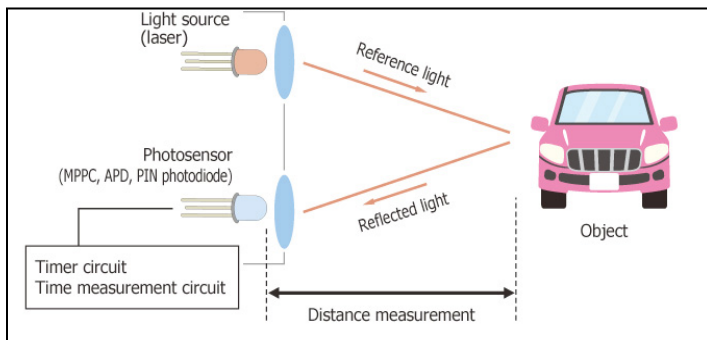


Figure 4.3f: Diagram of LiDAR sensor functionality reproduced as is from [23]

When looking into sensors that could communicate to the robots that they were holding an object, pressure and force sensors stood out the most. For instance, pressure sensors measure the amount of force applied to an area on the robot [24]. Meanwhile, force sensors measure both linear and rotational forces applied to an area on the robot [25]. Although similar in performance, force sensors allow for more versatility in their applications and come in a variety of different geometric shapes, which is ideal when working with robots with limited attachment space.

Additionally, force sensors (shown in Figures 4.3g and 4.3h) are reliable, accurate, and cost effective.

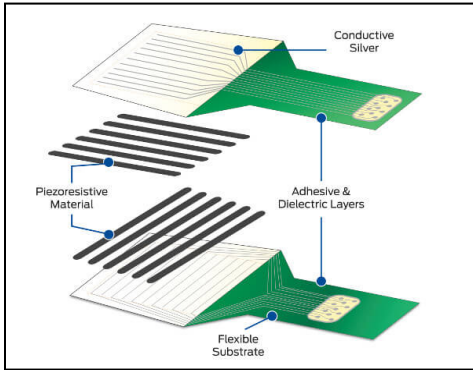


Figure 4.3g: Diagram of pressure sensor functionality reproduced as is from [26]

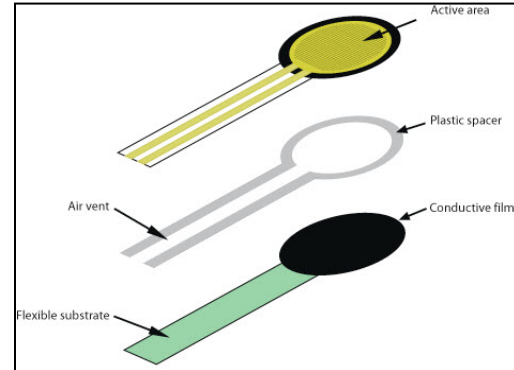


Figure 4.3h: Diagram of force sensor functionality reproduced as is from [27]

Alongside the distance and force sensors, an inertial measurement unit (IMU) can help the robots maintain balance and stability while they move due to the built in 3-axis gyroscope and accelerometer (shown in Figure 4.3i). Although some IMU's come with built-in magnetometers or even barometers, these extra functions would not be necessary for our project.

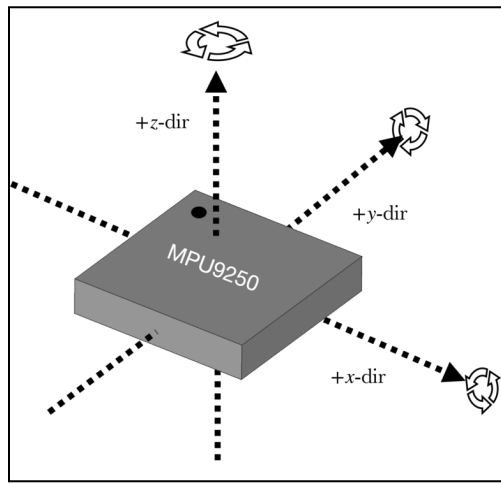


Figure 4.3i: Diagram of an IMU's 3-axis gyroscope and accelerometer reproduced as is from [28]

Lastly, in order for the robots to pick up objects, they not only need to confirm that they are holding an object, but also know what the object looks like and where it is located. This can be done with the use of a camera with AI object detection. Utilizing this method, we would be able to train the robots to recognize specific objects and inform them of where to send their gripper to pick the objects up. However, this camera would have to easily fit within the head of the robot since the head is the most independently movable body part and best emulates human anatomy.

Electromagnets

Unlike traditional magnets, electromagnets can be turned on and off by controlling the flow of electricity through a coiled wire. When electricity is present, this coil creates a magnetic field which enables the electromagnet to function as a traditional magnet. However, when the electricity is cut off, it no longer performs like a magnet [29]. This type of magnet is ideal when you do not wish to have a magnet that is constantly active.

4.4 Exoskeleton

Exoskeletons offer important structural support for human motion. They are used to decrease pain for the user and to increase their efficiency as well. This is done by decreasing the load on the body. During the motion of picking up an object, the lower back region carries the largest load. Relieving this stress is a major focus on the design of exoskeletons.

There are two styles of exoskeletons: rigid and soft [30]. Rigid exoskeletons transmit both tensile and compressive forces, whereas soft exoskeletons only impact compressive forces. A common style for a rigid design is based around the waist. It is attached to the torso and thigh, rotating about the pelvis (Figure 4.4a). One of the early pioneers for soft exoskeletons was the Personal Lift Augmentation Device (PLAD) [31]. This design uses ropes and braces connected throughout the body (Figure 4.4b). Another design is the Passive SPEXOR prototype [30].

One of the key design focuses to consider is the likelihood of misaligned joints. If the exoskeleton does not align with the human's movements, it can create parasitic forces and torques. The SPEXOR prototype uses a flexible rod connected to a linear slider and ball joint to minimize the parasitic forces while still being able to output 36 Nm [30]. The added support to

normal human actions may prove beneficial to more complex humanoid robots. This is applicable to humanoid robots since the motion being enacted is similar to that of a human.

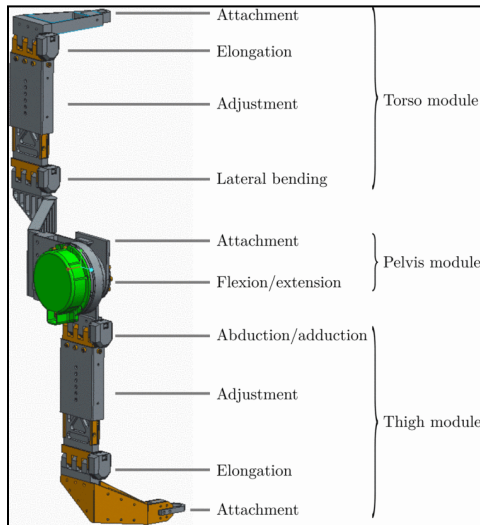


Figure 4.4a: Rigid Style Exoskeleton reproduced as is from [32]

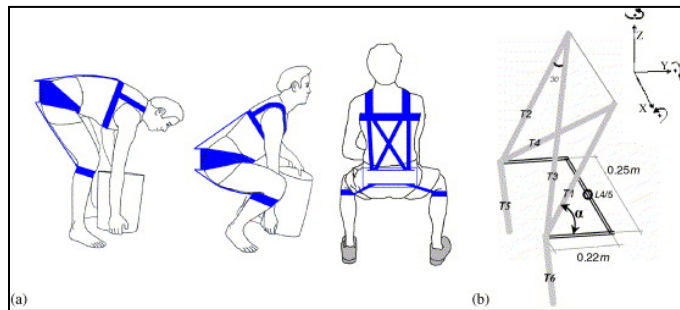


Figure 4.4b Personal Lift Augmentation Device reproduced as is from [31]

4.5 Printing

Similar to Koalby, Ava was designed to be manufactured using 3D printing so she could be an open source 3D printed humanoid robot. To do this, two different methods of 3D printing were utilized for both prototyping and final manufacturing. These methods included Fused Deposition Modeling (FDM) and Digital Light Processing (DLP). FDM is a 3D printing technique that employs a thermoplastic continuous filament. This filament is fed from a large spool and deposited on the growing work by a moving, heated printer extruder head. On the other hand, DLP printing technology makes use of liquid photopolymer resin that can cure solidified layers onto a print bed when exposed to the light of an LCD screen.

4.5.1 FDM Printing

For preliminary testing, polylactic acid (PLA) filament on FDM 3D printers was used. Compared to other filament types, Polylactic Acid (PLA) is more rigid and has a tensile modulus of 3600 MPa. This type of printing is more suitable for parts under less stress or load. For FDM printing the Creality Ender 3 Pro and the Prusa MK3S+ were utilized as seen in the figure below [33].

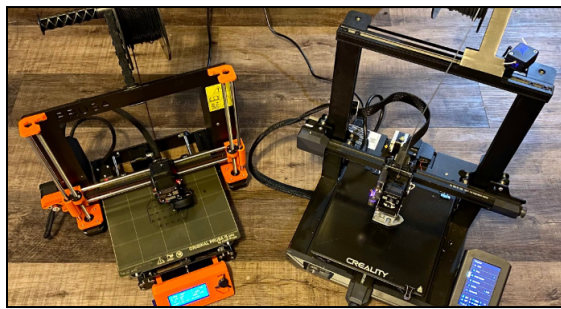


Figure 4.5.1a: FDM Printers

4.5.2 Resin Printing

Given its material properties and precision, DLP t was used to print the majority of Ava. For DLP printing, two resin printers were utilized; the Elegoo Mars2 Pro 2, as seen in the figure below, with the print area of 129 x 80 x 160 mm and the Elegoo Saturn with a print area of 192 x 120 x 200 mm. The Elegoo Mars 2 Pro printer was capable of printing most of the parts for the humanoid robot; however for parts exceeding the print area - the torso, legs, and shins - the larger Saturn printer was used. The printer setup can be seen in the figure below.

Depending on the situation, DLP may be a better choice when looking to reduce product development time, de-risk manufacturing operations, and create a unique model design due to its faster speed, better surface finishing, and isotropic material properties. Using an LCD screen instead of an FDM printer allows for much higher resolution parts to be created, as well as the creation of an entire layer at the same time.

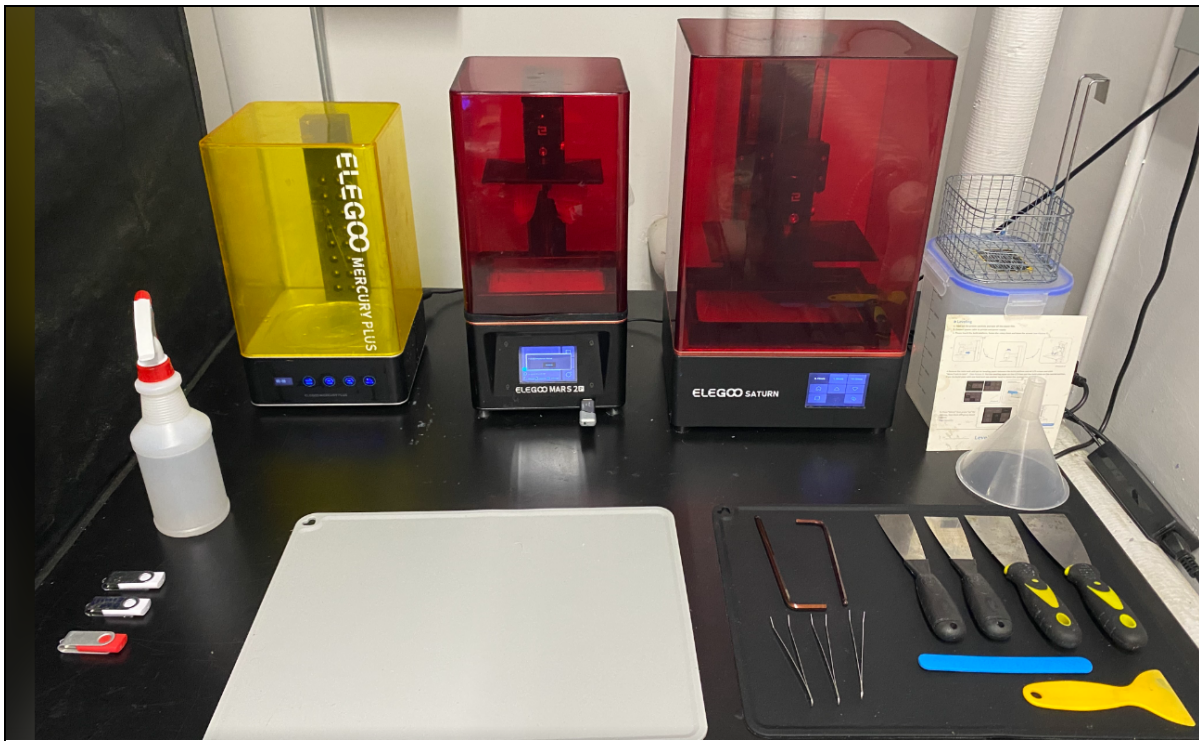


Figure 4.5.2a: Resin Printers Setup

5.0 Project Goal

Our mission was to create Ava, an open source, 3D-printed, humanoid robot that would act as a lab assistant with a focus on lifting objects and assisted walking via pushing a cart. The Koalby Project gave us a starting point of a humanoid robot with a 2-finger grip while our research taught us more about the different applications of a humanoid robot. To achieve our goal of a humanoid robot lab assistant, we needed to implement design changes that can be divided into 4 key categories: structural integrity, walking, gripping addition, and standardizing components.

Redesigning for structural integrity meant modifying parts, so they can withstand the new forces and weights acting on the robot; we were tasked with improving the strength of the robot. Modifications made to the robot for structural integrity are explained in Section 7.0.

For walking, new electrical components were required, so the robot could see its surroundings. Redesigns implemented for walking are discussed in Section 8.0.

We sought to develop a robust and versatile gripping mechanism. This mechanism would be used for lifting objects along with gripping onto a cart to help with assisted walking. We were tasked with creating the best grip for our robot's needs. More of our grip addition is discussed in Section 9.0.

Lastly, we were committed to creating uniformity to reduce parts and cost for the robot which meant standardizing components. This goal required changes to be made to various motor connection points. We further explain our changes based on these categories in Section 10.

5.1 Objectives

Following our research and understanding of Koalby, we established a plan to create an open-source, 3D printed humanoid robot that can be recreated for supply managers or engineers looking for a lab assistant. To achieve this, our objectives were:

- Improve the structural Integrity by redesigning parts to improve the strength of Ava
- Give Ava walking capabilities by integrating electrical components
- Add gripping functionality to lift objects and help with assisted walking
- Standardize components to reduce parts and create uniformity

As explained in Section 5: Project Goal, these key objectives, structural integrity, walking designs, gripping addition, and standardizing components, would help us in reaching the goal in creating a functional humanoid robot. In A-term, we first reviewed Koalby (2022, MQP) and researched humanoid robots applications. In B-term, we conducted analyses and created decision matrices to create our redesigns. Following our redesign plans, C-term was spent implementing design changes to improve overall functionality and strength. Lastly, in D-term, we assembled Ava.

6.0 Methodology

This section discusses our project goals and timeline throughout the year. A-term focused on familiarizing ourselves with the Koalby Project and conducting research on applications of humanoid robots along with gripping mechanisms. In B-term, we completed different analyses to identify areas of improvement and used design matrices to choose motors, sensors, and gripping designs. For C-term, we began to make modifications to various parts based on the information collected in A and B-term. D-term was used to assemble our new robot, Ava.

6.1 A-Term

Before conducting any work, a new goal for our new robot was established. This goal involved turning Ava into an everyday supply room assistant. During A-term, we conducted research into various applications of humanoid robots along with understanding Koalby, which can be found in Section 2 and 4 respectively. This allowed us to identify the different actions we wanted Ava to complete and focus on how to maintain her humanoid appearance. We determined that some important actions for Ava to do were standing, walking, and lifting objects. In order for her to stand and walk, we explored different sensors required to make it possible such as LiDar Sensors, Inertial Measurement Unit Sensors, and force sensors. In addition to this, we also researched different robotic gripping mechanisms to determine which grip type would be the best fit for Ava to grab and lift objects of any size and shape, located in Section 4.2. By adding these additional sensors and a new mechanical grip, we were making Ava heavier than what she originally was. The added weight required us to look into new motors and new batteries. Overall, A-Term was a time for us to truly understand the needs of a humanoid robot, and how we could implement the changes to make Ava as helpful and successful as possible.

In addition to all of our research, Ava was based on the built humanoid robot, Koalby, which we needed to familiarize ourselves with. This included keeping Koalby in good condition by repairing and replacing any broken parts along with understanding how he was structurally built. To do this, we analyzed the various CAD designs, analyzed the print settings for the FDM printed parts and Resin printed parts, and we spent time investigating Koalby to identify areas of improvement for Ava.

By the end of A-Term, we constructed a plan for the changes we wanted to make to allow Ava to be more functional. We finished A-Term with a better understanding of humanoid robots and a plan ready to be set in motion. In Section 4.3, you can find the research conducted with regards to sensors, batteries, motors, grips, and Koalby.

6.2 B-Term

Following A-term, we began investigating which areas of Koalby needed improvements along with what new components would be added to create Ava. These components are discussed in Section 3. To determine which parts needed to be redesigned for structural integrity, we conducted several analyses to test the strength and torque of each part. These different analyses were done through the use of ANSYS and free body diagrams (FBD), which allowed us to find accurate values for forces, moments, and the specific locations where those forces would be acting on. By doing this, we were able to easily identify the structural issues that needed to be addressed in Ava. ANSYS and FBDs are further explained in Sections 7.1.1 and 7.1.2 respectively.

We used decision matrices for multiple aspects of this project such as motors, grips, and sensors. Originally, Koalby was composed of Dynamixel motors and HerkuleX DRS motors; however, we determined that the motors would need to change to allow for uniformity in design and programming and to increase strength as we were adding a gripping mechanism. The motor matrix, which can be found in Section 10.2, shows 2 alternative motor options. We conducted Multi-Link Torque Analysis using free body diagrams; these calculations assisted with confirming whether or not the new motors and various parts of the robot (printed or not) would be strong enough to withstand the current load and any additions. With our calculations and motor matrix, we chose to use HerkuleX DRS motors. During B-term, we also identified which electrical components would be added to Ava and how to integrate them. Similar to the motors, we used a decision matrix for the sensors which is located in Section 8.1. Our team decided to implement Inertial Measurement Unit Sensors (IMU) in various areas of the robot, such as the chest, feet, and head to assist with balance and walking. We also planned to install an additional Arduino and Raspberry Pi in Ava's head to account for the increase in electrical components. We created a decision matrix for various grip designs as well. Once we settled on the best design for our needs, we wanted to enhance the capabilities, so we incorporated an electromagnet. All of

these components were taken into consideration with regards to our redesigns, and by the end of B-term, we compiled a list of the necessary modifications and established a plan to achieve them.

6.3 C-Term

C-term was dedicated to working on the various modifications for Ava. The redesigns, which were created using Solidworks, needed to address a new grip mechanism, the walking component, new motors, and new electrical components. The new gripping mechanism was designed to pick up objects, manipulate tools, and aid in assisted autonomous walking. The grip chosen was an underactuated, 3-point finger grip from ALARIS [15], which we redesigned to accommodate for our new electromagnet. This grip was then attached to the base of the forearm to strengthen the ability to lift lab tools. The forearm was redesigned to accommodate the new motors used for the grip. With the use of this gripping mechanism, Ava would be able to hold onto and push a cart allowing her to walk. In addition to the grip, the spine was created, connecting to the chest and pelvis, to assist with walking and stability. While the chest was redesigned to have an attachment point for the spine, it was also altered to fit the new sensors and motors. Similarly, the feet were redesigned to include sensors that would improve walking abilities as well. Another redesign aspect was modifying all of the motor connection points throughout the robot. We wanted to make Ava more cost effective, so all of the Dynamixel motors were replaced with HerkuleX DRS motors. By changing the motors, we created uniformity throughout the design and reduced the overall cost. Lastly, we altered the head to add more space for the additional electrical elements and compartments were added to allow for better organization within the controls.

All of these changes made during C-term were to make Ava as functional as possible. Redesigns about the pelvis and spine can be found in Sections 7.2 and 7.3. Changes to the head, chest and feet are located in Sections 8.3-8.5. Gripp information can be found in 9.3 while the forearm changes are located in Section 9.4. Various components that underwent redesigns could be found in Sections 10.3- 10.10. A full Solidworks assembly of Avs is located in Appendix J. As we tackled each redesign element, we printed prototypes to test our designs and made new modifications when necessary. Thus, C-term ended with the completion of our redesigns.

6.4 D-Term

D-term's focus was printing, assembling Ava, and presenting our work. After prototyping in C-term, we determined which designs worked best for functionality. We printed some of Ava's parts like the thigh and arms using a resin printer and other parts like the head with an FDM printer. Once all of the parts were printed, we began assembling. This included integrating the new motors into the 3D-printed parts, securing the sensors and electromagnets, and wiring everything together. We also presented Ava during WPI's Project Presentation Day for Major Qualifying Projects (MQP). The end of D-term resulted in a complete assembly of Ava with new abilities.

7.0 Structural Component Redesign

This section focuses on the analysis we conducted to determine which parts needed to be designed to improve the structural integrity of Ava. This section will also highlight the areas changed such as the pelvis and spine.

7.1 Analysis

Before we could make any part changes, we needed to conduct static and dynamic analyses. These analyses were important as it guided our findings in areas of improvement for strength and areas to integrate new components. At first, we used ANSYS, a 3D design engineering software that can produce simulations of how products would function in the real world. ANSYS was chosen because it was a software that can be learned quickly within our given time frame while still providing helpful information with regards to the different parts of the robot, and it was readily available. ANSYS assisted in highlighting areas that experienced the most stress under any force. Furthermore, we created free body diagrams, graphics that visualize the applied forces and moments of Koalby's 3D-printed components. Diagrams were created for each part experiencing force from the y-direction, x-direction, and z-direction. These free body diagrams (see Section 7.1.2) allowed for a clearer understanding of how the 3D-printed components acted with respect to the movement of the motors. In addition to both ANSYS and free body diagrams, we conducted a service level Multi-Link Torque Analysis to determine how much torque the new motors would need to produce to compensate for the new weight additions.

7.1.1 ANSYS

When using ANSYS, a multi-purpose modeling software for mechanical engineering simulation, we selected a 3D printed part and designated areas that would represent where the force and moments were being applied. For example, we can look at the pelvis in the figures below. 'A' represents the moment from the motor, 'B' represents upper body force, and 'C' and 'D' represent the fixed supports. Figure 7.1.1a shows the different letters and the direction of the force and moment. Figure 7.1.1b shows the greatest and weakest areas of deformation while Figure 7.1.1c shows the greatest and weakest areas of stress. Areas in red underwent large amounts of stress and deformation while areas in blue underwent no stress or deformation. To

generate these diagrams, each part was treated as a static structural object, more specifically as a cantilever beam, that underwent forces in the y or x direction. We then used the “equivalent (von-mises) stress” function to calculate the values we needed, which was maximum stress and maximum deformation. For the pelvis, the moment was set to 2 Nm, and the force was set to 20 N. These values were chosen because the 20 N force represents half of the weight of Koalby and the 2 Nm moment is an estimate for the moment of the lever arm. The lever arm is less than $\frac{1}{3}$ of a meter and would have a small angle of bend. These ANSYS analyses provided a maximum deformation value of 1.7051e^{-3} m and a maximum stress value of 4.2e^7 Pa. These values represent the most extreme scenarios; however, we needed more realistic analysis of actual arm and leg movements, which we were unable to do in our available time frame. Although we were unable to reproduce the constraints and loads that the parts would be experiencing, ANSYS was helpful in highlighting the areas we should be worried about.

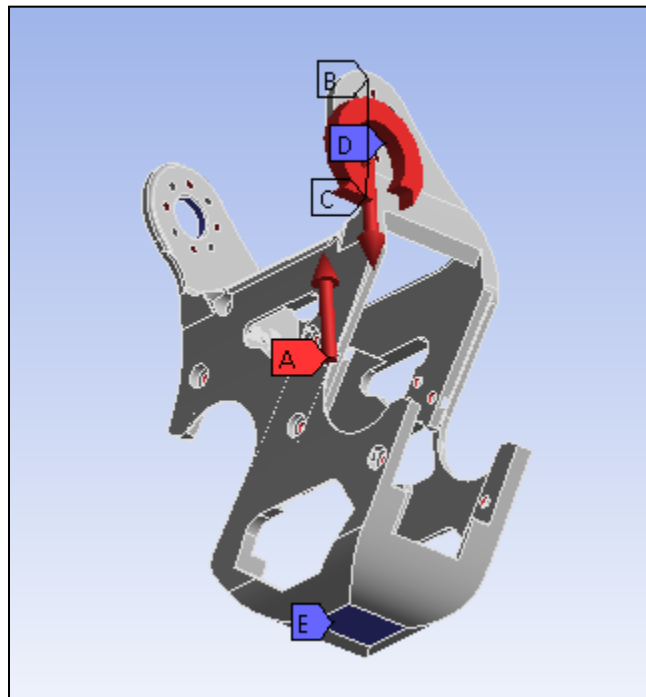


Figure 7.1.1a: Pelvis ANSYS set up

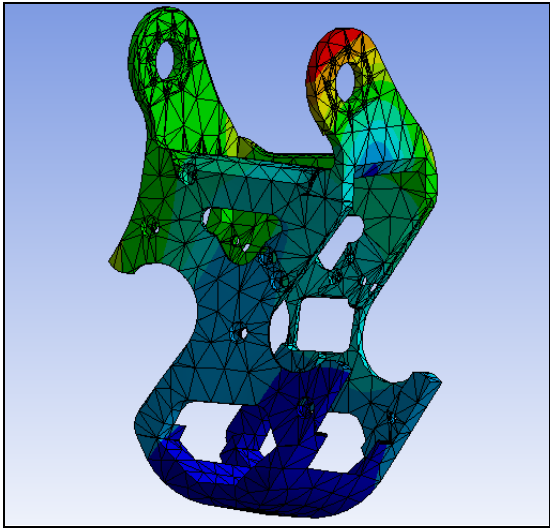


Figure 7.1.1b: Pelvis ANSYS deformation

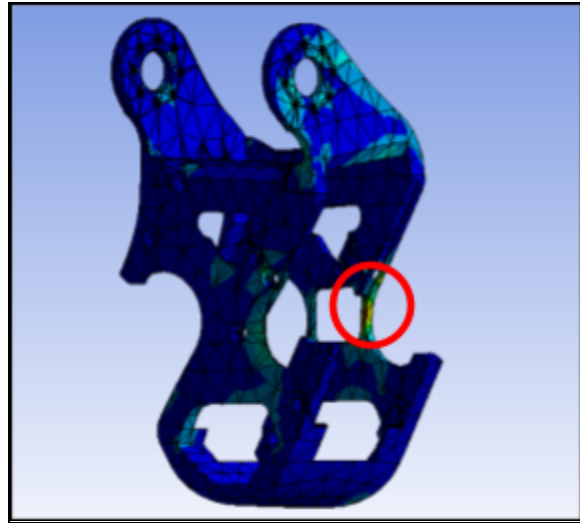


Figure 7.1.1c: Pelvis ANSYS stress

Along with the pelvis, we conducted ANSYS analysis on the foot, rib, shin, and abdomen which can be found in Appendix L. However, we still experienced issues with producing realistic values. We were unable to find adequate tutorials, so we did not know how to accurately replicate arm and leg movements in ANSYS. ANSYS was a useful tool in displaying areas that may be prone to failure, but we were unable to use its values.

7.1.2 Free Body Diagrams

After utilizing ANSYS, we decided to create Free Body Diagrams (FBD). FBD provided a better understanding of how the parts interact with one another, but it required calculations done by hand. Figure 7.1.2a shows all of the robot's parts in their correct locations with x-y-z coordinate axis to explain the direction of rotation. We started from the feet and worked our way up. We first focused on movements about the z-axis; rotation about the z-axis was designated as front and back movement (bending). The figures below show the parts that rotate about the z-axis: foot (Figure 7.1.2g), arm (Figure 7.1.2f), hip (Figure 7.1.2e), thigh (Figure 7.1.2d), shin (Figure 7.1.2c), and head (Figure 7.1.2b). An example for the foot moving would be the flexing of an ankle. As for the shin, the motor that it is attached to acts as a knee giving it the ability to bend. For the hip and thigh, the motors located at those locations allow the robots to essentially bend over at the waist. The shoulder motor allows for the arm to move back and forth. Lastly, the

motor located in the neck area gives the head the ability to nod. In the figures below, you can see the shape of the part, arrows indicating the various forces and moments acting on the parts, and a x-y-z coordinate system. The grounded areas are the locations of where the motors were connected, and they were denoted by a line with slashes. The calculated values of force and moments are located in Section 7.1.3.

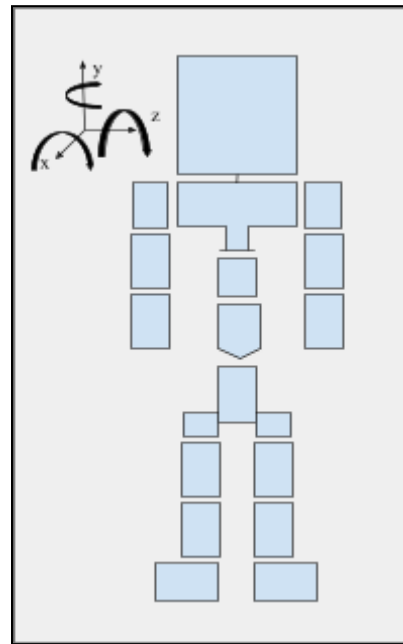


Figure 7.1.2a: Full body reference for FBD

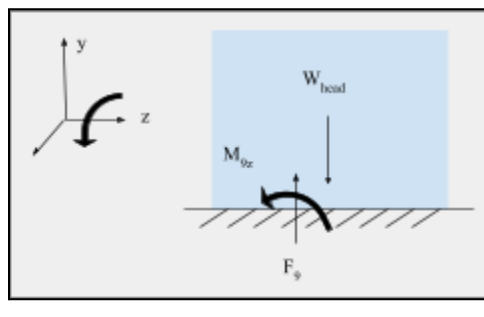


Figure 7.1.2b: Head FBD about Z-axis

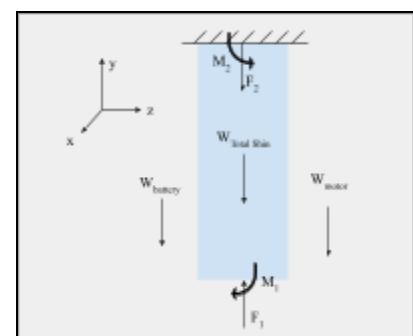


Figure 7.1.2c: Shin FBD about Z-axis

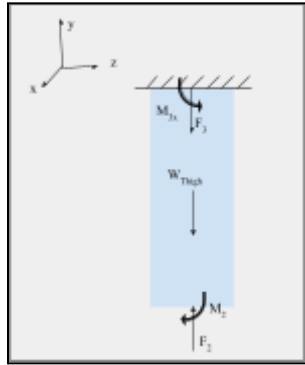


Figure 7.1.2d: Thigh FBD about Z-axis

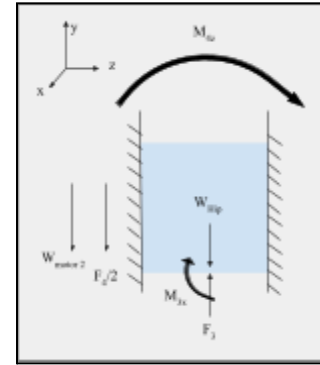


Figure 7.1.2e: Hip FBD about Z-axis

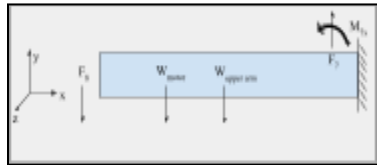


Figure 7.1.2f: Arm FBD about Z-axis

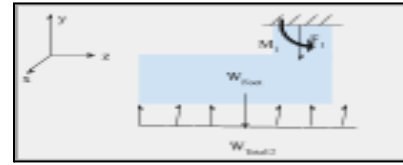


Figure 7.1.2g: Foot FBD about Z-axis

Following the creation of FBD about the z-axis, we created FBD for rotation about the x-axis which was designated as a tilting motion. The following parts were able to tilt: chest (Figure 7.1.2h), forearm (Figure 7.1.2i), abdomen (Figure 7.1.2j), and hip (Figure 7.1.2k). Parts like the hip can rotate about the z-axis and x-axis due to the two motors within the part. Within the arm, there is a motor to act as an elbow to create a flexing motion which can be described as making a muscle. There is a motor located in the rib area that gives the chest the ability to move side to side. The use of these motors gives the robots the most human-like movements.

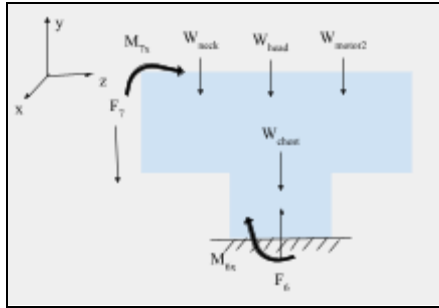


Figure 7.1.2h: Chest FBD about the X-axis

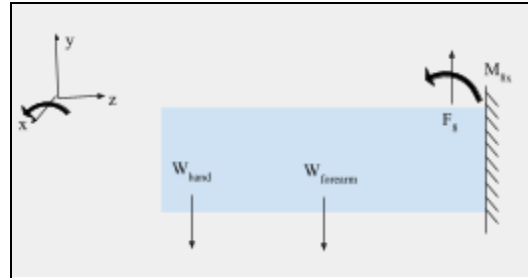


Figure 7.1.2i: Forearm FBD about the X-axis

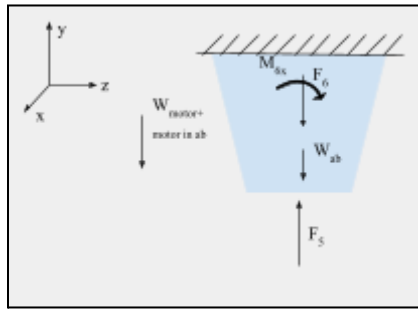


Figure 7.1.2j: Abdomen FBD about the X-axis

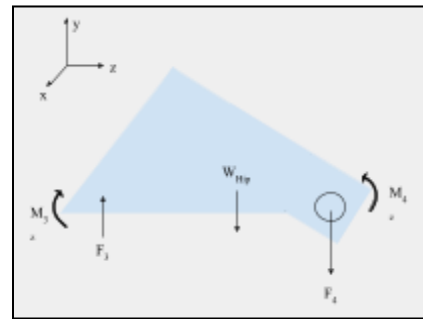


Figure 7.1.2k: Hip FBD about the X-axis

Lastly, we constructed FBD for the pelvis (Figure 7.1.2m) and looked at rotation about the y-axis, a twisting motion. The rib, head, and shoulder were able to twist; however, we were able to determine that the torque of these parts was negligible. For the pelvis, it was not rotation about any axis. The pelvis was composed of 3 motors that allowed hip and abdomen movement, but the pelvis itself would not move. We can see the various moments and forces that the pelvis experienced due to other parts in the figure below. The FBD below shows the forces of the pelvis when grounded at the top.

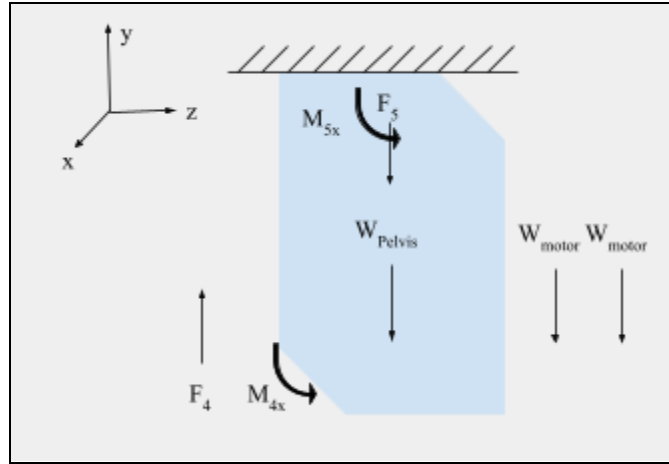


Figure 7.1.2m: Pelvis FBD about the Y-axis

These FBD were useful in providing clear visuals about how each part moved. Because there are so many motors to allow for so many different types of moment, the FBD helped with understanding each rotation and track the movements and how each motor was being used. The forces were used to perform the torque analysis to measure the torques acting on each joint of the robot. These calculations were used to determine the loads that each motor would need to handle. This in turn optimizes the selection process for the motors based on the torque and power requirements of that joint. Our torque analysis is further explained in Section 10.1.1 and Appendix F.

7.1.3 FBD Equations

As we worked on our FBD, we denoted the values with variables such as W_{pelvis} and W_{motor} . We force equations to calculate the numerical values of the forces, weights, and moments. These equations are listed below for each part.

$$\text{Forearm: } \sum F = F_8 - W_{\text{forearm}} - W_{\text{grip}}$$

$$F_8 = 0.57879 \text{ N}$$

$$\sum M = M_{8x} = 0.06367 \text{ Nm}$$

$$\text{Full Arm: } \sum F = F_7 - F_8 - W_{\text{upperarm}} - W_{\text{motor}}$$

$$F_7 = 0.57879 \text{ N} + 0.1952 \text{ N} + 0.5886 \text{ N} = 1.36259 \text{ N}$$

$$\sum M = M_{7x} = 0.06367 \text{ Nm}$$

$$Chest: \sum F = F_6 - F_7 - W_{neck} - W_{motor} - W_{head} - W_{chest} - W_{motor}$$

$$F_6 = 1.363 \text{ N} + 0.07749 \text{ N} + 1.5107 \text{ N} + 0.7436 = 5.27378 \text{ N}$$

$$\sum M = M_{7x} - M_{6x} \rightarrow M_{7x} = M_{6x}$$

$$Abdomen: \sum F = F_5 - F_6 - W_{abdomen} - W_{motor1} - W_{motor2}$$

$$F_6 = 10.1601 \text{ N} - 0.4777 \text{ N} - 1.5107 \text{ N} = 8.1717 \text{ N}$$

$$\sum M = M_{6x}$$

$$Pelvis: \sum F = F_4 - F_5 - W_{pelvis} - W_{motor} - W_{motor}$$

$$F_5 = 11.66 \text{ N} - 0.3227 \text{ N} - 2 * (0.5886 \text{ N}) = 10.16 \text{ N}$$

$$\sum M = M_{4x} - M_{5x} \rightarrow M_{4x} = M_{5x} = 0.4028 \text{ Nm}$$

$$Hip: \sum F = F_3 - F_4 - W_{hip} - W_{motor1} - W_{motor2}$$

$$F_4 = 13.128 \text{ N} - 0.755 \text{ N} - 0.125 \text{ N} - 0.5886 \text{ N} = 11.66 \text{ N}$$

$$\sum M = M_{3x} - M_{4x} \rightarrow M_{3x} = M_{4x} = 0.4028 \text{ Nm}$$

$$Thigh: \sum F = F_2 - F_3 - W_{Thigh}$$

$$F_3 = 13.61 \text{ N} - 0.48167 \text{ N} = 13.128 \text{ N}$$

$$\sum M = M_2 - M_{3x} \rightarrow M_2 = M_{3x} = 0.4028 \text{ Nm}$$

$$M_{3z} = 1.0503 \text{ Nm}$$

$$Shin: \sum F = F_1 - F_2 - W_{battery} - W_{motor}$$

$$F_2 = 20.1379 \text{ N} - 2.669 \text{ N} - 0.5886 \text{ N} = 13.61 \text{ N}$$

$$\sum M = M_1 - M_2 \rightarrow M_1 = M_2 = 0.4028 \text{ Nm}$$

$$Foot: \sum F = -F_1 - W_{foot} - (\frac{1}{2} * W_{total})$$

$$F_1 = -0.5611 \text{ N} + 20.6691 \text{ N} = 20.1379 \text{ N}$$

$$\sum M = M_1 - M_2 \rightarrow M_1 = M_2 = 0.4028 \text{ Nm}$$

The equations in conjunction with the FBD were useful in providing information on how each part interacts with one another and how large of loads the robot was experiencing.

7.2 Pelvis

The pelvis was a component that continuously broke (as mentioned in Section 3) and desperately needed a redesign. The two areas with the most notable weakness were located in the back where the switch was attached and the left waist servo connection. To remedy this, we removed the cuts for the switch and added a 5mm extrude in the shape of a box with extra branches in the shape of an X as a back reinforcement. On top of this extrude, a clamp attachment was added for the spine (Figure 7.2a). To strengthen the servo connection, we added a 3 mm extrusion on the inside (Figure 7.2b). Then the holes on the waist motor mounts were adjusted to fit the Herculex 0601 motors instead of the prior Dynamixel MX-64 motor.

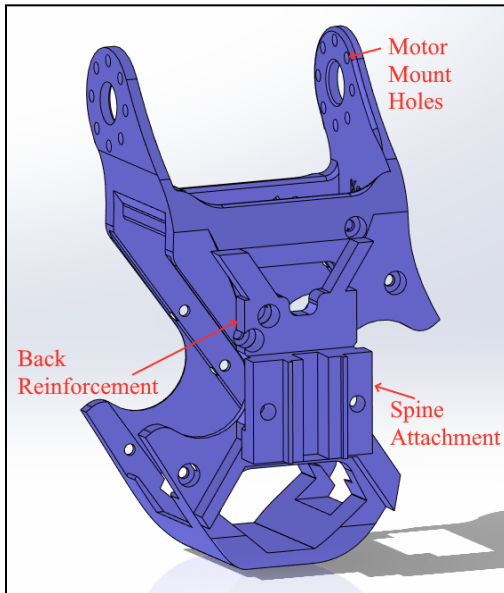


Figure 7.2a: Full pelvis part

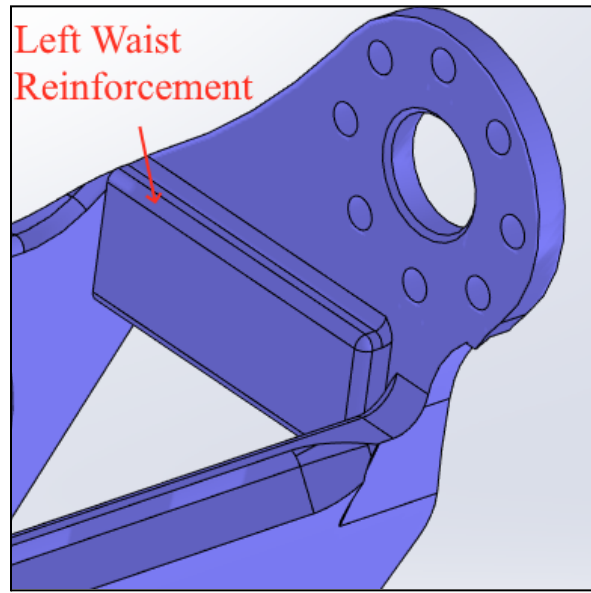


Figure 7.2b: Zoomed in pelvis

7.3 Spine

In order to increase the structural stability of Ava, a spine was determined to be a benefit to the system. The rod was designed to have a large area moment of inertia while still being easily printable, and the shape chosen was similar to that of a T (shown in the left image of Figure 7.3a). Along with the cross section shape, we made the spine into smaller 4 inch sections

that could be attached later on for printing purposes. This was because the length of over 0.3 m long was larger than any print bed we had access to.

In order to implement the spine, two attachment points were designed. The lower attachment clamped the spine to the pelvis, meaning that the dimensions fit the spine closely (shown in the right image of Figure 7.3a). For the upper attachment we gave it freedoms similar to the SPEXOR exoskeleton mentioned in Section 4.4 in order to negate parasitic forces [15]. This part attachment was designed to have a gap larger than the spine, allowing for the linear sliding of the spine rod, and was attached to the chest with a fastener allowing it to rotate.

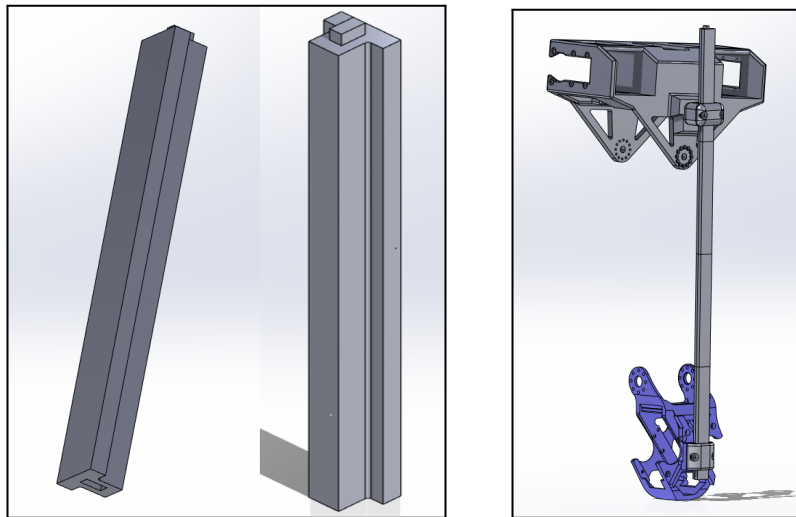


Figure 7.3a: Spine addition

8.0 Walking Redesigns

When it came to walking capabilities, there were several things to consider. To successfully walk, a multitude of electronic components are necessary, and the robot's new design needed to accommodate them. This section discusses the electronic components we implemented and how we incorporated them into our design.

8.1 Sensor Integration

Sensor integration plays a crucial role in enabling a robot to walk with stability and efficiency. As such, to allow for stability and balance we chose to implement three Inertial Measurement Units (IMU): a BNO055 for Ava's chest and an MPU6050 for each foot. To integrate obstacle detection, there were a variety of LiDAR distance sensors to choose from. To determine which one would be the best fit for our project, we created a sensor decision matrix that compared three different LiDAR sensors: Ultrasonic, TF Luna, and TF-LC02 (Table 8.1a).

Utilizing the decision matrix method, we created a list of criterias and assigned each of them a weighted value from 1-5 (5 being most important, 1 being least important) to identify which criterias were valued more. When choosing which sensors we wanted to compare, we looked at sensors that were low in cost, easily obtainable, and had good detection speed. Due to the success of this method, we also used decision matrices to determine our grip design and motors, which are located in Section 9.2 and 10.2 respectively. These matrices allowed us to narrow down our options and find the best possible design paths we could take.

Table 8.1a: Sensor Decision Matrix

Sensor Criteria	Weight	Current Situation	Alternative 1	Alternative 2
Price	4	0	-1	-1
Error Margin	3	0	1	-1
Hazard to health	5	0	0	0
Size	4	0	-1	1
Ability to Attach/install	5	0	1	1
Detection speed	5	0	1	-1
Detection Distance	4	0	1	-1
Software Capability	5	0	1	1
Weighted Total		0	14	-2

Based on our set of weighted criteria within the matrix, we concluded that the TF Luna sensor was our best option. Although, more expensive than the Ultrasonic and TF-LC02 sensors, the TF Luna outshined its competitors with its low error margin, and its better detection speed and detection distance. In addition to these sensors, we chose to use a Huskylens, an AI camera

that is both easy to use and to integrate, for object detection because one was readily available, and it fit the requirements of our projects.

8.2 Electrical Integration

Due to all of the modifications made to the robot, a new electrical diagram was constructed and can be seen in Appendix G. To accommodate for the different voltages across the sensors and motors, a series of adjustable voltage regulators were implemented. Meanwhile, the previous 7.4V batteries were upgraded to two 11.1V batteries. Then to improve the durability and reliability of the circuit, old and worn components were replaced and higher quality wires were used.

8.3 Head Lid

The lid of the head was redesigned to house the AI Huskylens Camera and LiDAR TF Luna. A 52mm ledge was added to the top of the lid with cutouts for the fasteners of each sensor. Additional 17-20mm cutouts were made on the ledge and the top of the lid for wire management of the sensors. Figure 8.3a shows the head lid designed by the 2022 MQP team. Figure 8.3b shows the redesigned head lid with the new ledge and cutouts for sensors. Figure 8.3c shows the full head assembly and how the head lid attaches to the head.

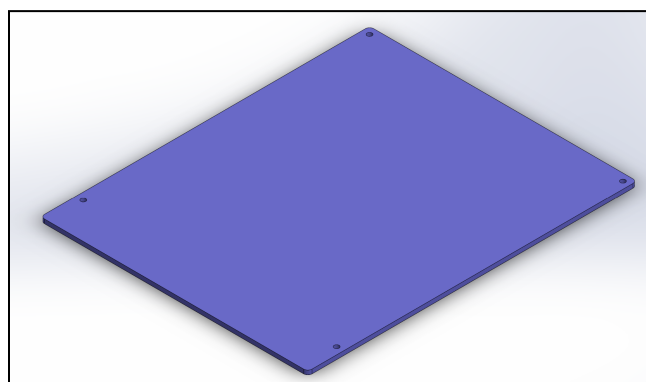


Figure 8.3a: 2022 MQP Team Head Lid Design

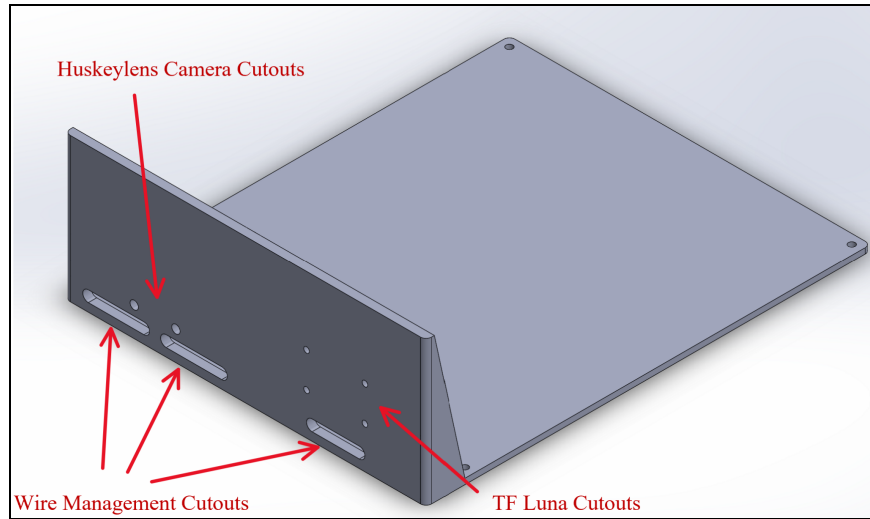


Figure 8.3b: Redesigned Head Lid

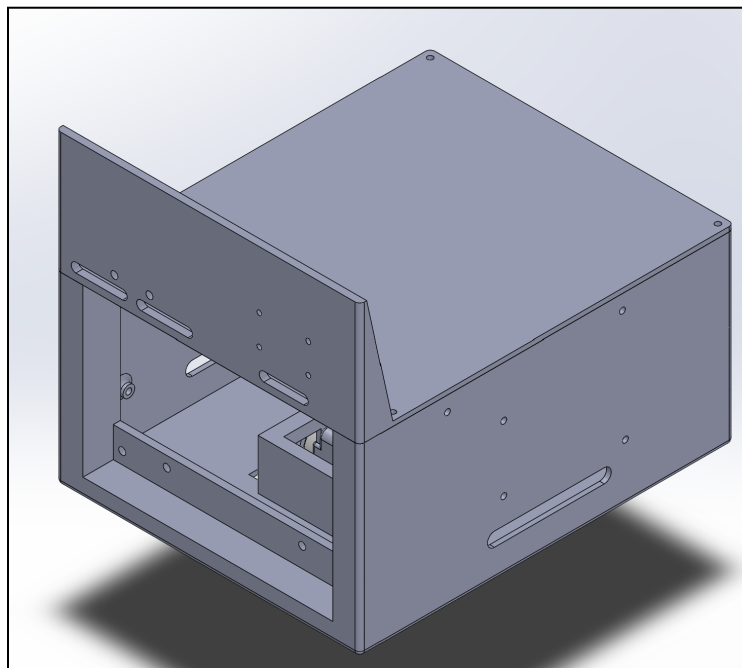


Figure 8.3c: Head Assembly

8.4 Chest

Multiple new components were added to the chest. Herculex 0601 motors were added to the shoulders to aid with lifting heavier objects. To accommodate this, we increased the width by 26 mm and height of the chest by 27.2 mm, which is highlighted in Figure 8.4a. We cut holes to

fasten the neck and chest motors. An IMU was also added; however it needed to be located as close to the center of mass as possible. A cut was made into the chest to fit an IMU holder (Figure 8.4d) along with the IMU shown in Figure 8.4a. To protect the IMU, we added a breast plate, (in Figure 8.4c), that is held on by a dovetail joint and a single fastener. We made cuts throughout the chest, which is shown in Figure 8.4b, to remove unnecessary parts to decrease the mass.

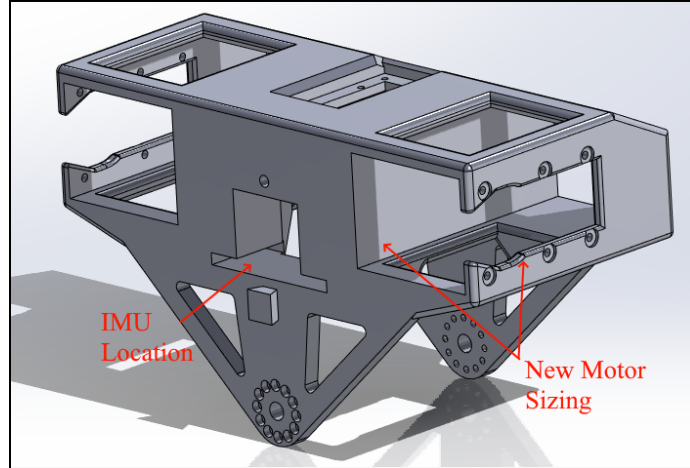


Figure 8.4a: Front Chest Design

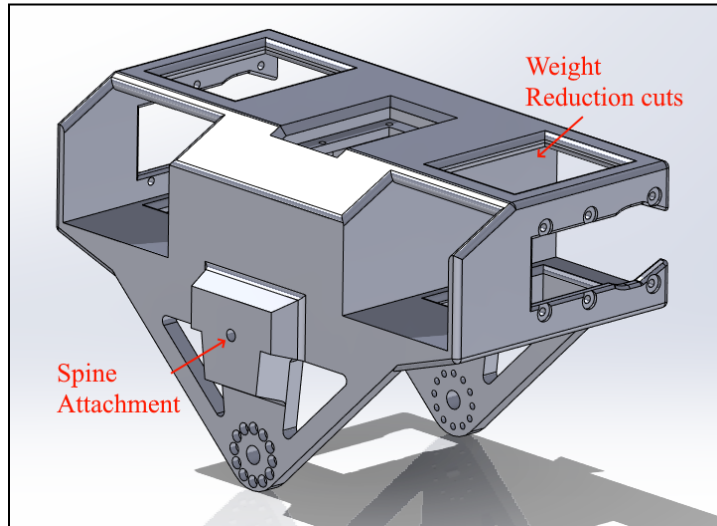


Figure 8.4b: Back Chest Design

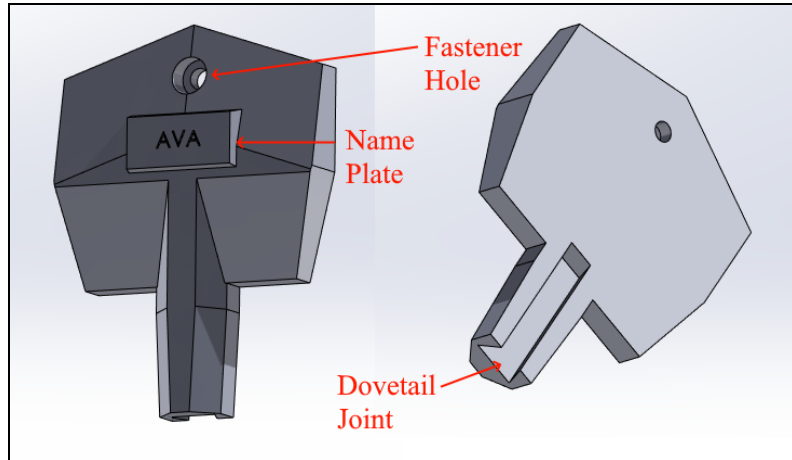


Figure 8.4c: Breast Plate

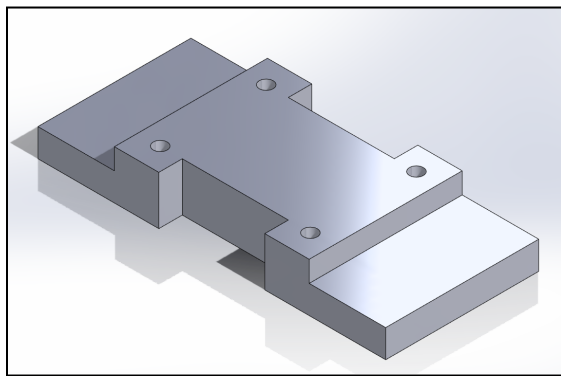


Figure 8.4d: IMU Holder

8.5 Feet

To improve Ava's balance while walking, each foot base was widened by 9.8mm displayed in Figure 8.5a. This change widened the foot enough to increase stability while simultaneously keeping the general humanoid foot shape. Then to improve traction, the feet were first printed in Thermoplastic Elastomer (TPE) shown in Figure 8.5b. However, this material did not provide enough traction and was found to make the part too flimsy. Instead, Polyvinyl Chloride (PVC) was secured to the bottom of each foot as seen in Figure 8.5c. Additionally, a hole was cut into the top of each foot to create a small opening where the MPU6050 could be wired and placed securely inside (Figure 8.5d).



Figure 8.5a: Widened Foot



Figure 8.5b: Foot Printed in TPE



Figure 8.5c: Foot with PVC Attached



Figure 8.5d: Foot with IMU Integration

9.0 Grip Addition

In order to make Ava a successful lab assistant, we needed to consider which type of gripping mechanism would be able to pick up a variety of objects, as well as hold onto a cart for assisted walking. In this section, we discuss the different types of grip designs we considered and

the design we chose. We also discuss the tools the grip needed to lift along with how we altered the forearm to fit our new grip

9.1 Grip Tools

In order to decide between a variety of grips, we first had to determine what objects were going to be handled. Given that Ava would be performing as a lab room assistant, we created a list of standard tools you would find in a lab shown in Figure 9.1a, and their corresponding masses as displayed in Table 9.1a.



Figure 9.1a: Lab Tools

Table 9.1a: Lab Tool Specifications

Object Name	Mass
Plier	165g → 0.165kg
Metal Caliper	148g → 0.148kg
Screwdriver: 88593 P 2X4	104g → 0.104kg
Blackhawk: 2X5	77g → 0.077kg
Screwdriver: 88395 P 1X3	66g → 0.066kg
Paramount: 1X3	58g → 0.058kg
Plastic Caliper	53g → 0.053kg
Safety Glasses	35g → 0.035kg
Paramount: 0X2	15g → 0.015kg

9.2 Grip Matrix

There were several possible grip approaches we could take. To handle this, we created a decision matrix to help us determine which grip was best for our redesigns. As mentioned in Section 8.1, the matrix helped with ranking the various criterias we needed to consider for the grip. There were many factors to consider like scalability, motor power, sensor integration, finger count, and much more. To make the grip decision matrix, we started with understanding the customer needs and translating it mechanical needs. For example, we had the following criteria as customer needs: human-like hand, versatility to grab multiple shapes, capability to sense the object, strength to lift anything, and interchangeability. The next steps were to understand what these needs would mean for the design aspect. When looking at “human-like hands” and “versatility to grab multiple shapes”, we determined it would translate to how many fingers a grip would have (2, 3, 4, or 5) and how many joints a grip hand. Being able to bend fingers to

create an encompassing grip would help with picking up different objects, especially circular ones. Whether a grip was strong enough was determined by the type of motor and number of motors along with how much torque/pressure would be required to lift an object. Ava would be using a cart for assisted walking, so the robot would need a grip to hold on to a knob while also still being able to grab objects resulting in interchangeability being a key factor in the decision matrix. We looked at grips that would be easy to take on and off. Next, we looked into scalability. Of the grips we researched, we wanted to know how easy or hard it would be to scale it down to the size of Ava; it was important to keep the robot proportional. In addition to design and mechanical needs, we considered the grip would work for software. We wanted to include an electromagnet and force sensors to the grip. We needed to ensure there would be space for these electronic components and wiring.

The grip used for the current situation was “The Claw”, a 3-point, equidistant grip [14]. This grip uses a N20 DC Motor that moves a worm gear in the center. With the “claw” as our starting grip, we compared alternate options. Alternative 1 was the Model O design, a grip using 4 Dynamixel XM430-W350-R motors and torsional springs at the base of the palm to help move the 3D-printed fingers. Following Model O was the Underactuated Robotic Grip for Alternative 2. This grip uses a Dynamixel MX-28 motor and has a mechanical linkage system for fingers with an underactuated worm wheel gear transmission. Alternative 3 was a jamming grip. A jamming grip uses an elastic material covered ball, filled with a granular material that uses pneumatics to lift objects. Lastly, alternative 4 was DFRobot Bionic Hand [34]. This hand option had 5 fingers; however, it wasn't necessarily open source [35].

Table 9.2a: Grip Decision Matrix

Grabber Criteria-Design	Weight	Current Situation	Alternative 1	Alternative 2	Alternative 3	Alternative 4
Digits to move at joints	3	0	1	1	-1	1
Capability to grab multiple shapes	5	0	1	0	1	1
The hand knows its grabbing	4	0	0	0	0	0
Strong enough ability to lift anything we want	3	0	0	0	1	0
Motor count	5	0	-1	0	-1	0
Modularity	4	0	0	0	-1	-1
Scalability	5	0	-1	0	-1	-1
Software accessibility	5	0	-1	0	-1	-1

Sensor Capability	4	0	0	0	-1	-1
Magnet Capability	2	0	0	0	-1	0
Total		0	-1	1	-5	-2
Total with Weight		0	-7	3	-20	-10

After weighing the criteria with 1 (least important) to 5 (most important), we gave each alternative a -1, 0, or 1. We determined that alternative 2, Underactuated Robotic Grip was the best option for us to pursue. The Underactuated Robotic Grip was very similar to The Claw; however, it had the ability to bend the fingers to create an encompassing grip. Alternative 1 had too many motors and was not the best for scalability. Alternative 3 had no fingers and required an air tank in addition to motors making scalability, modularity, sensor capabilities, and electromagnetic capability impractical. Alternative 4 may have had more fingers, but it was not ideal for modularity, scalability, or software capability overall. From the grip decision matrix, we chose to proceed with alternative 2 for Ava.

9.3 Grip Design

Our team started with an open source 3D printed underactuated gripper, which we then scaled down to meet the size requirements of everyday objects that can be found in a mechanical engineering lab environment. The base attachment of the gripper was also modified to better connect with the forearm. To actuate the fingers of the gripper, we installed a worm wheel that was connected to a HerkuleX DRS 0201 motor located inside the forearm. To ensure that the rotation was easier and the connection was intact between the misaligned motor and worm wheel, we incorporated a Cardan universal joint to connect the two components, which were not aligned initially. The connection for the wrist movement of the gripper was also modified to connect with the HerkuleX 0201 motor located in the forearm. This allowed for better control of the wrist movement while keeping the overall design compact. Lastly, an electromagnet cutout

was integrated onto the palm of the gripper to accommodate the electromagnet. These modifications allowed us to create a grip that was better suited for our robot while maintaining the overall robustness of the forearm. Figures 9.3a and 9.3b show the grip mechanism along with the electromagnet we used while figure 9.3c shows the palm of the grip in an assembly with the motor connection.

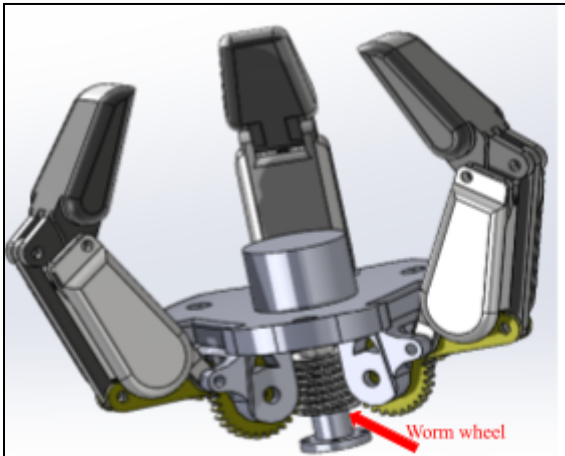


Figure 9.3a: Implemented grip design



Figure 9.3b: Electromagnet

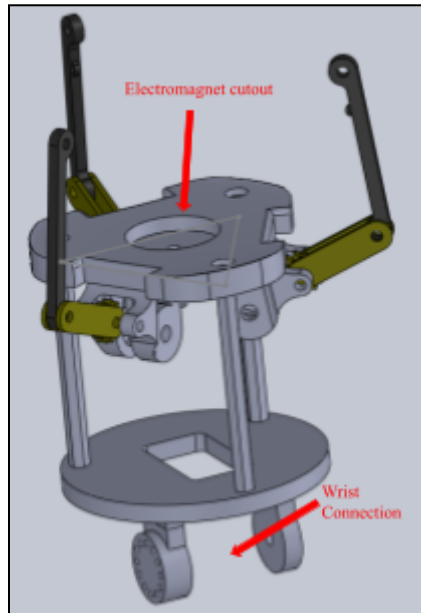


Figure 9.3c: Wrist connection with palm of grip assembly

9.4 Forearm Redesign

Once we established a grip design, we looked at the forearm. The forearm needed the greatest redesign in the arm because we were connecting another mechanism to the base, but we also wanted a design that would allow for modularity. The gripping mechanism needed a motor, a HerkuleX DRS 0201 motor, to create the grasping functionality of a grip. To place it in the center of the forearm, we created a motor mount to secure it. Due to this motor, we widened the forearm to fit everything. Secondly, we needed another HerkuleX DRS 0201 to allow for wrist movements, which increased grabbing capabilities. We added a motor connection point to the outside of the forearm to place this motor. Since we wanted to implement modularity, we redesigned the forearm to be two different pieces, the elbow and lower forearm. The elbow piece would stay connected to the elbow motor, the HerkuleX DRS 0601. We added a hole for a clevis and cotter pin in both the forearm and elbow. The lower forearm piece would be able to be removed to replace it with a different kind of grip if wanted. Figure 9.4a shows the new design of the forearm.

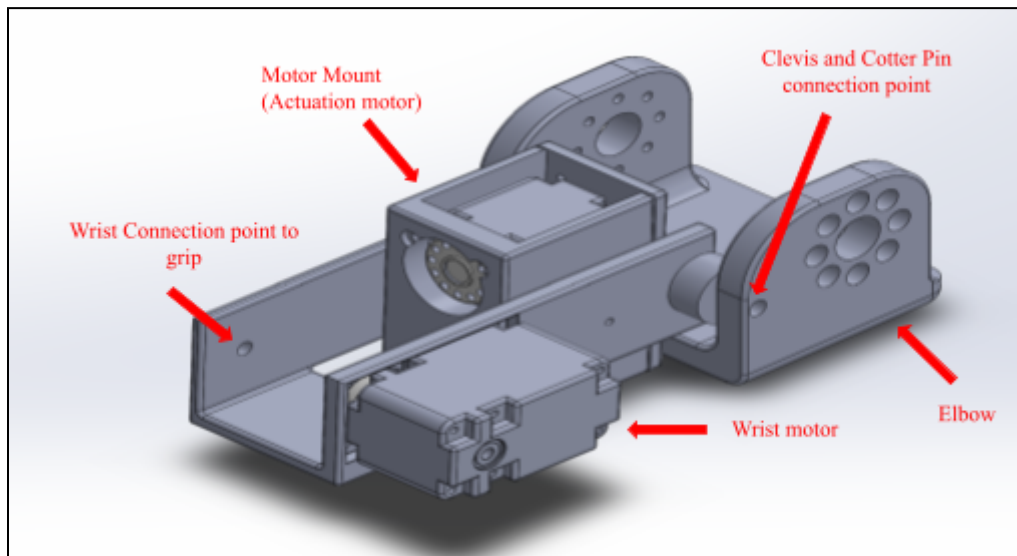


Figure 9.4a: Forearm redesign assembly

10.0 Standardizing Components

Another goal we had was standardizing components which entails creating uniformity throughout the robot. This section will review the various changes made to the type of motors we used, and cover the various redesign to reduce added hardware and parts.

10.1 Motor Matrix

For our motor matrix, we needed to address the upper body needs and lower body needs separately. Ava, originally, used an HerkuleX DRS 0201 motor, and the alternative options we were considering were a HerkuleX DRS 0401 for the upper body, HerkuleX DRS 0601 for the lower body, or a Dynamixel MX-64. The upper body motor needed to meet the shoulder torque requirement we calculated along with the elbow torque requirement. The lower body motor needed to meet the leg torque requirement and the hip torque requirement. In addition, we looked at the voltage requirement for each motor. One of our goals was to make the robots more affordable, so we considered the price of the motors. With our given time frame, we also considered lead time. Lastly, we needed to account for compatibility with resin, which is understanding the complexity of the changes needed to integrate the motors. The tables below show the ranking for each motor criteria and how each alternative compares to the current situation.

Table 10.1a: Upper Body Motor Decision Matrix

Motor Criteria	Weight	Current Situation Herkulex 	Alternative 1	Alternative 2
Meet Shoulder Torque Requirement	3	0	1	1
Meet Elbow Torque Requirement	3	0	1	1
Price	5	0	-1	-1
Lead Time	5	0	-1	1
Voltage	2	0	0	0
Compatibility with Resin→ changes needed to implement it	2	0	0	0
Weighted Total		0	-4	6

Table 10.1b: Lower Body Motor Decision Matrix

Motor Criteria	Weight	Current Situation	Alternative 1	Alternative 2
		Herkulex		
Meet Leg Torque Requirement	4	0	-1	1
Meet Hip Torque Requirement	4	0	-1	1
Price	5	0	-1	-1
Lead Time	5	0	-1	1
Voltage	2	0	0	0
Compatibility with Resin→ changes needed to implement it	2	0	0	0
Weighted Total		0	-18	8

However, after consideration of the programming aspect of the motor, we determined that keeping all the motors HerkuleX would be more beneficial for software and overall cost. We chose to keep the HerkuleX DRS 0201 in their respective locations. We needed to find a HerkuleX motor that was able to provide the same strength as a Dynamixel motor. The equivalent of Dynamixel MX-64AT is a HerkuleX DRS 0401 or HerkuleX DRS 0601. The HerkuleX DRS-0601 proved to have a higher stall torque than MX-64AT. We ultimately decided

on the HerkuleX DRS 0601 because 0401 were proving to have longer lead times along with the possibility of being discontinued.

10.1.1 Torque Analysis

After finalizing our tool selection in Section 9.1, we needed to determine whether or not our motor of choice, the Herkulex 0201, could provide enough torque to lift them. To do this, we performed Multi-Link Torque Analysis to ensure feasibility by calculating how much mass the Herkulex 0201 motor could lift at 15%, 20%, and 100% stall torque at different joint locations. To begin, we started with how much mass the elbow could hold by configuring it in the position where it would experience the most stress (Table 10.1.1a).

Table 10.1.1a: Elbow Torque: Arm is resting at the side and the elbow is bent 90 degrees upward.

Stall Torque (Herkulex 0201 2.25 Nm)	Object Mass It Can Lift
15%	0.1965 kg
20%	0.2765 kg
100%	1.555 kg

This torque analysis highlighted that at max stress, the Herkulex 0201 motor could lift and hold the heaviest object, pliers at 0.165 kg, at an ideal stall torque of 15%. Following the elbow, we did the same process for the shoulder including analysis for both axis of rotation, and the chest. These calculations can be found in Table 10.1.1b, Table 10.1.1c, and Table 10.1.1d respectively.

Table 10.1.1b: Shoulder Torque (y-axis): At the shoulder, the arm was held straight out to the right (horizontal) and the palm of the hand was rotated to face the ceiling.

Stall Torque (Herkulex 0201 2.25 Nm)	Object Mass It Can Lift
15%	0.0282 kg
20%	0.0712 kg
100%	0.7562 kg

Table 10.1.1c: Shoulder Torque (x-axis): At the shoulder, the arm was held out straight to the right (horizontal) and the elbow was bent inwards 90 degrees where the palm was facing the ground.

Stall Torque (Herkulex 0201 2.25 Nm)	Object Mass It Can Lift
15%	0.0883 kg
20%	0.1363 kg
100%	0.9036 kg

Table 10.1.1d: Chest Torque: At the shoulder, the arm was held out straight to the right (horizontal) and analysis was done about the central chest connection point.

Stall Torque (Herkulex 0201 2.25 Nm)	Object Mass It Can Lift
15%	X
20%	X
25%	0.0167 kg
100%	0.466 kg

Finally to ensure that the new motor was strong enough to lift the batteries in the shin of each leg, we performed the same analysis as shown in Table 10.1.1e.

Table 10.1.1e: Leg Torque: Hip was bent upward 90 degrees, and the knee joint was bent downward to create a 45 degree inner angle.

Stall Torque Required to Lift Leg	Effort
1.3256 Nm	22.09%

Overall, we found the Herkulex 0201 to be successful as it provided enough torque for our purposes and would allow us to standardize all of our motors without issue. For further insight into the torque calculations, refer to Appendix F.

10.1.2 Comparing Specifications

Dynamixel motors generally have a more complex functionality, such as faster larger operating angles and higher resolutions, compared to HerkuleX motors, causing a higher cost. However, both Dynamixel and HerkuleX motors have similar functionality related to feedback and control. The HerkuleX DRS-0601 and DRS-0602 were compared to the Dynamixel MX-64AT and MX-64T as possible replacement options. Detailed motor specifications and pictures are in Appendix D.

The only difference in the specifications of the MX-64T and MX-64AT is the cost and weight, where the MX-64AT is heavier and costs more. The MX-64AT is a special version of the MX-64T with an aluminum front plate. This plate acts as a heat sink, providing better heat dissipation, allowing the servo to run cooler. The aluminum front plate has threaded holes, allowing for easier assembly as no nuts need to be seated on the front plate. The back plate still required nuts. Figure 10.1.2a shows the Dynamixel MX-64AT motor.



Figure 10.1.2a: Dynamixel MX-64AT Motor

The key differences between these Dynamixel and HerkuleX motors are the resolution and operating angle. The HerkuleX DRS-0601 motor is shown in Figure 10.1.2b. The Dynamixel MX-64AT has a more precise resolution of 0.088° and a larger operating angle of 360° compared to the HerkuleX DRS-0601 which is 0.163° and 320° , respectively. For the purpose of this project, the resolution and operating angle of the HerkuleX motor was determined to be

sufficient. Considering the different motor types, the Maxon RE-MAX of the Dynamixel motor has higher speed capabilities of 78 RPM; a coreless motor, like the HerkuleX, has slower speeds of 61.73 RPM. However, the HerkuleX DRS-0601 motor weighs less at 123g compared to the 135g Dynamixel MX-64AT. Overall, the simple movements and gripping actions that were expected of this project did not require extremely precise or fast maneuverability. Furthermore, the HerkuleX motors cost \$50 less and have slightly smaller dimensions (35 x 56 x 38 [mm]) than the Dynamixel motors (40.2 x 61.1 x 41.0 [mm]). This change in size required redesigning most of the parts to fit the HerkuleX motors. However, this redesign is worth it because of the greater benefits of cost and production time reduction that this replacement would cause.



Figure 10.1.2b: HerkuleX DRS-0601 Motor

Additionally, the HerkuleX DRS-0101 was compared to the Dynamixel AX-12 as a possible replacement for the neck motors. Figure 10.1.2c shows the HerkuleX DRS-0101 motor, and Figure 10.1.2d shows the Dynamixel AX-12. These motors have similar functionality differences as the Dynamixel MX-64AT and HerkuleX DRS-0601. The Dynamixel AX-12 has a more precise resolution of 0.29° compared to the HerkuleX DRS-0101 which is 0.325° . However, the Dynamixel AX-12 has a smaller operating angle of 300° compared to the 320° operating angle of the HerkuleX DRS-0101. The other key differences between these motors are the cost, weight, and stall torque. The HerkuleX DRS-0101 is cheaper (\$40) and lighter (45g) than the Dynamixel AX-12 (\$50 and 55g). However, the HerkuleX DRS-0101 has a smaller (1.18Nm) compared to the Dynamixel AX-12 (1.5Nm). Based on torque calculations (see Section 10.1.1), it was determined that the smaller stall torque of the HerkuleX DRS-0101 is sufficient for the neck motors.



Figure 10.1.2c: HerkuleX DRS-0101 Motor



Figure 10.1.2d: Dynamixel AX-12 Motor

Overall, it was determined that the HerkuleX DRS-0601 and DRS-0101 are sufficient to replace the Dynamixel MX-64AT and AX-12 motors, respectively. However, the HerkuleX motor replacements are different dimensions than their Dynamixel counterparts, so this required redesigns in the parts to fit the new motors. Additionally, the HerkuleX motors have more limited control and communication speeds compared to the Dynamixel motors. Replacing these Dynamixel motors with HerkuleX motors reduces the cost of the robot by approximately \$375. It was determined that the benefits of replacing the Dynamixel motors with HerkuleX motors outweighed the costs.

In addition to analyzing the Dynamixel motors, the torque requirements for all of the HerkuleX motors throughout the robot were considered to determine if other replacements with higher stall torques were required, which was found to not be the case in Section 10.1.2. For the purpose of lifting and placing various objects with a maximum weight of 165g, the elbow and shoulder motors required a higher stall torque than their original HerkuleX DRS-0201 motors. These motors were replaced with HerkuleX DRS-0601 motors which have a 5.25Nm higher stall torque. Lastly, two HerkuleX DRS-0201 motors were added to each wrist for gripping capabilities which were further explained in Section 9.

Based on these replacements, Koalby now has 19 HerkuleX DRS-0201 motors, eight HerkuleX 0601 motors, and two HerkuleX DRS-0101 motors.

10.2 Hip

The hip underwent a significant redesign in order to remove unnecessary motor mounts and reduce the overall weight of the part. These changes are shown in Figure 10.2a. These mounts added to the complexity and weight of the part, thus, to simplify the design and reduce weight, we decided to directly connect the hip to the HerkuleX DRS 0201 motor.

Additionally, since the hip was susceptible to deformation, we increased the thickness of the connection to the pelvis to 3mm. This added strength and durability to the part, ensuring that it would remain stable and functional during operation. Overall, the hip was redesigned to be simple and efficient.

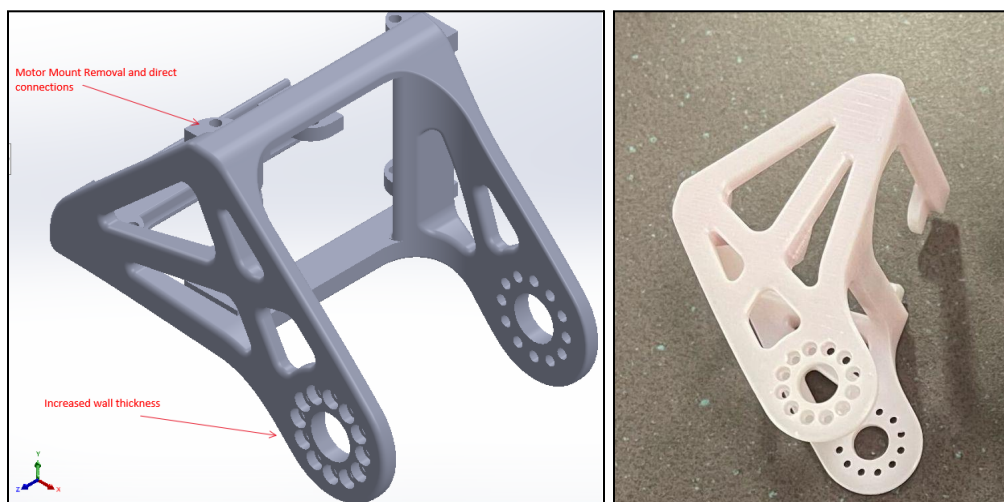


Figure 10.2a: Redesigned Hip Piece

10.3 Thigh

The thigh underwent minor changes to fit the new Herkulex DRS-0601 motors. The motor horn holes were adjusted to align with the new motor, the radius of the fastener holes were changed to 2.7mm, and the radius of the circle of holes of the motor horn was decreased by 2mm. Figure 10.3a shows the redesigned thigh part. Additionally, a custom servohorn was made to align with the Herkulex DRS-0601 motors and the fastener holes on the thigh. Figure 10.3b shows the custom servohorn, and Figure 10.3c shows the thigh sub assembly and how these parts fit together.

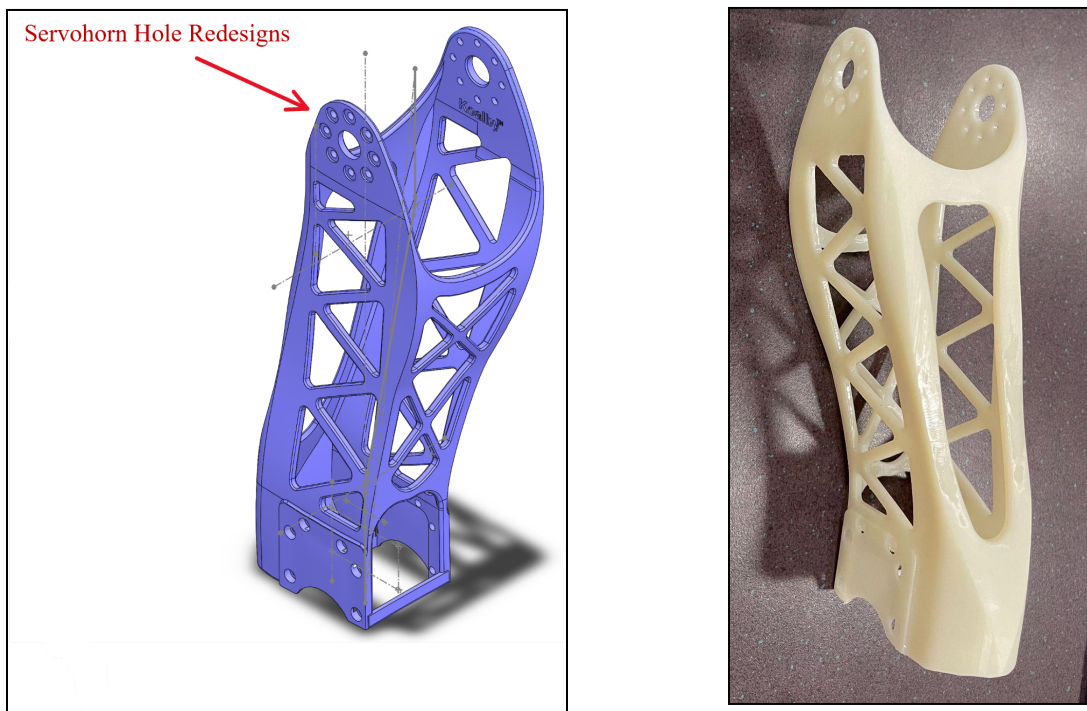


Figure 10.3a: Redesigned Thigh Part



Figure 10.3b: Custom Servohorn for HerkuleX DRS-0601 Motor

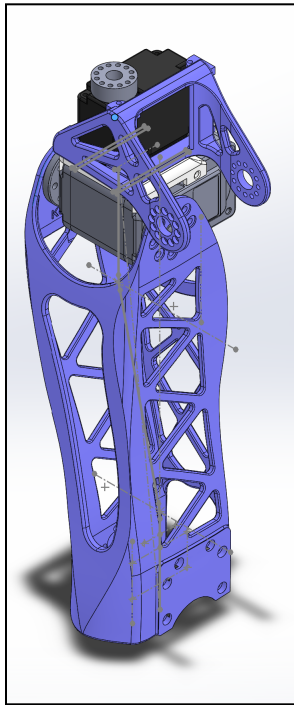


Figure 10.3c: Thigh Sub-Assembly

10.4 Shin

The shin underwent significant changes to improve its structural integrity, accommodate new batteries, and improve the design for ease of assembly and disassembly of motors. Due to the constraints of the 3D printer dimensions, the shin was printed as two separate parts: the top shin (Figure 10.4a) and the bottom shin (Figure 10.4b). However, we observed that the connection points of the two parts were susceptible to breakage, so changes were made to adjust for this. We increased the wall lines for the part connection and increased the thickness to keep the part from breaking. Additionally, we removed the threading from the holes, which was interfering with the structural integrity of the connection points, replacing it with a regular hole for a bolt and nut connection. Although this increased the number of components, it was an effective tradeoff compared to having to frequently reprint this part.

Additionally, changes were made to the bottom shin. To accommodate the new 11.1V batteries, we increased its length by 18mm. This was done by introducing a new shape geometry that the design was modeled on. Meanwhile, to improve the design and reduce weight, we removed the motor mounts for the HerkuleX DRS 0201 motor in the ankle. Instead, we changed

the dimension of the part and introduced L brackets with M2 holes to connect to the motor. We also added extra extruded cuts to the part near the motor connection for ease of assembly and disassembly of the motors (Figure 10.4b). These modifications helped us create a more robust and efficient design for the shin while still accommodating the new batteries and motor requirements.

In conclusion, the redesign of the shin was a necessary and effective modification that resulted in a more durable and efficient design. The changes made to the connection points, geometry, and motor mounts were necessary to counteract the limitations of the 3D printer dimensions, and improved the overall performance of the leg.

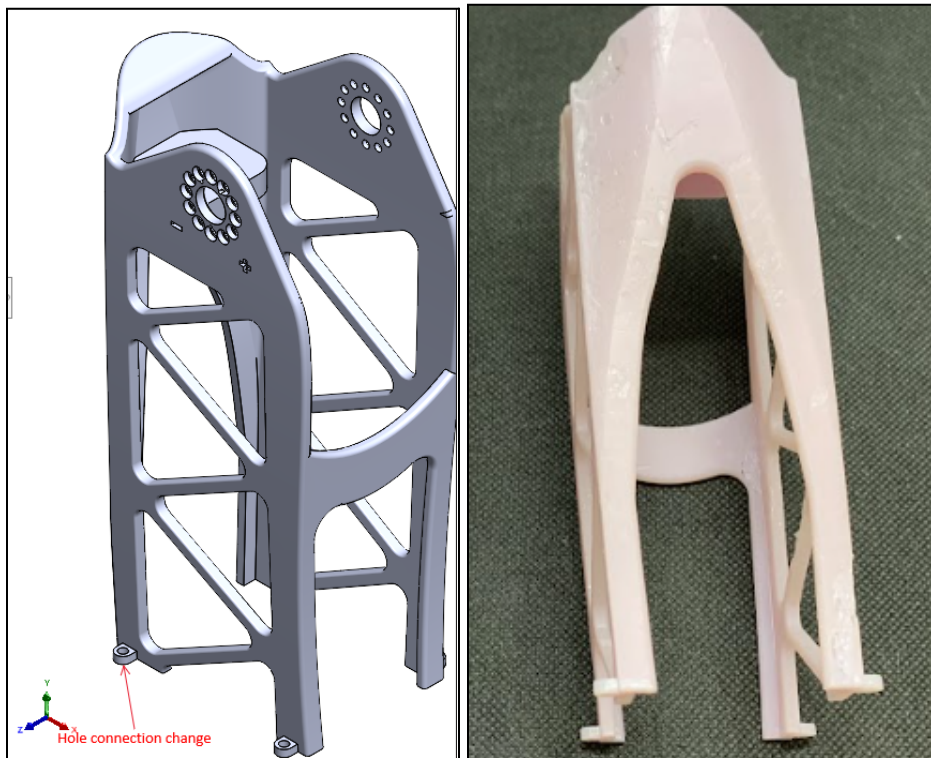


Figure 10.4a: Redesigned Top Shin Part

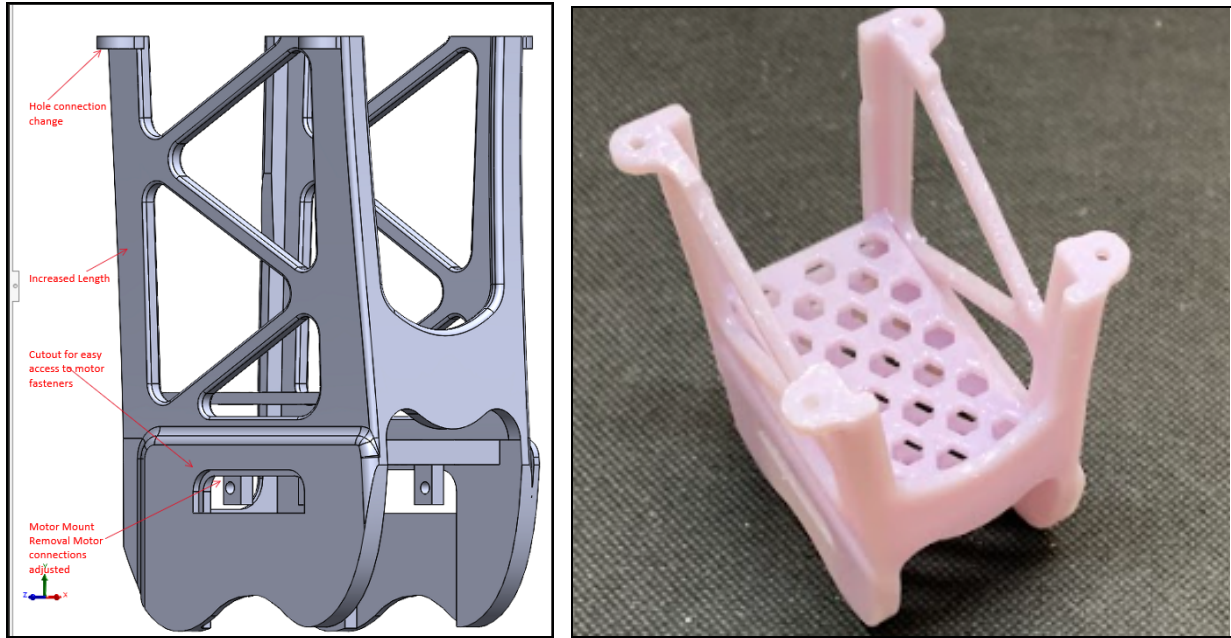


Figure 10.4b: Redesigned Bottom Shin Part

10.5 Abdomen

Changes were made to the abdomen components to fit the new HerkuleX DRS-0601 motors. The abdomen horn holder and abdomen motor connector were made 3mm wider and 5mm longer to fit the slightly larger motors and realign the fastener holes. These two pieces, shown in Figures 10.5a and 10.5b, connect the two HerkuleX DRS-0601 motors which are then encompassed by the large abdomen piece. Similar to the thigh, the large abdomen piece was adjusted to realign the servo horn holes by changing the radius of the fastener holes to 2.7mm, and decreasing the radius of the circle of holes of the motor horn by 2mm. Additionally, the hole along the top of the large abdomen piece was widened by 3 mm to provide more space for wire management. Figure 10.5c shows the large abdomen piece. Figure 10.5d shows the entire abdomen assembly, and Figure 10.5e shows where the abdomen assembly fits into the full assembly.

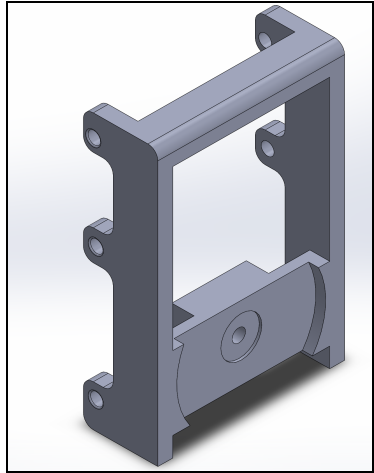


Figure 10.5a: Abdomen Horn Holder

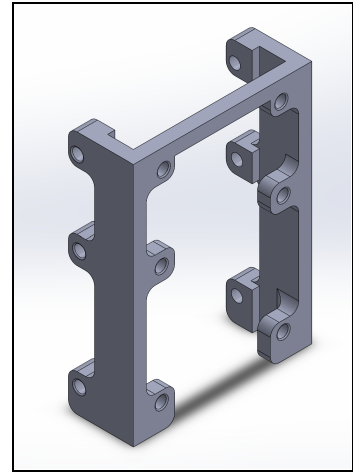


Figure 10.5b: Abdomen Motor Connector

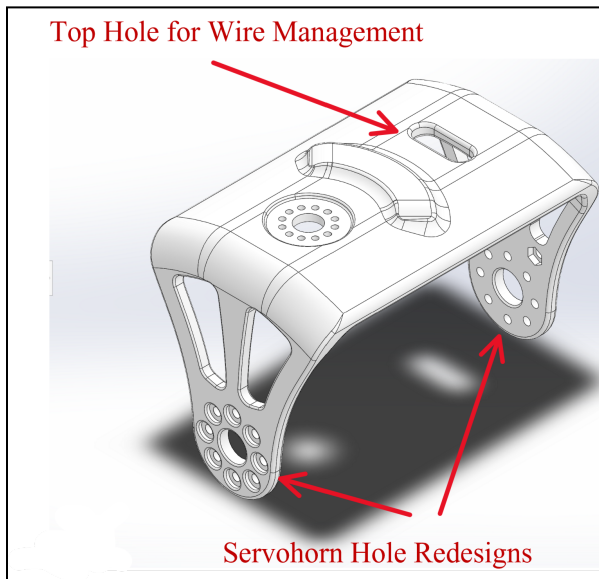


Figure 10.5c: Large Abdomen Piece

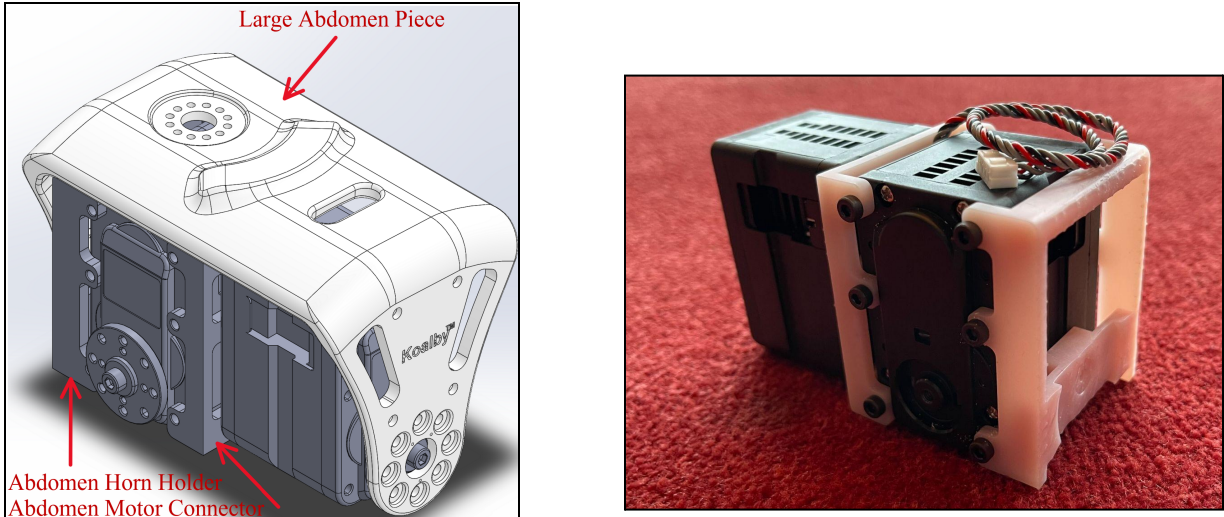


Figure 10.5d: Abdomen Assembly

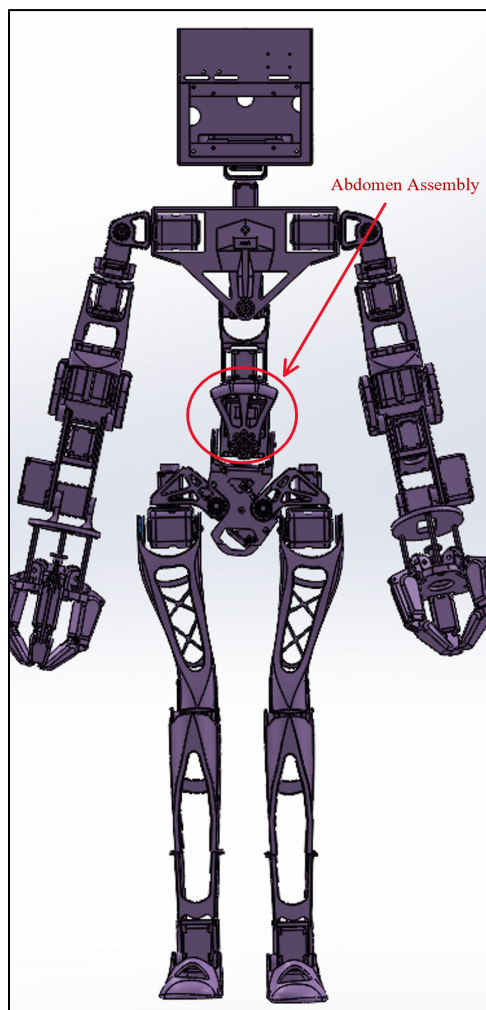


Figure 10.5e: Abdomen Location in Full Assembly

10.6 Neck

Minor changes were made to the neck for the new HerkuleX DRS-0101 motors. The radius of the fastener hole was adjusted to 2.4mm, and the radius of the circle of holes was decreased to 14mm. Figure 10.6a shows the neck piece, and Figure 10.6b shows where the neck piece fits into the head assembly.

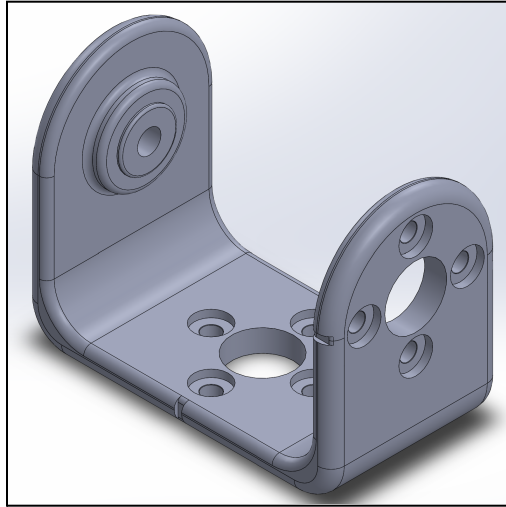


Figure 10.6a: Neck Piece

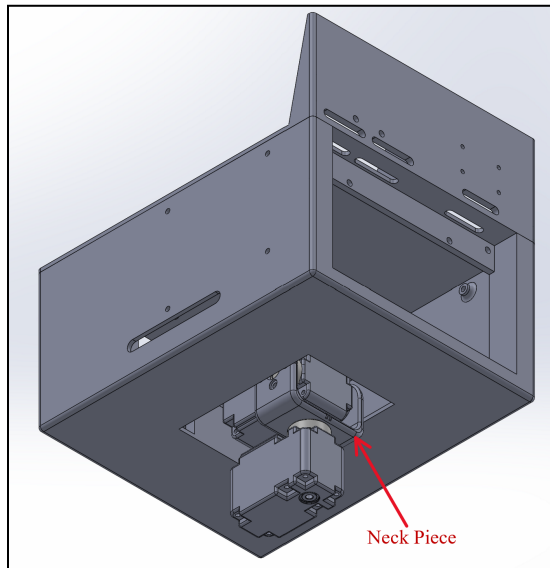


Figure 10.6b: Head Assembly with Neck Piece

10.7 Head

To incorporate the new Herkulex 0101 neck motors, the head was split into two separate parts: the head bracket (depicted in Figure 10.7a) and the head base (shown in Figure 10.7b). Originally one piece, the head was altered to allow the head bracket to be inserted through the bottom of the head base and secured in place by screws from the top down as illustrated in Figure 10.7c. Furthermore, attachments were added to the head bracket to accommodate for the new Herkulex motor. This major redesign not only allowed for the new motor attachments, but made the assembling process more manageable and less time-consuming.

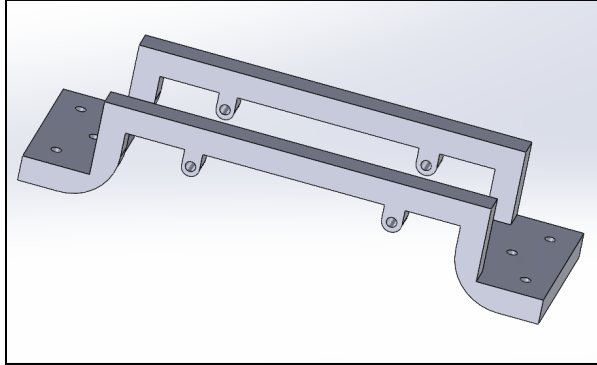


Figure 10.7a: Head Bracket

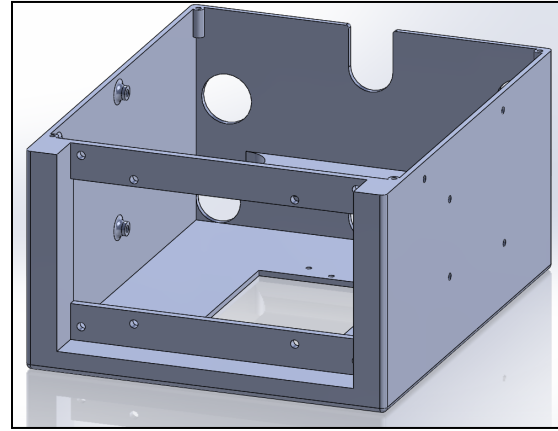


Figure 10.7b: Head Base

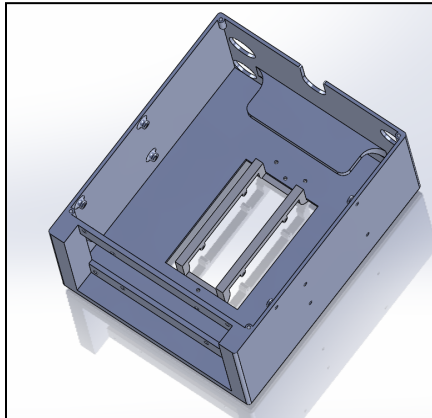


Figure 10.7c: Full Head Assembly

10.8 Shoulder and Shoulder Connector

To work with the new motors, minor changes were made to the shoulder of the arm. Specifically, the hole placement and size were adjusted to accommodate the HerkuleX DRS 0601 motor. These changes were necessary to ensure a proper fit and operation of the new motor as well as to increase its structural integrity. In addition to adjusting the hole placement and size, we also increased the thickness of the shoulder to 3mm to compensate for the different hole sizes. This was necessary to maintain the structural integrity and stability of the part and to prevent any potential deformation or breakage. Overall, the changes made to the shoulder, shown in Figure 10.8a, were minor, but necessary to ensure compatibility with the new motors. The adjustments made to the hole placement and size, as well as the thickness of the part, helped create a more robust and efficient design for the arm.

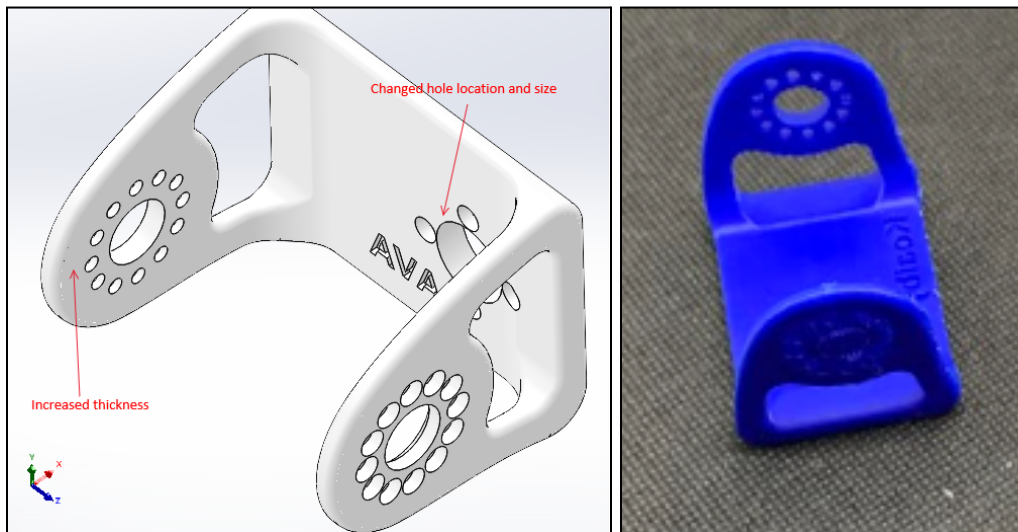


Figure 10.8a: Redesigned Shoulder Part

The shoulder connector underwent significant changes to improve its efficiency and reduce the number of components. We removed the motor mounts, which reduced the number of components and simplified the design. To accommodate this change, we increased the wall thickness to 6.8 mm to maintain the structural integrity of the part. Furthermore, we extruded the hole connection to align with the actual motor holes, which improved the accuracy and stability of the connection. This ensured proper fit and operation of the motor and reduced the likelihood of any potential damage or breakage. We also changed the cutout in the part to allow for easy

access to the fasteners, making it easier to remove and replace. This modification improved the efficiency of the assembly process and reduced the time required for maintenance and repairs.

Overall, the changes made to the shoulder connector, highlighted in Figure 10.8b, were significant and effective in improving the efficiency and simplifying the design of the arm. The removal of the motor mounts, increase in wall thickness, and modification of the cutout resulted in a more durable and easy-to-use part.

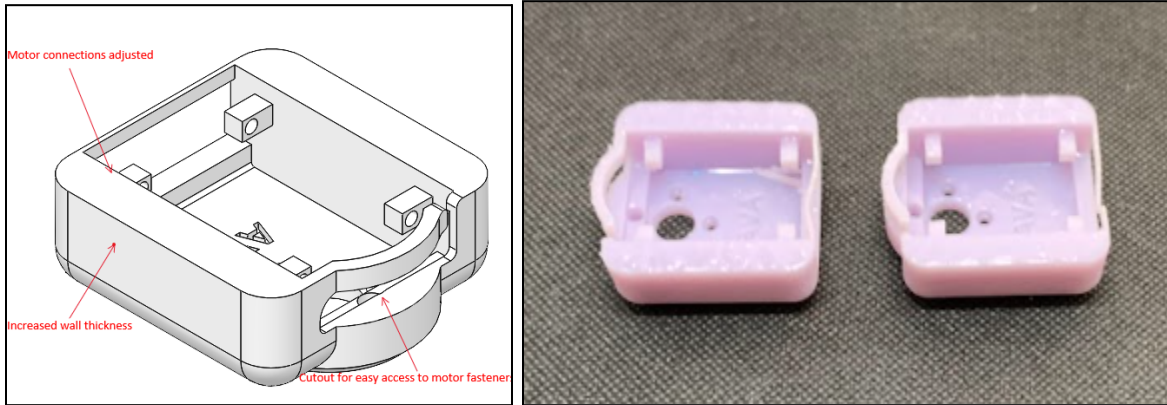


Figure 10.8b: Redesigned Shoulder Connector Part

10.9 Bicep

The bicep of the arm underwent significant changes to adjust to the new HerkuleX DRS 0601 motor and to reduce the number of parts. To accomplish this, the motor mounts were removed from the top of the bicep, and the part was extruded to align directly with the HerkuleX DRS 0201 motor holes. This was done with consideration to the stress that the part would need to withstand.

Additionally, we expanded the base of the bicep to adjust for the new HerkuleX DRS 0601 motor. Specifically, we adjusted the base of the bicep to a size of 42 x 40 mm. We then created new holes for the motors at the base to align with the 0601 motor. Overall, the changes made to the bicep, as seen in the figure below, were necessary to ensure compatibility with the new motor and improve the overall functionality of the arm. By removing the motor mounts and adjusting the base, we were able to create a more efficient and effective design (see Figure 10.9).

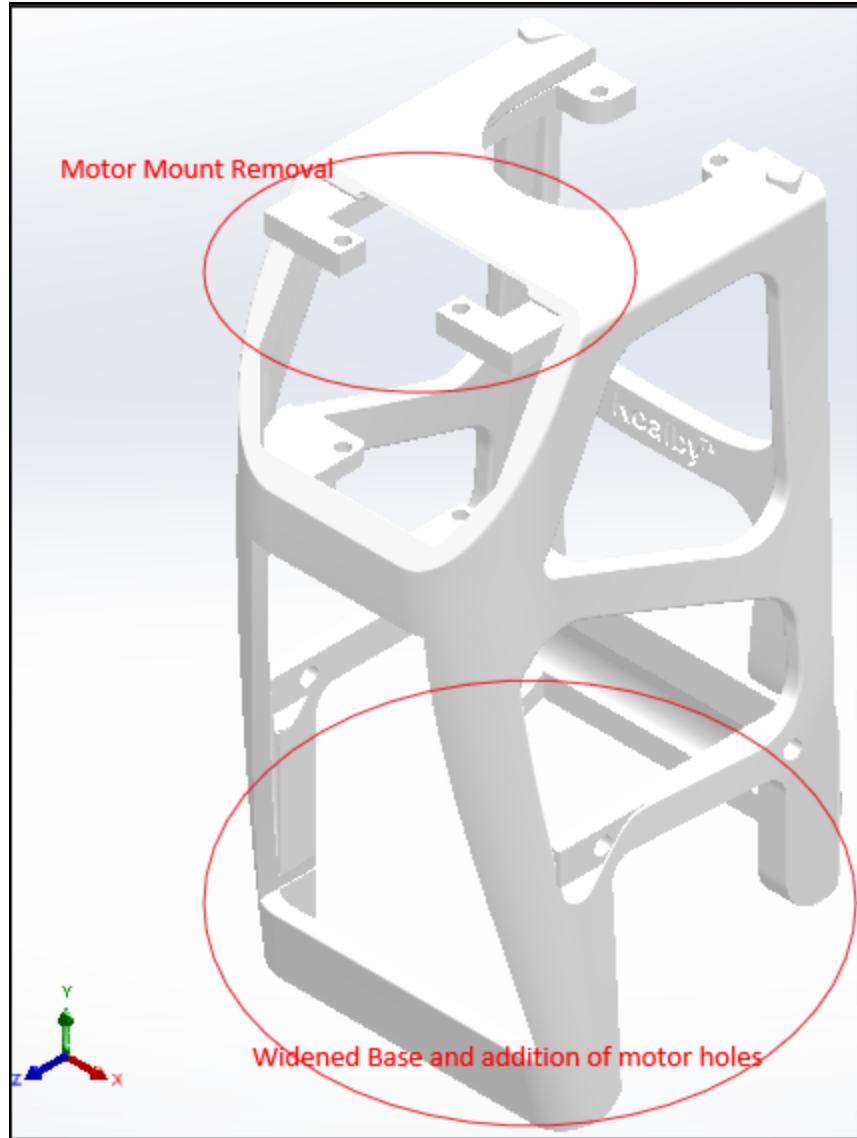


Figure 10.9a: Right Hand Bicep Piece

11.0 Manufacturing and Assembly

This section provides an overview of the manufacturing and assembly processes used to physically construct all the components of the robot and assemble the system together.

Manufacturing of the parts primarily used resin and FDM 3D printing. Resin printing was used for parts that required high resolution and more durability, while FDM 3D printing was used for larger parts that did not require high resolution or were under considerably less stress or load. These printing techniques allowed for quick and efficient production of the parts.

Assembly of the robot itself was done using various fasteners, mainly M2 and M2.6 fasteners. These were used to connect various parts of the robot together into subassemblies, including the arms, legs, torso, and head. The fasteners were chosen for their compatibility to the Herkulex DRS 0201 and 0601 motors, ensuring that the robot would remain securely assembled during operation.

During the assembly process, great care was taken to ensure that all parts were properly aligned and connected. This involved close attention to detail and careful measurement of each component to ensure that it was printed correctly and were compatible with other parts and motors (see Section 11.3).

Overall, the manufacturing and assembly processes were crucial in ensuring that the robot was constructed and assembled to the highest possible standards. The use of resin and FDM 3D printing techniques allowed for efficient production of the parts, while the use of high-quality fasteners and careful assembly ensured that the robot was durable and reliable during operation.

11.1 3D Printing

Similar to Koalby, Ava was designed to be manufactured using 3D printing so she could be an open-source 3D printed humanoid robot. To do this, two different methods of 3D printing were utilized for both prototyping and final manufacturing. These methods included Fused Deposition Modeling (FDM) and Digital Light Processing (DLP).

11.1.1 Resin 3D Printing

Resin 3D printing was a critical component of the manufacturing process for the Ava robot. Nineteen structural components used on Ava were resin DLP printed using the Elegoo Saturn and Mars2 Pro model printers. A full list of all printed parts used in the Ava robot can be found in Appendix I.

To ensure that the parts would not be brittle and could handle the stress from the weight of all the components, the team used eSun's Hard-Tough type resin. This resin type is also useful for creating longer-lasting parts because of its ability to survive wear and tear. White resin was ordered, which costs \$60 per liter for production, and epoxy resin dyes were used to make different color parts. The properties of the Hard-Tough resin are given in the table below.

Table 11.1a: Physical Properties of Hard-Tough Resin (Appendix H)

Resin	Shore Hardness	Tensile Strength (MPa)	Flexural Strength (MPa)
Hard-tough	81	50-60	70-80

The resin parts were sliced using the Chitubox Software, and multiple parts were set up on one bed to maximize print speed. An example of the print bed is shown in the figure below. The curing parameters, as well as the printing instructions, are given in Appendix H. The curing parameters were changed slightly depending on the dye color used for the parts.

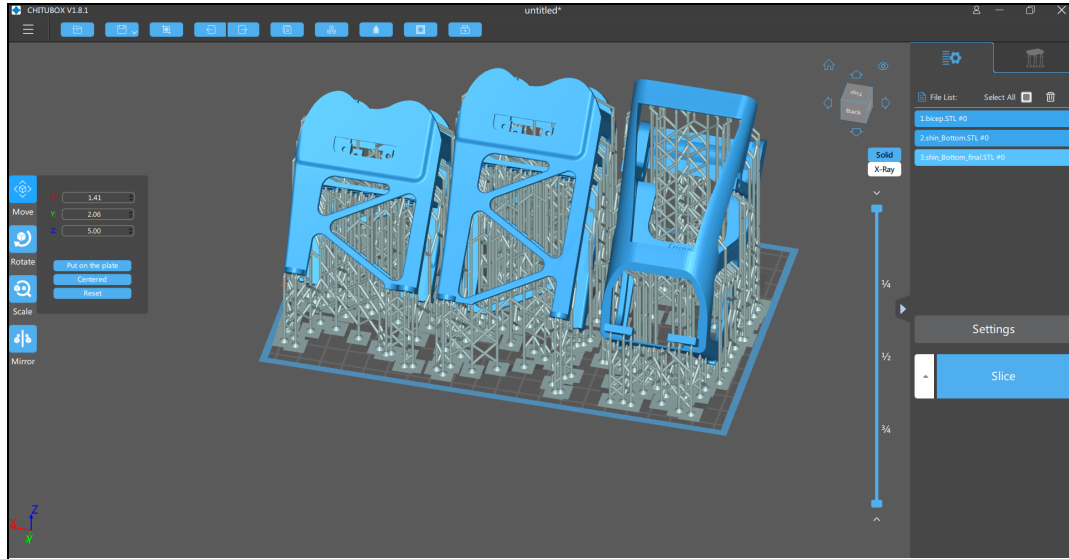


Figure 11.1a: CHITUBOX setup

Overall, Resin printing was a critical component of the manufacturing process for the Ava robot. By using high-quality resin and carefully managing the printing process, the team was able to create durable, long-lasting parts that could withstand the stresses of the robot's operation.

11.1.2 FDM 3D Printing

FDM 3D printing played a critical role in the manufacturing of 48 structural components for Ava, using both Creality Ender 3 Pro and Prusa MK3S+ printers. A list of the parts can be found in Appendix I.

The team used FDM printing with PLA material for components that were structurally sound, had less complex geometry, and were under comparatively less stress or load. Blue and Purple PLA were used, with an estimated cost of \$22 per liter for production. The physical properties of PLA are given in Appendix H. The parts were sliced using the Cura software, and multiple parts were set up on one bed at a time to maximize printing speed. The infill settings and supports varied according to the part's structure.

Overall, FDM 3D printing was an essential component of the manufacturing process for the Ava robot. By using high-quality PLA and carefully managing the printing process, the team

was able to create durable, long-lasting parts that could withstand the stresses of the robot's operation.

11.2 Assembly

The Ava robot is assembled using a total of 48 FDM and 19 resin printed components, 29 HerkuleX motors of different types, and several hundred M2-M2.6 fasteners. Full assembly, which takes approximately 24 hours excluding part print time, can be done by following the instructions in Appendix I.

The general assembly process involves setting up each motor with the required adaptors and then building subassemblies, building your way in from the limbs. The team divided the building process into multiple subassemblies, including the Head, Torso, Arm, and Leg (Figures 11.2a-11.2d). The component list and sub assembly instructions can be found in Appendix I. The full assembly of Ava is shown in Figure 11.2e.

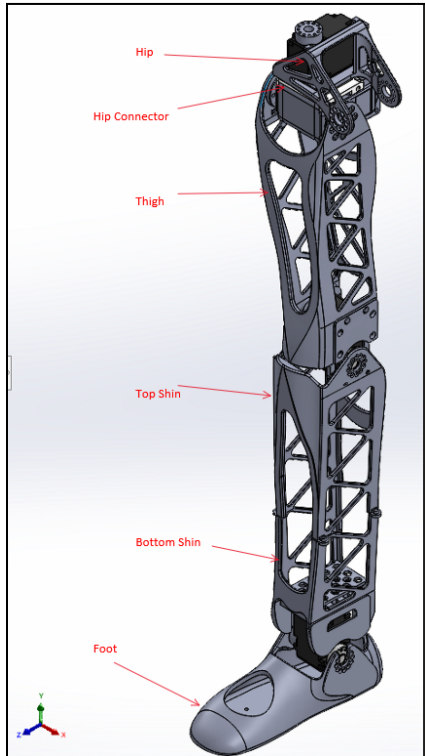


Figure 11.2a: Leg Subassembly

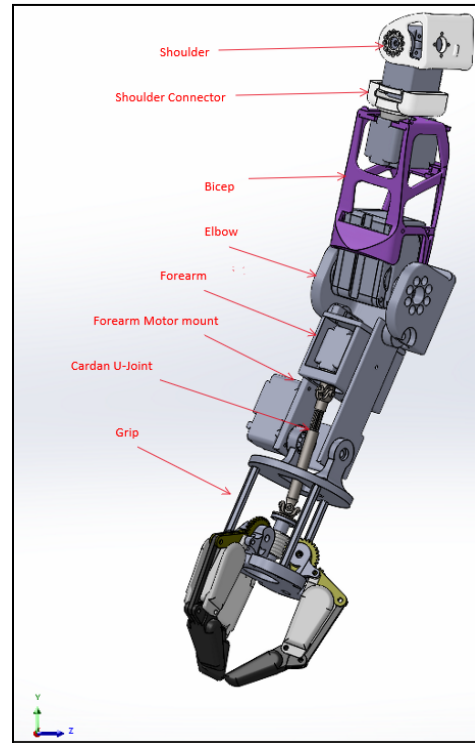


Figure 11.2b: Arm Subassembly

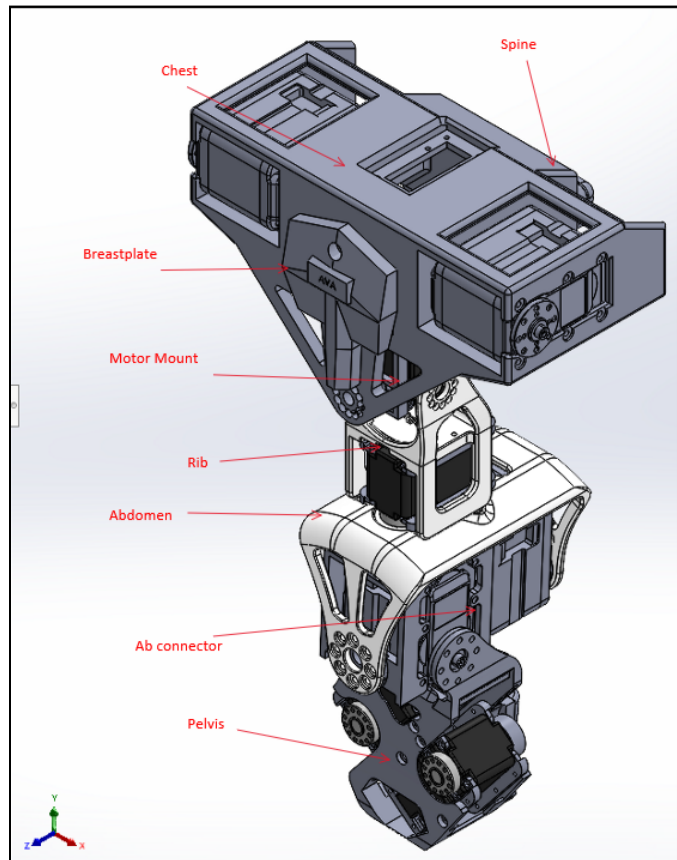


Figure 11.2c: Torso Subassembly

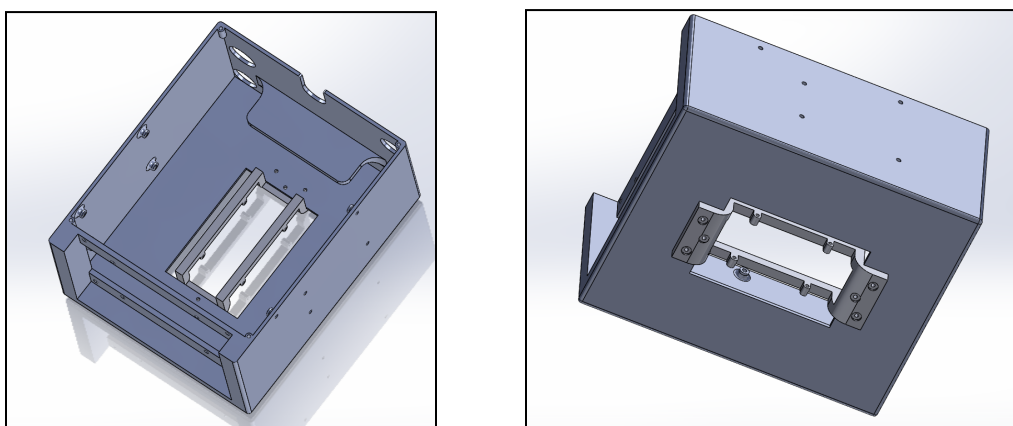


Figure 11.2d: Full Head Subassembly

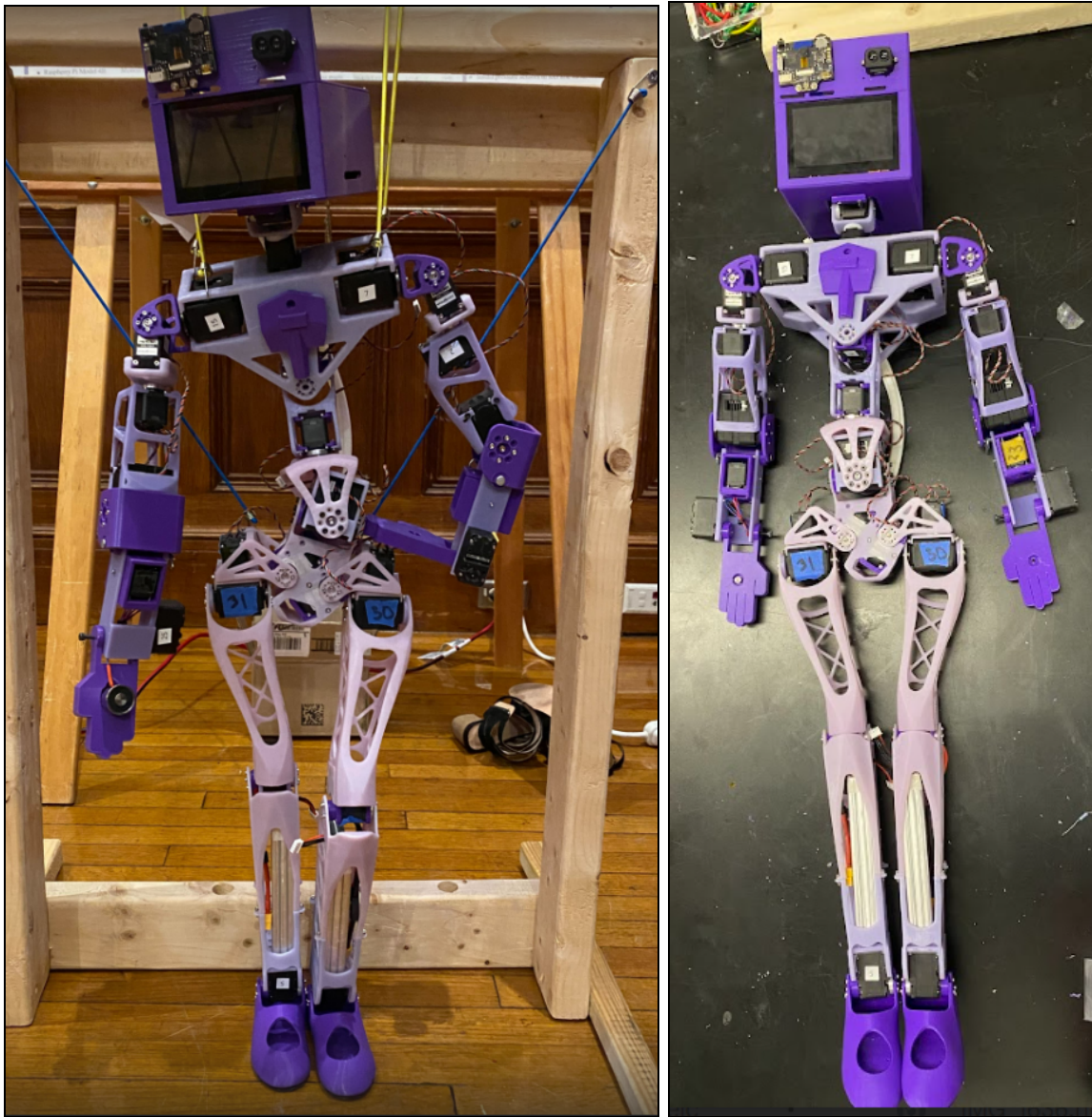


Figure 11.2e: Ava Assembly without Grip Attached

The Herkulex DRS 0101 & 0201 motors are attached to the parts via four M2 screws, and the Herkulex DRS 0601 motors are attached via four M2.6 screws. Each piece is either at the rotation axis or at the motor connection points. By carefully following the assembly instructions and properly torquing the fasteners, the Ava robot can be assembled into a fully functional system.

Overall, the assembly process for the Ava robot is complex but well-organized, with clear instructions and detailed component lists to guide the process. By carefully managing the

assembly process and properly connecting each component, the team was able to create a durable and reliable robot that can perform a range of functions. Detailed costs for the assembly can be found in Appendix K.

11.3 Part Compatibility

Throughout the printing and assembly of components, the 3D printed parts were measured and compared to their CAD measurements to understand the tolerance of the 3D printers (see the Part Compatibility Document in Appendix E). Specific areas on each part were measured where low tolerance was important (i.e. connection points and hole alignments) and where it was easiest to measure with calipers to minimize the error (i.e. flat sections rather than curves). Based on these measurement comparisons, it was determined that the most common deviation across the parts was between 0.1 and 0.4 mm. Larger deviations went up to 1.5mm which were found in the right hip and rib parts which are shown in Figures 11.3a and 11.3b. These larger deviations can be accounted for by some bowing in the parts and grooves left by the resin print supports. Deviations occurred most frequently with the fastener holes, but this can be accounted for as physical measurement errors due to the difficulty in measuring small radii with calipers. Overall, the 3D printed parts are highly compatible with minimal deviations. All of the parts were successfully assembled together, even with the higher 1.5mm deviation and bowing.



Figure 11.3a: Right Hip Deviation



Figure 11.3b: Rib Deviation

12.0 Discussion

This section reviews the original goals of this project and how we addressed each one. The main goals this team focused on achieving this year were to:

1. Improve Structural Integrity
2. Design for Walking
3. Grip Addition
4. Standardize Components

12.1 Improve Structural Integrity

This project made key changes to improve the structural integrity of the robot through analysis and redesigns of critical parts (see Section 7.1). ANSYS was used to determine areas requiring improvement, with high stress identified in the pelvis. Next, free body diagrams were created to understand the forces and moments acting on each part. This analysis was useful in providing clear visuals about how each part moved and how each motor is required in its movement. After this analysis, redesigns were made to the pelvis with 3 mm extrusions added along the sides to act as reinforcements, and a new spine was created to improve the structural integrity of the torso (see Sections 7.2 and 7.3). The new spine was designed as a flexible rod that attaches to the pelvis and chest to provide support throughout the torso (see Section 7.3). Both of these new parts were successfully printed and assembled into the new robot, Ava.

These implementations showed improvement in the structural integrity because the torso parts stopped breaking. The old pelvis design broke three times during the initial three months of the project, and the new pelvis design has been implemented for over four months and has not broken. However, due to time constraints more quantitative testing on the strength of the new parts were not completed. The next steps towards improving the structural integrity of the humanoid robots would be to first complete more testing on the physical components and then identify more components to improve.

12.2 Design for Walking

This project made key developments towards humanoid robot walking through sensor integration and related electrical and part redesigns (see Section 8). Based upon a sensor decision matrix (Table 8.1a), three sensors were chosen to be integrated into the robot's design: LiDAR TF Luna, IMU (BNO055 and MPU6050), and AI Huskylens Camera. To accommodate the addition of new sensors and motors, a new electrical diagram was constructed (see Appendix F). A series of adjustable voltage regulators and higher power 11.1V batteries were implemented for the different voltages across the sensors and motors. Additionally, a few parts were redesigned to integrate the new sensors into the design of the robot (see Section 8.3-8.5). The head lid was extended by 52mm with cutouts made to attach the Huskylens Camera and TF Luna sensor. The chest was redesigned to house an IMU near the center of mass and fit the new HerkuleX DRS-0601 motors. Lastly, the foot base was made 9.8mm wider to improve stability, PVC was attached to the bottom of the foot to improve traction, and a hole was cut into the top of each foot to create a small opening to house the MPU6050.

The sensors were successfully attached and fit to the redesigned parts. However, due to time constraints, the new electrical diagram was not completely assembled and tested. The next steps would be to finish wiring all of the new components, integrating the new systems into the circuits, and testing their functionality together.

12.3 Grip Addition

This project successfully developed an underactuated robot grip after measuring a variety of lab tools to determine the specifications required for gripping (see Section 9). The team chose an underactuated robot grip based on a grip decision matrix, and an electromagnet was integrated to assist lifting metallic objects (majority of the lab tools that we examined). This design was successfully assembled in CAD and FDM printed. The grip was physically assembled, but due to time constraints it was not tested. Next steps would be to test the functionality of the grip and then integrating it into the arm capabilities of the robot.

12.4 Standardize Components

This project successfully standardized the motors to a single brand, HerkuleX, and completed relevant redesigns to fit the new motors (see Section 10). The team performed torque analysis to determine the required torque for lifting specific lab tools, and used a motor decision matrix to choose HerkuleX brand motors. By replacing the original Dynamixel MX-64AT and AX-12 motors with HerkuleX DRS-0601 and DRS-0101, respectively, the cost was reduced by approximately \$375. The smaller size of the new motors required adjustments to several parts, including the hip, thigh, shin, abdomen, neck, head, shoulder, and biceps. The key changes made to these parts, to accommodate the new motor, were adjusting the fastener hole size and the radius of the servo horn holes to align with the new motor horns. These changes were successfully designed in CAD, 3D printed, and assembled. Due to time constraints, the new motors were not tested as part of the robot. The next steps include integrating the wiring, motors, and parts into the robot and performing load and torque testing on the new motors.

12.5 WPI Undergraduate Research Project Showcase

This project was showcased at WPI's Undergraduate Research Projects Showcase. This event allowed the team to successfully demonstrate and present the project at a higher level, speaking to WPI faculty and engineering professionals. Ava was fully assembled and displayed in a wooden support frame. Although Ava was not electronically operational, we manually demonstrated the movements of different joints throughout the robot, as well as highlight the parts that were redesigned. The team presented to WPI faculty and engineering professionals in the Mechanical and Materials Engineering Department (MME) and Robotics Engineering Department, and Ava did not experience any parts failure throughout the event. Figure 12.5a displays this team's poster presentation at the Showcase. The 2023 3D Printed Humanoid Robot Software MQP Team presented Koalby adjacent to our team at the MME presentation; Figure 12.5.b shows Ava and Koalby together.

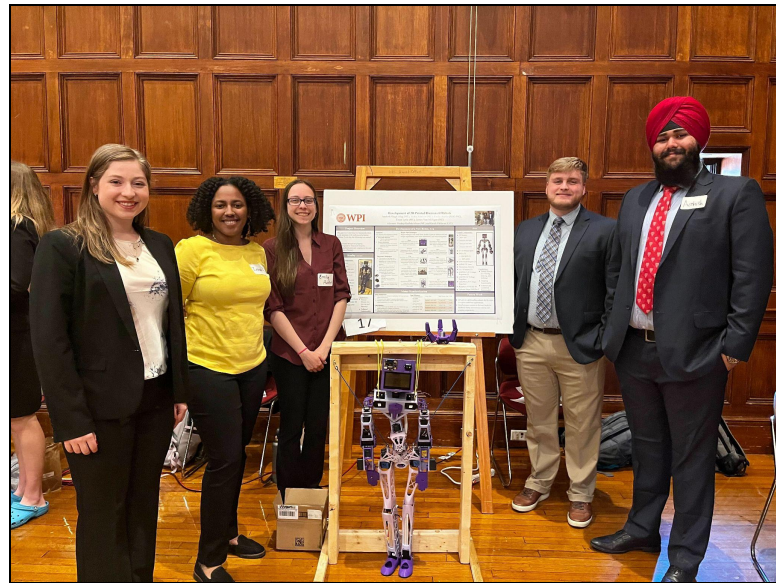


Figure 12.5a: Mechanical and Materials Engineering Department Presentation

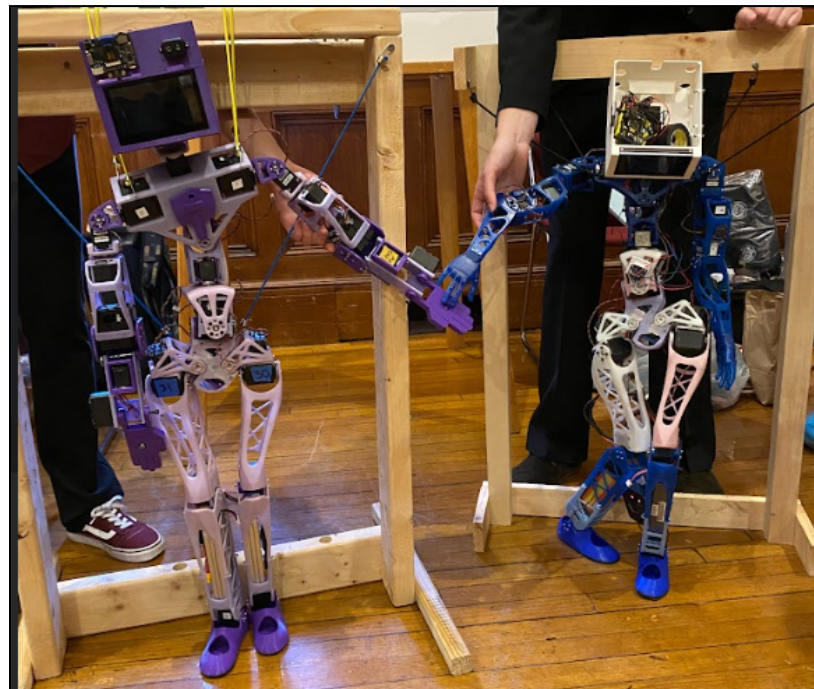


Figure 12.5b: Ava and Koalby at the Mechanical and Materials Engineering Department Presentation

13.0 Conclusions

Overall, as discussed in Section 12, this project successfully developed two open-source 3D-printed humanoid robots, Koalby and Ava, towards the application as versatile lab assistants with a focus on lifting objects, pushing a cart, and walking. Static and dynamic analyses were carried out to guide a series of redesigns to improve strength and integrate new components. A new spine was designed and integrated into Ava to improve the structural integrity of the torso. New sensors (LiDAR TF Luna, Husky Lens Camera, and IMU) were selected and integrated into the robot's design. The chest, head, and feet were redesigned to attach these new sensors. Additionally, an underactuated, 3-point finger grip with an electromagnet was designed and assembled for grasping capabilities. Lastly, all of the Dynamixel motors were replaced with HerkuleX DRS motors allowing for uniformity in design and programming and reduced the cost by $\sim \$375$. Various parts throughout the robot were redesigned to accommodate the new motors (i.e. abdomen, hip, thigh, etc.). These designs were created in Solidworks, then 3D printed and assembled. This project successfully assembled a new robot, Ava, which was demonstrated at WPI's Undergraduate Research Project Showcase. The modifications made on Ava were retro-fitted on Koalby to also improve its functionality and structural integrity.

The following section will cover how this project can be taken to a broader level and affects people and economics. Lastly, we will cover the future work that the robot can undergo.

13.1 Broader Impacts

The development of the humanoid robot has implications that go beyond the technical aspects of the project. As such, this section aims to reflect on the broader impacts of the project on people, culture, the environment, and economics.

13.1.1 Social and Global Impact

Individuals and groups of people can be significantly affected by the field of humanoid robotics. One anticipated outcome for this project was improving the interaction between humans and robots in a more intuitive manner. These types of interactions have important implications in the manufacturing and healthcare industries. The robot is designed to handle complicated activities such as aiding in lab conditions and dealing with patients in the healthcare

setting. This can increase both human and environmental safety. This robotic project, however, has unexpected repercussions. Increased use of robots in the workplace can result in job displacement leading to a negative impact on individuals' and communities' social and economic lives.

13.1.2 Environmental Impact

The materials used in building this humanoid robot have several potential impacts on the environment. The team used resin printing as well as IPA for the making and curing of the 3D printed parts. These components can have negative environmental effects if not stored or disposed properly. Keeping this in consideration, the team has taken measures to handle and dispose of these components safely. Additionally, we switched to FDM printing for several components to reduce the use of hazardous material; PLA is comparatively safer and more environmentally friendly than resin. Furthermore the robot's ability to handle certain hazardous materials or other such things in labs may help lessen the environmental damage caused by harmful substances.

13.1.3 Economical Impact

Considering the cost of manufacturing and application in the field, the team has created an open source 3D printed design. Usually, the humanoid robotics field is limited due to the excessive cost associated with the hardware components. This project utilized 3D printing, specially FDM printing, which is readily available to the public to make it easy to manufacture. The use of economical motors for this project has increased its potential to be used in various industries. This project demonstrates that the small scaled 3D printed Humanoid robot can be produced to work just as well as their larger market counterparts.

The humanoid robot project has a substantial overall influence, and it is crucial to take into account the project's effects on people, society, the environment, and economics. The team has worked to make sure the robot was created responsibly and with consideration for society's and the environment's welfare.

13.2 Future Work

This section will discuss recommendations we have for future work on the robots such as more testing, implementation of pressure sensors, and creation of hazardous resistances.

13.2.1 Testing

As outlined in the Analysis and Testing sections (Section 7.1 and 8.1), our team has conducted individual tests on various electronic components to ensure their proper functioning. However, due to time limitations, the grips and spine components were not implemented on the Koalby robot in time to conduct testing. This has left us unable to test the compatibility of the gripper in picking up objects, as well as the accuracy of the torque values calculated. Similarly, we have not been able to test the spine's ability to provide additional stability, balance, and support in bending motion.

In addition to testing the gripper and spine, we have also added new features to our electronics setup. The group has tested and trained the various sensors, AI camera, electromagnet, and motors individually. These components have been fully integrated into the humanoid robot. Moving forward, we hope the project conducts further integrated testing of the components to ensure compatibility and coordination of these electronics. Also to see whether the implementation of these components further align with our project goals. This will involve testing the functionality and performance of the arm as a whole, assisted walking, and navigating through a lab environment. Additionally, we plan to calibrate the compatibility of the components to ensure optimal performance and functionality. This may involve adjusting the programming or settings of the components to better align with the goals of the project.

13.2.2 Pressure Sensors

Another area of future work for the humanoid robot involves implementing pressure sensors in the feet and hands to aid in autonomous walking and gripping [36]. Currently, the gripping mechanism works with a start-stop function for the motors, but the integration of pressure sensors on the fingers will provide feedback to help improve the gripping function. The ability of robots to touch and feel objects is a critical area of research in robotics, mimicking the behavior of human touch. Adding pressure sensors to the fingers, the robot can better sense the

pressure and force being applied to the object and adjust its grip accordingly. In addition to the hands, adding pressure sensors to the feet can help create a more bio-inspired feet design to improve balance and stability. The contact forces measured by the sensors can be used to determine the manipulation of the robot. Overall, the implementation of pressure sensors in the feet and hands is an important area of future work for the humanoid robot. This will mimic human touch and add more advanced sensing capabilities.

13.2.3 Hazardous Resistance

Another area of future work for the humanoid robot is creating hazard resistance solutions to enable the robot to operate in a variety of environments, thus increasing its range of applications [37]. One possible solution is to create a waterproof suit that can protect the robot's electronics and actuators from water damage. Typically, for humanoid robots, this suit is made from a silicone rubber coating and a pressure-compensated air chamber that provides buoyancy to the robot. However, this requires a hybrid control approach that combines a model-based control method and a sensory feedback control method. A sensory feedback control would improve the stability of the robot's walking motion and reduce the impact of the reaction forces from the water. Alternatively, a lower scale approach could be to install a water-resistant coating on the robot's components, actuators, and wiring. This coating can be achieved using sealant or epoxy and will protect the robot's electrical components from water damage as well. Although, it is important to ensure that the coating does not restrict the motion of the robot. Another area of concern is heat resistance, and this can be addressed by changing the wiring and insulating the actuators and other electrical components. Additionally, different types of materials for 3D printing can be explored, such as resins that can create parts for high-temperature environments but may be slightly weaker than the current materials being used. Identifying the right mix ratio for these materials would be helpful in creating a more heat-resistant robot. Overall, creating hazard resistance solutions for the humanoid robot is an important area of future work that will enable it to operate in a wider range of environments and increase its potential applications.

14.0 References

1. I. Pavan, S. Sikka, M. Garg, and M. Pandey, "A BRIEF REVIEW OF RECENT ADVANCEMENT IN HUMANOID ROBOTICS RESEARCH." Available: <https://pal-robotics.com/wp-content/uploads/2020/08/A-BRIEF-REVIEW-OF-RECENT-ADVANCEMENT-IN.pdf>
2. "Poppy Project - Poppy Humanoid," Poppy-project.org, 2016. <https://www.poppy-project.org/en/robots/poppy-humanoid/> (accessed Apr. 30, 2023).
3. R. Beazley, W. Engdahl, D. Fournet, A. Galgano, and A. Lehman , 3D Printed Humanoid Robot Project, Worcester Polytechnic Institute, Worcester, MA, USA, Tech. Rep 65291 E-project-042822-123507, April. 2022.
4. Agility Robotics "Robots," Agility Robotics. 2022. [Online]. Available: <https://agilityrobotics.com/robots>. [Accessed: 22-Nov-2022].
5. Kawada Robotics, "Concept," NEXTAGE, 2022. [Online]. Available: <http://nextage.kawada.jp/en/concept/>. [Accessed: 22-Nov-2022].
6. D. Merkusheva, "Top 10 Examples of Humanoid Robots," ASME, 25-Mar-2020. [Online]. Available: <https://www.asme.org/topics-resources/content/10-humanoid-robots-of-2020#:~:text=Humanoid%20robots%20are%20used%20for,%2C%20public%20relations%2C%20and%20healthcare>. [Accessed: 22-Nov-2022].
7. Macco Robotics, "Kime: Macco: Robotics Technology for hospitality: Spain," Maccorobotfoodtech, 2022. [Online]. Available: <https://www.maccorobotics.com/robot-camarero-kime?lang=en>. [Accessed: 22-Nov-2022].
8. Dwarakanath, Nagarjun (22 January 2020). "Gaganyaan mission: Meet Vyommitra, the talking human robot that Isro will send to space". India Today. 22-Jan-2020. [Online]. Available: <https://www.indiatoday.in/science/story/gaganyaan-vyommitra-talking-humanoid-isro-space-1639077-2020-01-22>. [Accessed: 22-Nov-2022].
9. Hanson Robotics, "Sophia," Hanson Robotics, 01-Sep-2020. [Online]. Available: <https://www.hansonrobotics.com/sophia/>. [Accessed: 22-Nov-2022].

10. E. Guizzo, “Iran unveils its most advanced humanoid robot yet,” IEEE Spectrum, 18-Aug-2022. [Online]. Available: <https://spectrum.ieee.org/iran-surena-iv-humanoid-robot>. [Accessed: 22-Nov-2022].
11. E. Brown, N. Rodenberg, J. Amend, H. M. Jaeger, A. Mozeika, E. Steltz, M. R. Zakin, and H. Lipson, “Universal Robotic Gripper Based on the Jamming of Granular Material,” The Proceedings of the National Academy of Sciences (PNAS), 25-Oct-2010. [Online]. Available: <https://www.pnas.org/doi/10.1073/pnas.1003250107>. [Accessed: 22-Nov-2022].
12. “Jamming Gripper,” Creative Machines Lab - Columbia University. [Online]. Available: <https://www.creativemachineslab.com/jamming-gripper.html#:~:text=Gripping%20and%20holding%20of%20objects,properties%20remains%2C%20however%2C%20challenging>. [Accessed: 22-Nov-2022].
13. “3-Finger Adaptive Robot Gripper,” Wevolver. [Online]. Available: <https://www.wevolver.com/specs/3-finger.adaptive.robot.gripper>. [Accessed: 22-Nov-2022].
14. K. J. U. D. O. M. Thingiverse.com, “3-finger robot gripper,” Thingiverse. [Online]. Available: <https://www.thingiverse.com/thing:3945968>. [Accessed: 02-May-2023].
15. Y. Tlegenov, K. Telegenov, and A. Shintemirov, “An open-source 3D printed underactuated robotic gripper - Alaris,” An Open-Source 3D Printed Underactuated Robotic Gripper. [Online]. Available: https://www.alaris.kz/wp-content/uploads/2014/10/MESA14_114.pdf. [Accessed: 22-Nov-2022].
16. R. R. Ma and A. M. Dollar, “Yale OpenHand Project - Optimizing Open-Source Hand Designs for Ease of Fabrication and Adoption,” YALE OPENHAND PROJECT, Mar-2017. [Online]. Available: https://www.eng.yale.edu/grablab/pubs/Ma_RAM2017.pdf. [Accessed: 22-Nov-2022].
17. L. Reese, “The working principle, applications and limitations of ultrasonic sensors,” Microcontroller Tips, 06-Aug-2019. [Online]. Available: <https://www.microcontrollertips.com/principle-applications-limitations-ultrasonic-sensors-faq/>. [Accessed: 02-May-2023].

18. "IR led sensor IR transmitter and IR receiver," [indiamart.com](https://www.indiamart.com/proddetail/ir-led-sensor-ir-transmitter-and-ir-receiver-19971311412.html). [Online]. Available: <https://www.indiamart.com/proddetail/ir-led-sensor-ir-transmitter-and-ir-receiver-19971311412.html>. [Accessed: 02-May-2023].
19. "CUAV TF-Luna Lidar Module: Short range distance sensor," CUAV Official Store. [Online]. Available: <https://store.cuav.net/shop/luna-lidar/>. [Accessed: 02-May-2023].
20. S Adarsh et al 2016 IOP Conf. Ser.: Mater. Sci. Eng. 149 012141
21. C. K J and A. V M, "Investigation on Accuracy of Ultrasonic and LiDAR for Complex Structure Area Measurement," 2022 6th International Conference on Trends in Electronics and Informatics (ICOEI), Tirunelveli, India, 2022, pp. 134-139, doi: 10.1109/ICOEI53556.2022.9777233.
22. "Micro bit lesson - using the Ultrasonic module," Micro bit Lesson - Using the Ultrasonic Module " [osoyoo.com](https://osoyoo.com/2018/09/18/micro-bit-lesson-using-the-ultrasonic-module/), 18-Sep-2018. [Online]. Available: <https://osoyoo.com/2018/09/18/micro-bit-lesson-using-the-ultrasonic-module/>. [Accessed: 02-May-2023].
23. B. Schweber, "Lidar and time of flight, part 2: Operation," *Microcontroller Tips*. [Online]. Available: <https://www.microcontrollertips.com/lidar-and-time-of-flight-part-2-operation/>. [Accessed: 02-May-2023].
24. "Pressure sensors," Pressure Sensors | What is a Pressure Sensor? [Online]. Available: <https://www.futek.com/store/pressure-sensors>. [Accessed: 02-May-2023].
25. "Force sensor," FUTEK. [Online]. Available: <https://www.futek.com/force-sensor>. [Accessed: 02-May-2023].
26. "Tactile Pressure Sensor Solutions," *Tekscan*. [Online]. Available: <https://www.tekscan.com/tactile-pressure-sensor-solutions>. [Accessed: 02-May-2023].
27. T. Agarwal, "Force sensing resistor - how it works and its applications," *ElProCus*, 28-May-2020. [Online]. Available: <https://www.elprocus.com/force-sensing-resistor-technology/>. [Accessed: 02-May-2023].
28. J. Hrisko, "Gyroscope and accelerometer calibration with Raspberry Pi," *Maker Portal*, 25-Jul-2022. [Online]. Available: <https://makersportal.com/blog/calibration-of-an-inertial-measurement-unit-imu-with-raspberry-pi-part-ii>. [Accessed: 02-May-2023].

29. *Electromagnets*. [Online]. Available: <https://ece.northeastern.edu/fac-ece/nian/mom/electromagnets.html>. [Accessed: 02-May-2023].
30. M. B. Naf, A. S. Koopman, S. Baltrusch, C. Rodriguez-Guerrero, B. Vanderborght, and D. Lefeber, "Passive back support exoskeleton improves range of motion using flexible beams," *Frontiers in Robotics and AI*, vol. 5, 2018.
31. M. Abdoli-Eramaki, J. M. Stevenson, S. A. Reid, and T. J. Bryant, "Mathematical and empirical proof of principle for an on-body personal lift augmentation device (PLAD)," *Journal of Biomechanics*, vol. 40, no. 8, pp. 1694–1700, 2007.
32. S. Toxiri, J. Ortiz, J. Masood, J. Fernandez, L. A. Mateos, and D. G. Caldwell, "A wearable device for reducing spinal loads during lifting tasks: Biomechanics and Design Concepts," *2015 IEEE International Conference on Robotics and Biomimetics (ROBIO)*, Dec. 2015.
33. J.A. Travieso-Rodriguez, Ramón Jerez-Mesa, Jordi Llumà Fuentes, Oriol Traver-Ramos, G. Gómez-Gras, and J. Rovira, "Mechanical Properties of 3D-Printing Polylactic Acid Parts subjected to Bending Stress and Fatigue Testing," *Materials*, vol. 12, no. 23, pp. 3859–3859, Nov. 2019, doi: <https://doi.org/10.3390/ma12233859>.
34. "An Open-Source Design of ALARIS Hand: A 6-DOF Anthropomorphic Robotic Hand | ALARIS," Alaris.kz, 2021. <https://www.alaris.kz/research/robot-hand/> (accessed May 01, 2023).
35. "Bionic_Robot_Hand_SKU__ROB0142_&_ROB0143-DFRobot," Dfrobot.com, 2017. https://wiki.dfrobot.com/Bionic_Robot_Hand_SKU__ROB0142_%26_ROB0143 (accessed May 01, 2023).
36. D. Lanigan and Y. Tadesse, "Low Cost Robotic Hand that Senses Heat and Pressure." Available: https://personal.utdallas.edu/~yonas.tadesse/data/ASEE_David.pdf
37. Y. Kojio et al., "Walking control in water considering reaction forces from water for humanoid robots with a waterproof suit," 2016 IEEE/RSJ International Conference on Intelligent Robots and Systems (IROS), Daejeon, Korea (South), 2016, pp. 658-665, doi: 10.1109/IROS.2016.7759123.

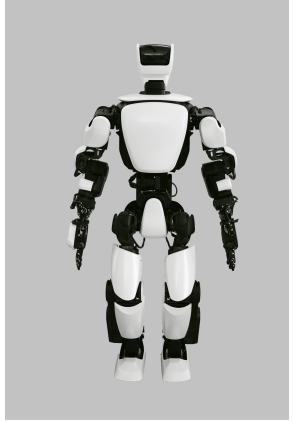
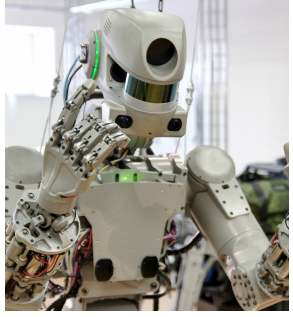
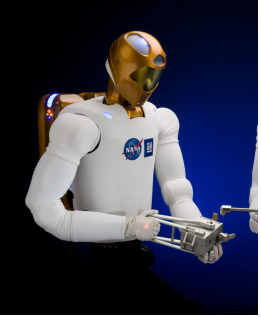
15.0 Appendices

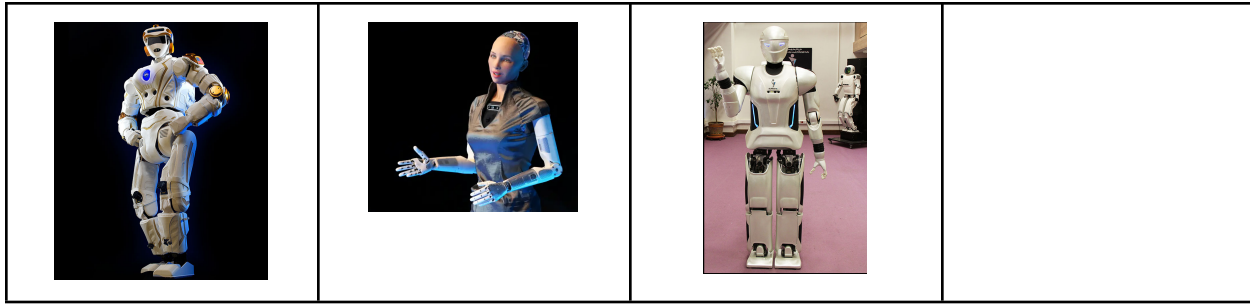
Appendix A Inventory

2022 MQP Supply Inventory

<https://docs.google.com/spreadsheets/d/1DgPiGQI4Hf66-sBon0um66BFSF47vr81UEjenN9kgmg/edit?usp=sharing>

Appendix B Humanoid Robot Application Pictures [6]

Digit (Ford Agility Robotics)	Nextage (Kawada Robotics)	T-HR3 (Toyota)	Kime (Macco Robotics)
			
Robotthespian	Vyammitra	Fedar	Robonaut 2 (NASA)
			
Valkyrie (NASA)	Sophia (Hanson Robotics)	Surena Robot (Iranian U)	



Appendix C Motor Movement Document

[☰ Motor Movement Document](#)

https://docs.google.com/document/d/1t_tMYS2VJ8auvmziVj6BmER5SNj7-b6WeYrIBfdJQM0/edit?usp=sharing

Appendix D Motor Specification Document

[☰ Motor Specification Document](#)

<https://docs.google.com/document/d/1I1Hc6FP-tjp3pim-tCEq7YIs4dnraPDDKmUtI4nidCU/edit?usp=sharing>

Appendix E Part Compatibility Document

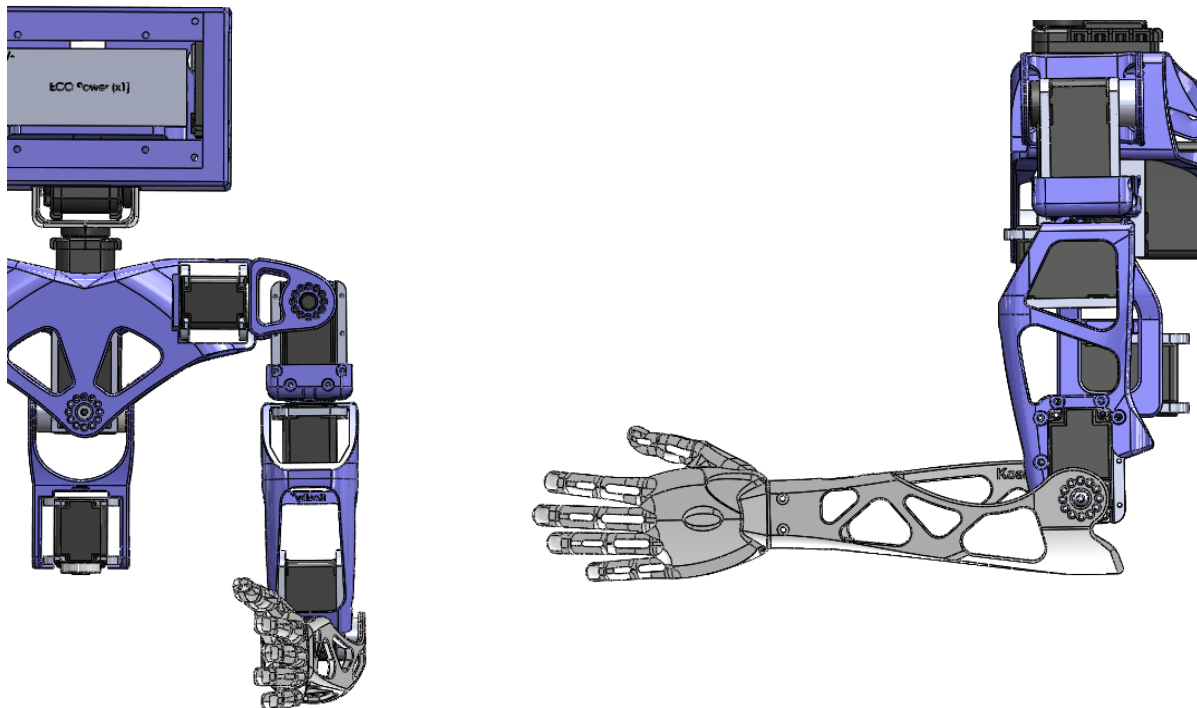
[☰ Parts Compatibility Document](#)

<https://docs.google.com/document/d/17o6BcccyMc62BL-O63BmJTNmalAvtsnJOqrDzYaHBxE/edit?usp=sharing>

Appendix F Torque Analysis

Elbow Torque: Arm is resting at the side and the elbow is bent 90 degrees upward.

Stall Torque (Herkulex 0201 2.25 Nm)	Object Mass It Can Lift
15%	0.1965 kg
20%	0.2765 kg
100%	1.555 kg

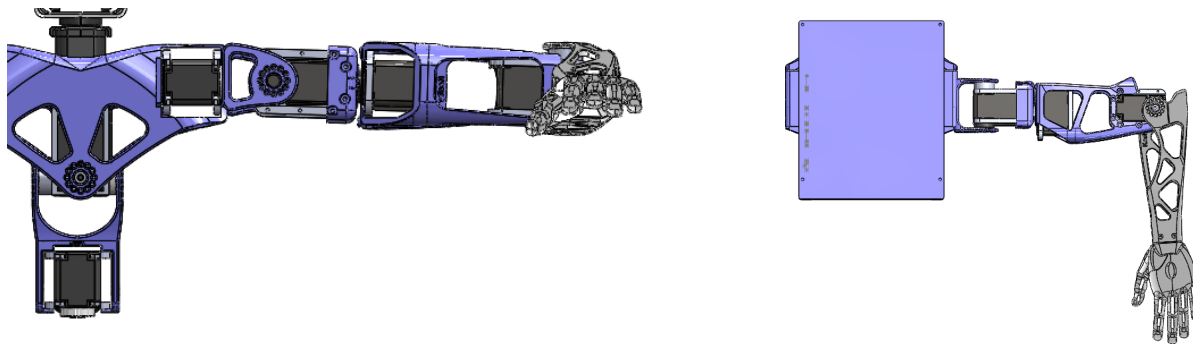


Shoulder Torque (y-axis): At the shoulder, the arm was held straight out to the right (horizontal) and the palm of the hand was rotated to face the ceiling.

Stall Torque (Herkulex 0201 2.25 Nm)	Object Mass It Can Lift
15%	0.0282 kg
20%	0.0712 kg
100%	0.7562 kg

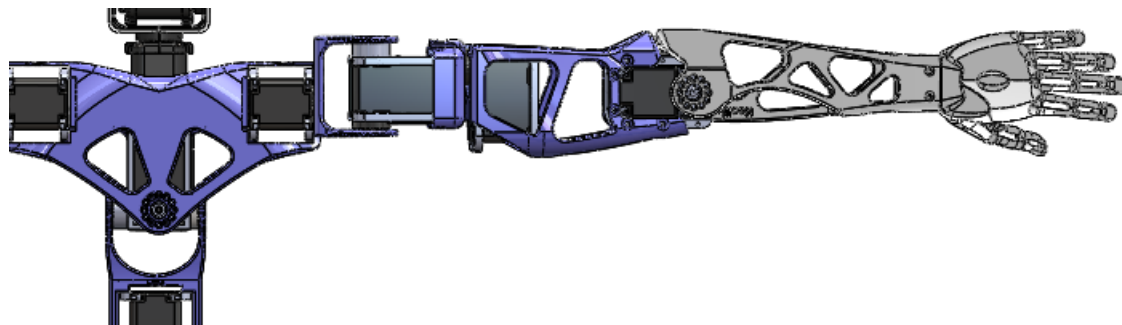
Shoulder Torque (x-axis): At the shoulder, the arm was held out straight to the right (horizontal) and the elbow was bent inwards 90 degrees where the palm was facing the ground.

Stall Torque (Herkulex 0201 2.25 Nm)	Object Mass It Can Lift
15%	0.0883 kg
20%	0.1363 kg
100%	0.9036 kg



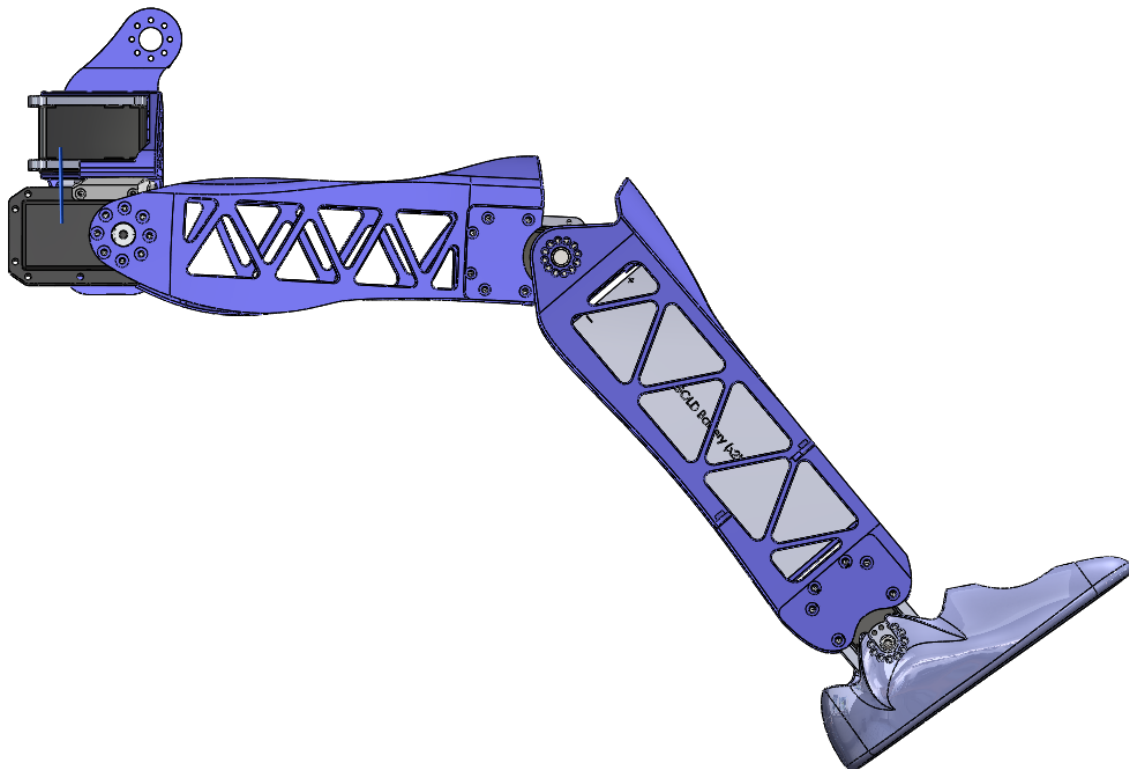
Chest Torque: At the shoulder, the arm was held out straight to the right (horizontal) and analysis was done about the central chest connection point.

Stall Torque (Herkulex 0201 2.25 Nm)	Object Mass It Can Lift
15%	X
20%	X
25%	0.0167 kg
100%	0.466 kg

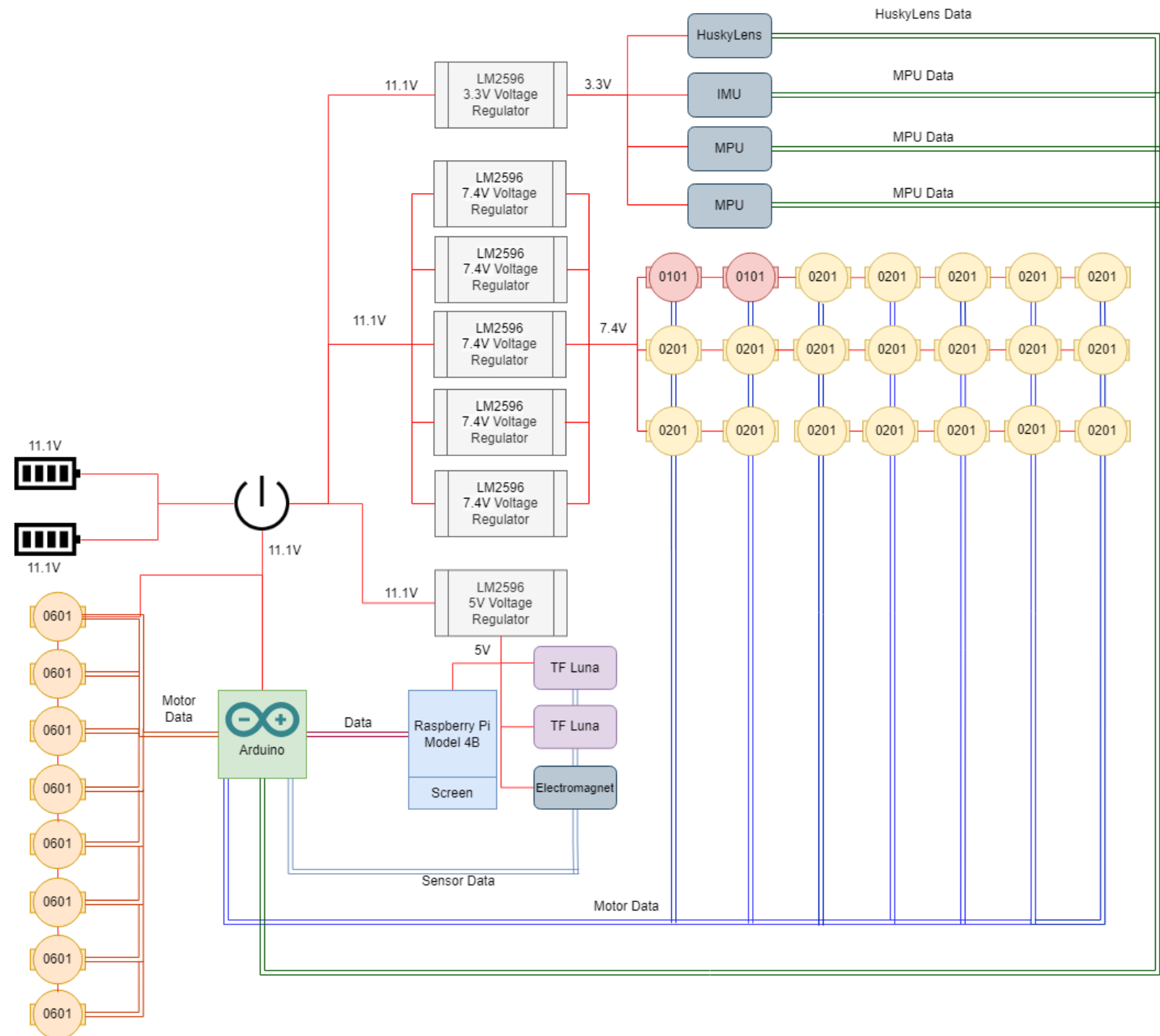


Leg Torque: Hip was bent upward 90 degrees, and the knee joint was bent downward to create a 45 degree inner angle.

Stall Torque Required to Lift Leg	Effort
1.3256 Nm	22.09%



Appendix G Electrical Diagram



Appendix H Printing Instructions

≡ Resin Printing Instructions

<https://docs.google.com/document/d/11REVxVn9yu2nXOchMf71bWQNSrN6A06C9SHvIzH0gLY/edit?usp=sharing>

✚ Resin compilation

<https://docs.google.com/spreadsheets/d/1KGv8B-8bG0lBbjzGa6qWPI-ITU9boGEJpVthxSiCs8/edit?usp=sharing>

Appendix I Assembly Instruction

≡ Ava Assembly Instructions

<https://docs.google.com/document/d/1Iv-MHw6AQRQZD2wzTs-EYQzZQxsOkkywe8XIPgF5b0M/edit#heading=h.11b7prq07nfd>

Appendix J CAD assembly

The CAD files and assemblies are saved in a OneDrive folder:

https://wpi0-my.sharepoint.com/:f/g/personal/aalag_wpi_edu/Ek3svFb1NeNGgxXppn0E04QBXQr0nkAOBMFzDqjv_g2_Cw?e=eOCp3h

Appendix K Cost

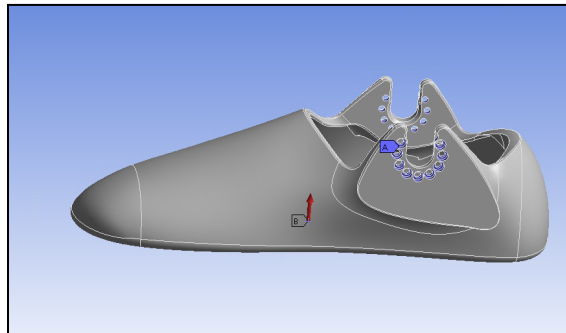
Here is a table of the components of the robot with their respective cost.

Component	Unit Cost	Quantity	Total Cost
3D Printed Parts (FDM)	\$21.45	1	\$21.45
3D Printed Parts (Resin)	\$73.95	1	\$73.95
Motors			
HerkuleX DRS 0101	\$40.00	2	\$80.00
HerkuleX DRS 0201	\$132.00	19	\$2,508.00
HerkuleX DRS 0601	\$320.00	8	\$2,560.00
Hardware			
"18-8 Stainless Steel Socket Head Screw M2 x 0.4 mm Thread, 8 mm Long"	\$8.10	2 packs	\$16.20

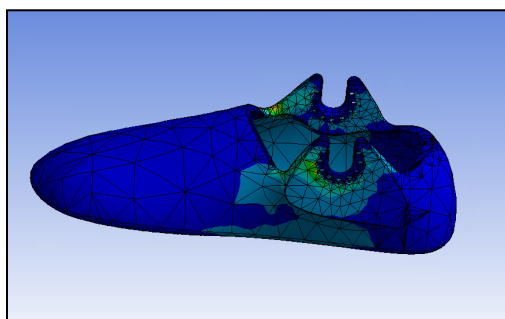
"Alloy Steel Socket Head Screw Black Oxide, M2.6 x 0.45 mm Thread, 6 mm Long"	\$11.18	4 packs of 25	\$44.72
"18-8 Stainless Steel Socket Head Screw M4 x 0.7 mm Thread, 6 mm Long"	\$7.63	1 pack of 100	\$7.63
18-8 Stainless Steel Hex Nut M2 x 0.4 mm Thread	\$6.14	1 pack of 100	\$6.14
"18-8 Stainless Steel Socket Head Screw M2 x 0.4 mm Thread, 8 mm Long"	\$8.10	2 packs of 100	\$16.20
Adjustable Clevis Pin, Zinc-Plated 1004-1045 Carbon Steel, 3/16" Diameter, 2.5" Long	\$6.59	1 pack of 10	\$6.59
Zinc-Plated Alloy Steel Socket Head Screw, M2 x 0.4 mm Thread, 12 mm Long	\$16.63	1 pack of 100	\$16.63
Electronics			
Raspberry Pi 4	\$35.00	1	\$35.00
Arduino Mega Clone	\$20.00	1	\$20.00
Waveshare Capacitive Touch Screen	\$48.99	1	\$48.99
5V 50N Electromagnet	\$9.99	1	\$9.99
MPU-6050 IMU	\$9.99	2 packs of 3	\$19.98
BNO055 IMU	\$34.99	1	\$34.99
TF-Luna LiDAR	\$28.59	1	\$28.59
HRB 11.1V 5000mAh Battery	\$63.19	1 pack of 2	\$63.19
LM2596 DC-DC Buck Converter	\$16.99	1 pack of 10	\$16.99
Huskeylens- AI Camera	\$54.90	1	\$54.90
Total Cost:			\$5,616.18

Appendix L ANSYS

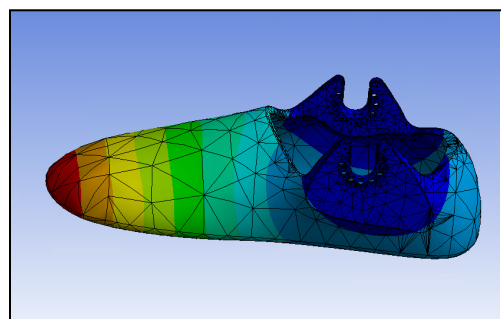
Foot ANSYS:



Foot ANSYS Set up

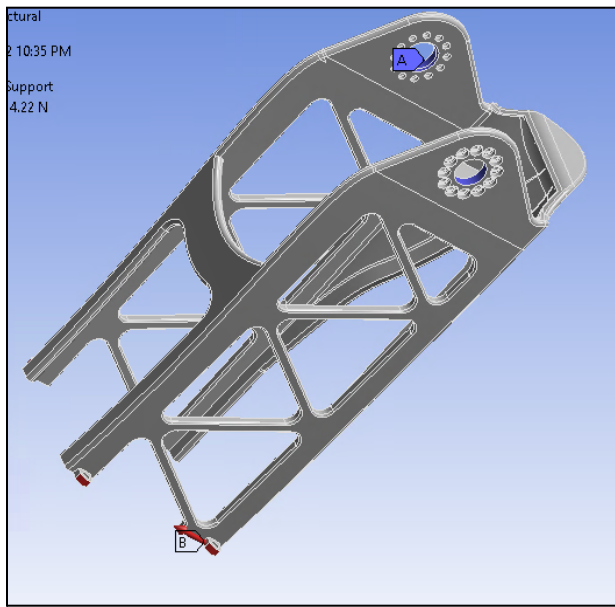


Stress Foot ANSYS

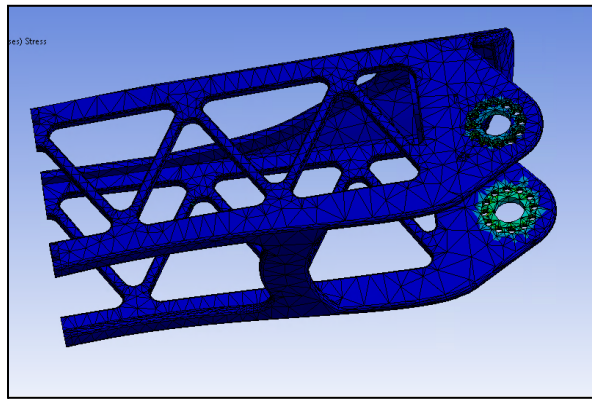


Deformation Foot ANSYS

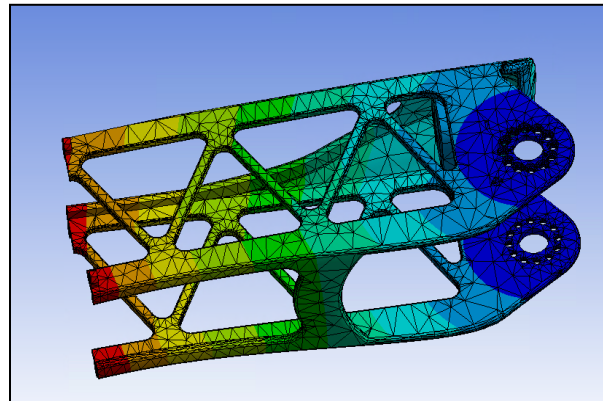
Shin ANSYS:



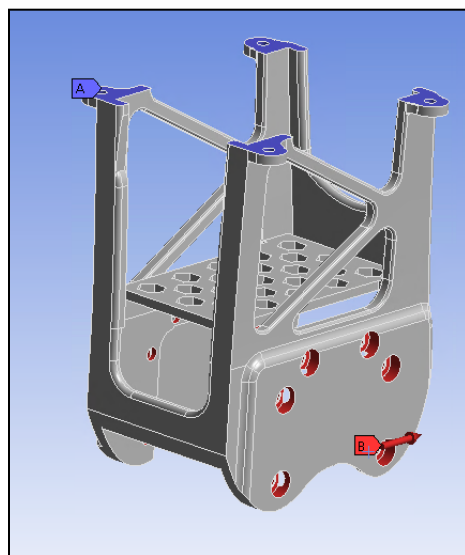
Top Shin ANSYS Set Up



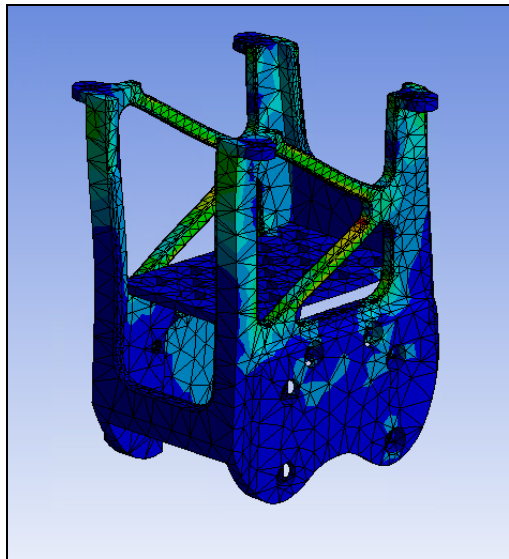
Stress Top Shin ANSYS



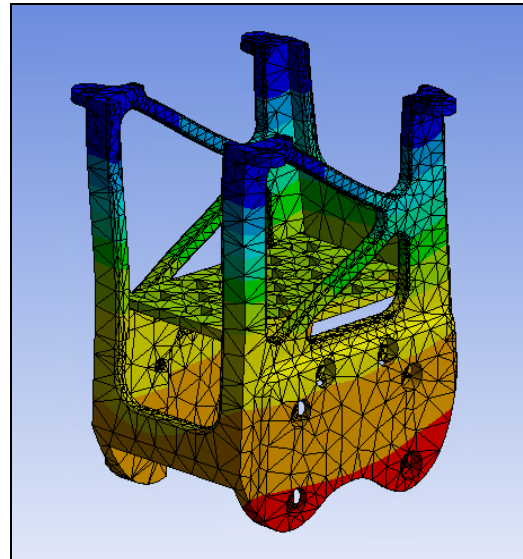
Deformation Top Shin ANSYS



Bottom Shin ANSYS Set Up

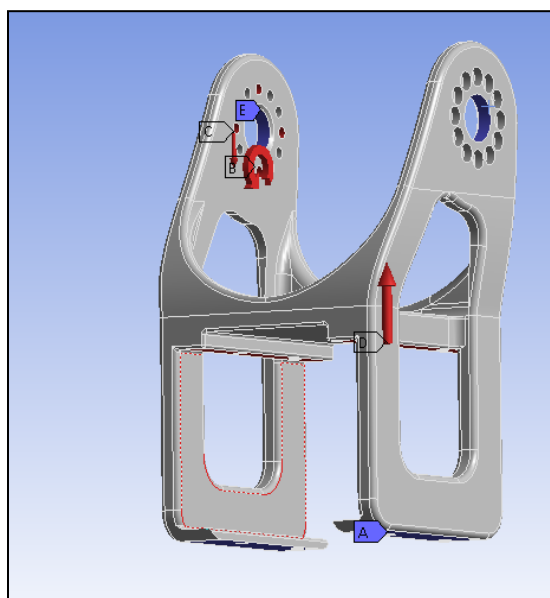


Stress Bottom Shin ANSYS

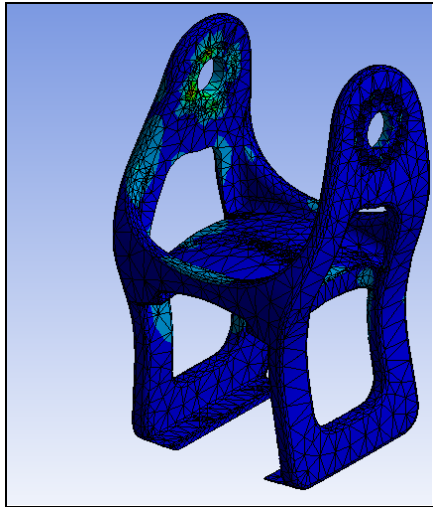


Deformation Bottom Shin ANSYS

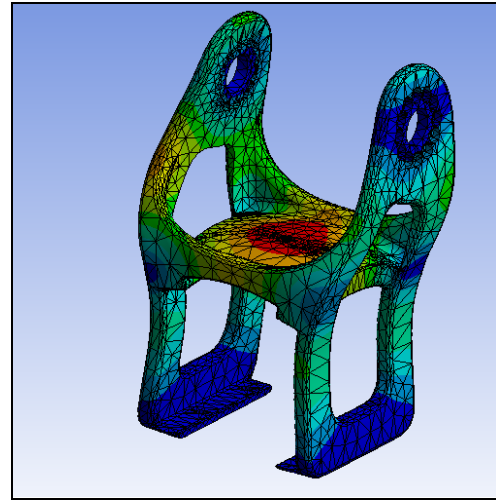
Rib ANSYS:



Rib ANSYS Set Up

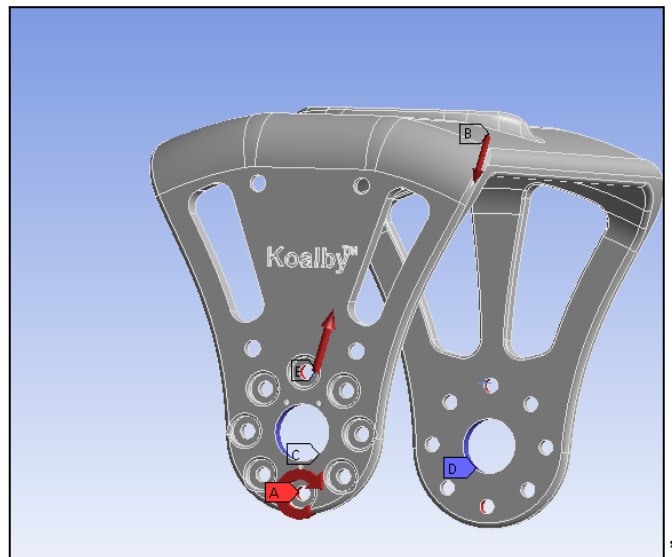


Stress Rib ANSYS

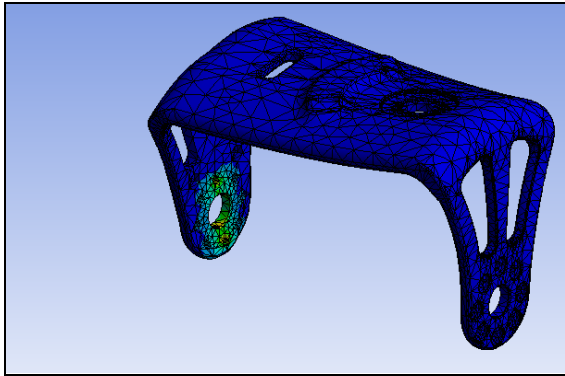


Deformation Rib ANSYS

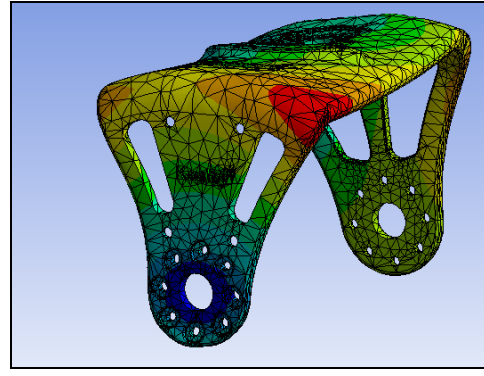
Abdomen ANSYS:



Abdomen ANSYS Set UP



Stress Abdomen ANSYS



Deformation Abdomen ANSYS

16.0 Reflections

This project required two valuable interpersonal skills from each team member to achieve all that we did throughout this year: communication and organization. This Major Qualifying Project required 15-17 hours of work per week from each member, so the ability to communicate effectively and timely between team members was crucial to the project's success. Strong organizational skills were required to delegate tasks and document our progress.

Additionally, various technical skills were brought to this project from individual team members. Our team members had a strong technical background in Solidworks CAD designs and assemblies, FDM printing, design for manufacturing techniques, and FBD analysis. Over the course of this project, new skills were developed related to ANSYS analysis, resin printing, sensor testing, and various electronic wiring and testing.

Overall, this project successfully continued the 2022 3D Printed Humanoid MQP Team's work by developing a grip addition, improving the structural integrity of the robot, integrating sensors for walking, assembling a new robot.